

T H E U N I V E R S I T Y O F M I C H I G A N
COLLEGE OF LITERATURE, SCIENCE, AND THE ARTS
Department of Physics

Technical Report No. 1

THE ACOUSTOELECTRIC EFFECT AND INTERVALLEY SCATTERING RATES
IN ANTIMONY-DOPED GERMANIUM

Benjamin Tell

ORA Project 04941

under contract with:

U. S. ATOMIC ENERGY COMMISSION
CHICAGO OPERATIONS OFFICE
CONTRACT NO. AT(11-1)-1112
ARGONNE, ILLINOIS

administered through:

OFFICE OF RESEARCH ADMINISTRATION ANN ARBOR
August 1963

This report was also a dissertation submitted in partial fulfillment of the requirements for the degree of Doctor of Philosophy in The University of Michigan, 1963.

TABLE OF CONTENTS

	Page
LIST OF TABLES	v
LIST OF FIGURES	vi
ABSTRACT	vii
ACKNOWLEDGMENTS	viii
CHAPTER	
I. INTRODUCTION	1
II. THE ACOUSTOELECTRIC EFFECT	5
A. Introduction	5
B. Band Structure of Germanium	8
C. Intervalley Scattering	10
D. Derivation of Acoustoelectric Voltage	13
E. Space Charge	29
F. Attenuation and Radiation Pressure	32
III. EXPERIMENT EQUIPMENT AND PROCEDURE	35
A. General	35
B. Samples and Transducer	37
C. Sample Holder	41
D. Electrical Equipment	45
E. Experimental Procedure	47
F. Resistivity Measurement	48
IV. RESULTS	50
A. Reduction of the Data	50
B. Estimates of Error	58
V. INTERPRETATION OF INTERVALLEY SCATTERING RATES	68
A. Preliminary Remarks	68
B. Theory of Donor States in Germanium	69
C. Introduction to the Ionized Donor Problems	76
D. Ionized Impurity Scattering-Direct	81
E. Ionized Donors-Compound Capture Re-Emission Process	87

TABLE OF CONTENTS (Concluded)

	Page
F. Concluding Remarks on Ionized Donors	102
G. Neutral Donor Induced Intervalley Transitions	107
APPENDIX	
A. MOBILITY AND CONDUCTIVITY IN A MANY-VALLEY SEMICONDUCTOR	116
B. THE USE OF MODULATED ACOUSTIC POWER	120
C. DELTA FUNCTION REPRESENTATION OF VALLEY-ORBIT SPLITTING	124
D. THERMAL TRANSITION RATES	128
E. VALLEY STATISTICS	138
BIBLIOGRAPHY	143

LIST OF TABLES

Table	Page
I. Thermal Emission Rates	98
II. Internal Transition Rates	98
III. Characteristic Rate of Changing Valleys	99
IV. Compound Capture Process for Antimony	99
V. Neutral Donor Data	113

LIST OF FIGURES

Figure	Page
1. Pictorial description of acoustoelectric effect for simple semiconductors.	7
2. Pictorial description of acoustoelectric effect in many-valley semiconductor (symmetric four-class system).	12
3. Energy band structure of germanium.	15
4. Typical germanium sample.	40
5. Sample holder with mounted crystal.	42
6. Layout of Dewar.	43
7. Block diagram of electrical system.	46
8. Intervalley scattering rates as a function of temperature for antimony-doped germanium.	52
9. Ionized and neutral donor concentrations as a function of temperature.	54
10. A(T) and B(T) for antimony-doped germanium.	56
11. Plot of $\frac{(N^+)^2}{N_0} T^{-3/2}$.	57
12. Theoretical spectrum and corrected spectra for energy levels of donors in germanium (S states only).	77
13. A(T) and B(T) for arsenic-doped germanium.	79

ABSTRACT

Theory and experiment are presented for the drag exerted on electrons in antimony-doped germanium by a traveling acoustic wave, using a method similar to that employed by Weinreich, Sanders, and White for arsenic-doped germanium. It is shown that the drag, or acoustoelectric voltage, indicates directly the intervalley scattering rates as a function of temperature and doping. Experimental data for five antimony-doped germanium crystals are given with impurity content ranging from 1.5×10^{14} to 8.3×10^{15} cm^{-3} and for temperatures of 15°K to 100°K .

Intervalley scattering rates are attributed, as previously, to phonons and to both ionized and neutral donors. In the temperature region where the phonon contribution is dominant, our results agree with the phonon rates previously determined.

The express purpose of this experiment was to determine the intervalley scattering rate due to antimony donors. Antimony was chosen because its valley-orbit splitting is approximately one-seventh that of arsenic, these donors representing the extremes in valley-orbit splitting of the commonly used Group V impurities, and the intervalley scattering rate due to arsenic donors had been previously measured.

The effective intervalley scattering cross section for ionized antimony follows a $T^{-2.5}$ temperature dependence, which is characteristic of recombination cross sections. Two possible contributions to the intervalley cross sections have been examined in detail, viz, the compound capture re-emission process and direct scattering by the central cell potential. They are found to be inadequate to explain the present experimental results. Two other possible mechanisms have been briefly discussed.

The neutral donor contribution has been attributed to exchange scattering and an order of magnitude agreement has been achieved by scaling appropriate calculations for atomic hydrogen.

As a subsidiary result of our experiment, and a definitive check on our experimental procedure, uniaxial deformation potential of 16.9 eV has been found. This is in good agreement with the previous determination of Weinreich, Sanders, and White and with other independent estimates.

ACKNOWLEDGMENTS

The author wishes to express his gratitude to Professor Gabriel Weinreich not only for his suggestion of the problem and his interest and encouragement throughout, but also for an undefinable aspect which goes beyond the above acknowledgment.

The interest and help of the other members of the doctoral committee is appreciated.

The author wishes to thank his fellow graduate students on the Resonance Project for their advice and suggestions.

The author wishes to thank Mr. Harry G. White and Dr. Ralph A. Logan, of the Bell Telephone Laboratories, for providing the doped single crystals of germanium, from which our samples were prepared.

The use and loan of equipment from various sources around the University is gratefully acknowledged. In particular, the author wishes to thank Professor C. W. Peters for use of his high vacuum evaporator, and the Chemical and Metallurgical Engineering Department for use of their X-Ray Diffractometer, diamond saw, and metallurgical wheels.

The support of this research by the United States Atomic Energy Commission under Contract No. AT-11-1-112 is gratefully acknowledged.

CHAPTER I

INTRODUCTION

This thesis is a report of the measurement of the acoustoelectric effect and of intervalley scattering rates in antimony-doped germanium. It is an extension of the experiment of Weinreich, Sanders, and White (1) on arsenic-doped germanium. Their work constituted the first experimental observation of the acoustoelectric effect, although there had been many previous and several subsequent theoretical papers (e.g., 2-6).

The W.S.W. experiment was also the first direct determination of intervalley scattering rates in n-type germanium. Previous attempts to measure these rates had, of necessity, been rough estimates because of the inability to separate intervalley scattering from the much faster intravalley rates. The acoustoelectric effect, however, provides a direct measure of these rates, since it depends on the relaxation of the electron distribution after a relative population shift of the valleys. Intervalley rates had previously been deduced from deviations in piezoresistance data from theoretical predictions (8,9), and had been attributed entirely to phonons. Weinreich, Sanders, and White* succeeded in determining the energy of the "intervalley phonon", and in showing that at low temperatures ($T \lesssim 100^\circ\text{K}$) a sizeable con-

*Called W.S.W. hereafter

tribution to the total rate is due to donors (both ionized and neutral).

As will be explained later, donor-induced intervalley scattering rates depend on the detailed structure of the donor potential in the central impurity cell. This potential gives rise to a splitting of the "hydrogen-like" energy levels, which would be degenerate in effective mass approximation (10). This splitting is called the valley-orbit splitting, and is about a factor of seven larger for arsenic than for antimony donors in germanium. Since W.S.W. measured intervalley scattering rates for arsenic, we felt it would be interesting to do a similar experiment for antimony. Our purpose was to see how these rates depended on the donor by virtue of the valley-orbit splitting, and to attempt to interpret the results.

There are not, to our knowledge, any detailed theories for either ionized or neutral impurity induced intervalley transitions. Certain hypotheses as to the dependence of intervalley scattering on the valley-orbit splitting have been made, and they are briefly discussed by Koenig (12). They are not in agreement with experiment.

We have attempted to make order-of-magnitude calculations for the several processes which are expected to contribute to the intervalley rates (1,11). Physical explanations and attempted calculations for donor induced intervalley scattering constitute the chapter on Interpretation.

The acoustoelectric effect is a direct measure of the electron-lattice interaction, aside from the determination of intervalley scattering rates which are peculiar to n-germanium, n-silicon, bismuth, and several other solids. Whereas such processes as resistivity and thermoelectricity depend on the coupling between the electron and the lattice (thermal phonons), the acoustoelectric effect allows us to study this coupling for a single lattice mode (an ultrasonic phonon).

The acoustoelectric effect or acoustic drag is determined by the electric potential set up by a traveling acoustic wave, so that if relevant relaxation times are known, we have a direct measure of this potential. From this electric potential, the appropriate deformation potential constants can be determined (i.e., electron-lattice coupling constants). If, however, neither the relaxation times or deformation potential are known, it may be possible to determine both by measuring the acoustoelectric effect at several frequencies. (See p 66.) It might be interesting to study the magnetic field dependence of the acoustoelectric effect (2,52), and also to determine the acoustoelectric effect in the presence of an external electric field (3,7, 53,54). We have not, however, attempted to do this.

Unfortunately, the electron-lattice coupling is usually weak, and when space charge diminution of the traveling potential is taken into account, the acoustoelectric effect becomes very small. It can be readily observed in n-germanium, however, because space charge ef-

fects can be eliminated as a result of the "many-valley" structure. The effect has been recently observed in Cds (7) which is a piezoelectric semiconductor in which the electron-lattice coupling (piezoelectric coupling constant) is several orders of magnitude larger than the coupling in germanium. It is conceivable that one might observe this effect in certain semiconductors by using ambipolar conduction (both electrons and holes) to alleviate space charge problems (3,4). It might also be possible to do experiments in n-type silicon similar to the present experiment and the previous experiment of W.S.W.

The format for this thesis consists of an explanation of the acoustoelectric effect (Chap. II), description of experimental techniques (Chap. III), presentation of results (Chap. IV), and the ensuing interpretation (Chap. V).

CHAPTER II

THE ACOUSTOELECTRIC EFFECT

A. INTRODUCTION

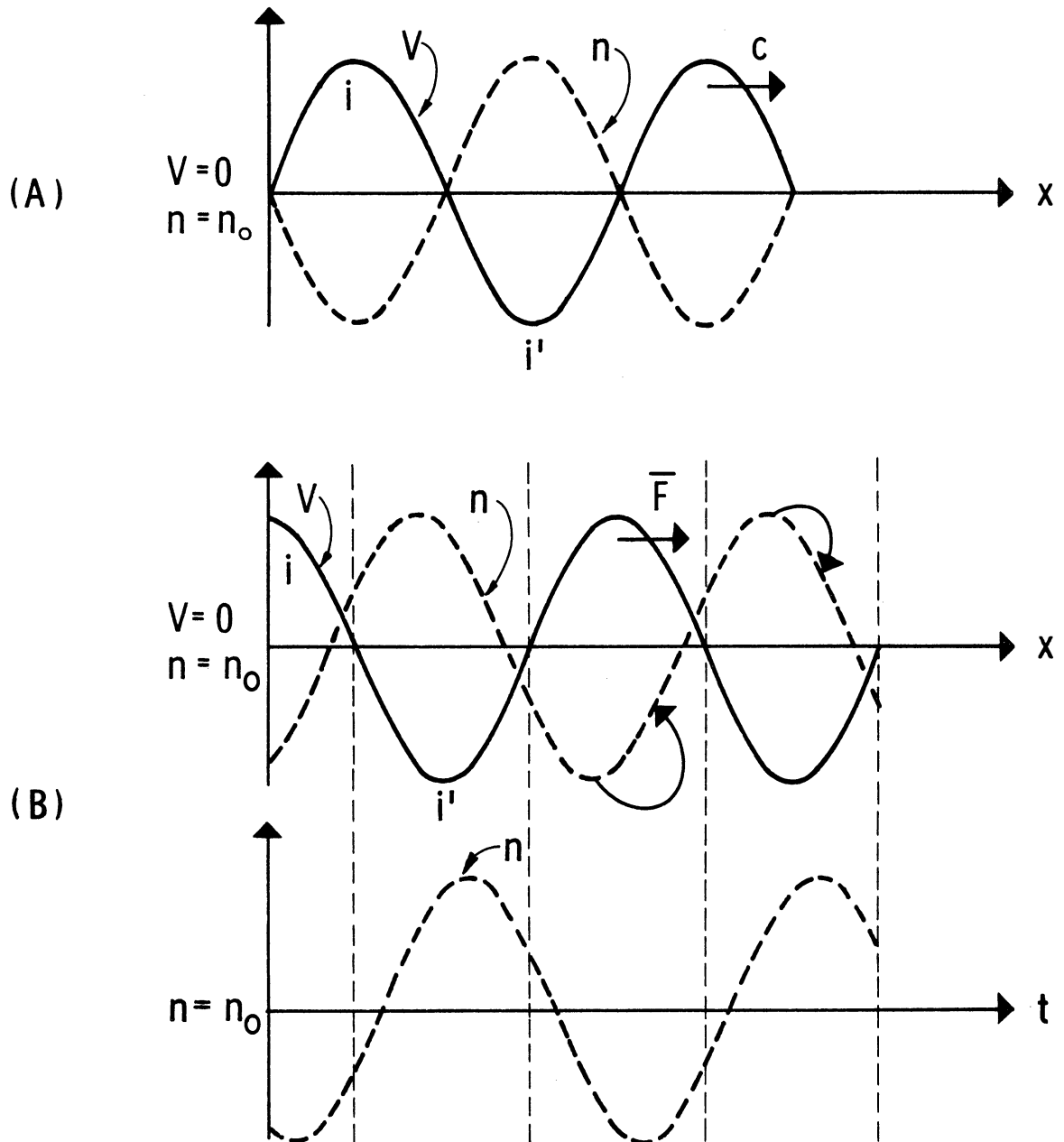
The acoustoelectric effect refers to the production of a dc electric field under the action of a traveling acoustic wave in a medium containing free carriers. In extrinsic n-type germanium, the conduction electrons are coupled to the wave by means of a deformation potential. The electrons, in the absence of the acoustic wave, perform a diffusive motion, being continually scattered by lattice vibrations and impurities. The perturbing effect of the traveling wave may result in a preferential scattering of electrons in the direction of the wave: That is, a net average force exerted by the wave on an electron along the direction of propagation. We will consider only the case where the thermal energy of the electron is much greater than its deformation potential energy, and its mean free path is short compared to the acoustic wavelength.

The simplest physical picture for this process is to visualize a sinusoidal potential traveling with the velocity of sound C , with the electrons attempting to attain equilibrium positions favoring regions of lower potential. If the electrons were capable of immediate redistribution with respect to the traveling potential, exact equilibrium would be attained. The electron density at any point in

space would then simply oscillate at the acoustic frequency. At the other extreme, the electrons would have a relaxation time long compared to the period of the wave. Then, the electrons would be almost unaffected by the wave, and the electron density would remain uniform in space. In the first case, the net average force exerted by the wave on the electrons would be zero. In the latter case (the ultrasonic frequency approaching infinity) an average force remains. This results despite the deviations from a uniform electron density approaching zero, since the local force approaches infinity. Their product, however, remains finite. (See Fig. 1A for the first case.)

For intermediate cases, where the electron relaxation time is short but still finite with respect to the period, the electron sees the potential but cannot attain exact equilibrium. The electrons get behind, and tend to bunch on the backward slope of the wave. (See Fig. 1B.) This implies a net average force (i.e., the local force weighted by the local electron distribution) in the direction of the wave. The magnitude of the force depends on the amount by which the electron distribution deviates from its equilibrium distribution.

The net average acoustic force per electron causes a certain number of electrons to flow down the crystal. These electrons then produce a dc electric field whose effect balances out the force due to the acoustic wave. This dc field, or equivalently, the corresponding dc voltage, is called the acoustoelectric voltage.



Traveling potential, V , with velocity, c , and electron density, n , for (A) low frequency case, and (B) intermediate frequency case (ii' is the backward slope of the potential, and the curved arrows indicate the relaxation mechanism). The net average force, \bar{F} , is in the direction of the wave propagation.

Fig. 1. Pictorial description of acoustoelectric effect for simple semiconductors.

The relaxation time described above is the spatial redistribution or diffusion process. As will be shown, it is both frequency and mobility dependent, and is the only process available for the carriers to attain equilibrium in a simple semiconductor.

We have so far neglected space charge effects due to the bunching of carriers. The electrons are assumed to move in a uniform positive charge density due to the ionized donors, and bunching of electrons will upset the charge neutrality. This will result in their mutual repulsion, and the restoration of a uniform electron distribution. Since the acoustoelectric voltage results from the bunching of carriers, we cannot produce a sizable effect without overcoming space charge inequalities.

Fortunately, space charge difficulties can be eliminated in a many-valley semiconductor such as n-type germanium, where we can produce considerable bunching without upsetting space charge neutrality. We can therefore produce a measurable acoustoelectric voltage, which will give a direct determination of intervalley scattering rates. We will next discuss the band structure of germanium, and the relationship between the acoustoelectric effect and intervalley scattering.

B. BAND STRUCTURE OF GERMANIUM

Germanium is an elemental semiconductor whose space lattice is face centered cubic. It has two atoms associated with each lattice point at $[000]$ and $[1/4, 1/4, 1/4]$; each atom forms covalent tetra-

hedral bonds with its four nearest neighbors. A donor (antimony, arsenic, phosphorus, and bismuth with five electrons in their outer shell) enters the germanium lattice substitutionally, and the extra electron is weakly bound. At low temperatures, it is only the extra electrons that contribute to conduction processes.

The simple model of a semiconductor is based on a nondegenerate energy minimum located at the center of wave vector or reciprocal lattice space, and spherical constant energy surfaces in the neighborhood of the energy minimum. This implies single isotropic effective masses for the carriers. In germanium, neither the valence band nor the conduction band follows this simple scheme. The conduction band contains a set of equivalent energy minima, or "valleys" symmetrically located at the points where the [111] axes intersect the surface of the basic cell in reciprocal space, i.e., the reduced Brillouin zone. Since the valleys are at the zone faces rather than in the interior, we have only four valleys instead of eight. This follows from the periodicity of the reciprocal lattice, where any points differing by a reciprocal lattice vector are identical. (See Figs. 3A and 3B.)

The constant energy surfaces are ellipsoids of revolution centered at the equivalent minima whose symmetry axes are the [111] axes. We now have an anisotropic effective mass whose component m_l along the symmetry axis has been measured to be approximately 20 times the components m_t perpendicular to the axis (10, p 273).

Electrons in the conduction band will have energy and crystal momentum corresponding to states in the neighborhood of one of the valleys, since these are the only states populated at low temperatures.

C. INTERVALLEY SCATTERING

To return to the qualitative description of the acoustoelectric effect, we will later show that a transverse elastic wave traveling in a [100] crystallographic direction, and polarized in an arbitrary direction destroys the energy degeneracy of the valleys. Two valleys are shifted equally but oppositely, and the other two also equally and oppositely but by a different amount than the first two. This case is called a symmetric four-class system. For a sinusoidal shear wave, the shifts occur at the acoustic frequency. If the shear wave is polarized in a [010] direction, the shifts of the two pairs become equal and this case is called a symmetric two-class system. We are assuming, as is customary, that the only effect of the strain is to shift the valleys rigidly by a certain energy called the deformation potential energy (13,14 p 167). The total number of electrons in the conduction band does not change as a result of the shear wave, since the sum of the energy shifts is zero. (See Fig. 2.)

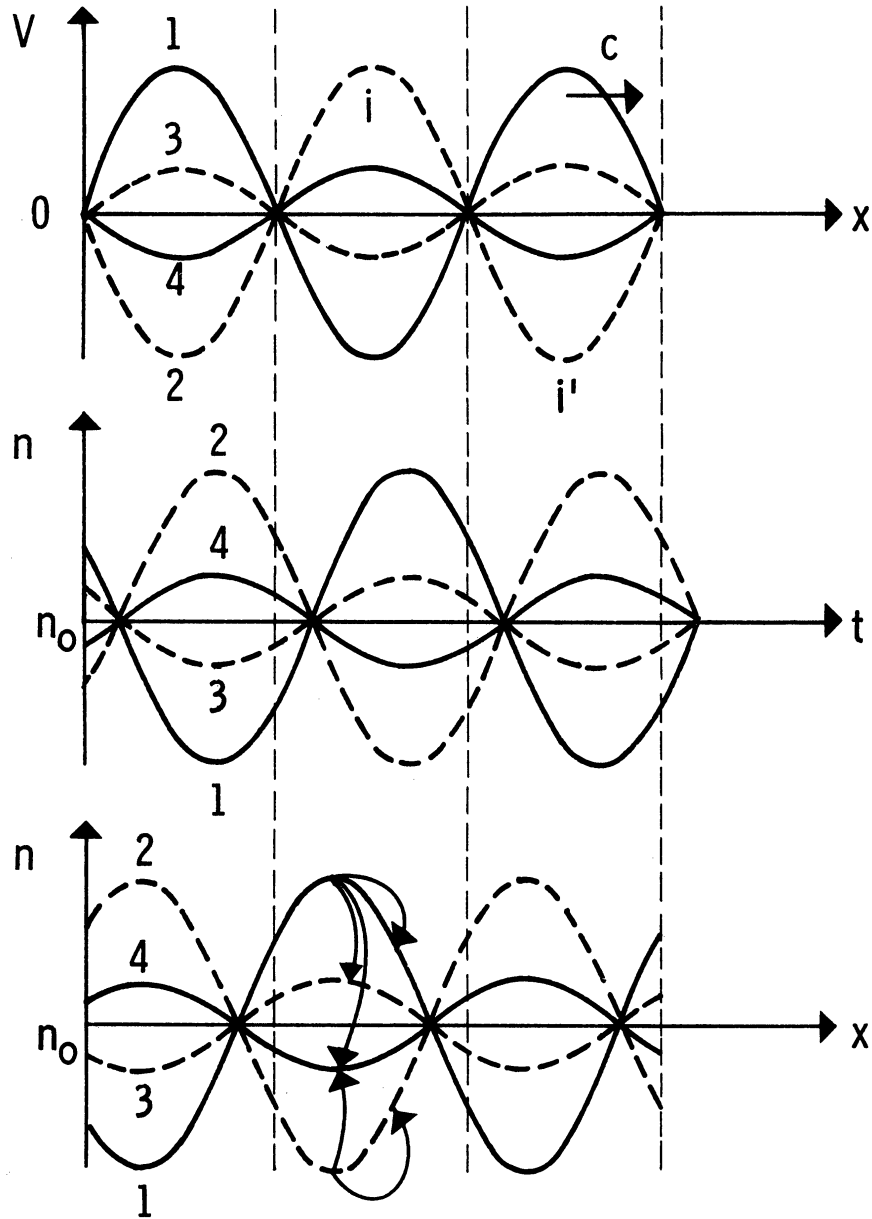
The electrons, because the valley degeneracy has been destroyed, will however attempt to redistribute themselves among the valleys according to a Boltzmann factor. The extent to which the electrons

can reach an equilibrium distribution is determined by the relation between the redistribution time or intervalley scattering rate and the acoustic frequency. We assume that electrons reach equilibrium within a valley in a time short compared to the redistribution time between valleys. In other words, the intravalley scattering time is fast compared to the intervalley time.

Analogously to the discussion in Part A on spatial redistribution, we do not get an acoustoelectric voltage if the electrons redistribute perfectly among the valleys. At the opposite extreme (the intervalley scattering rate approaching zero), the problem reduces to that of a simple semiconductor, but with no space charge problems (Sec. E). For intermediate cases, the electrons follow the changing valleys, but not perfectly, and we again develop a net average force and a corresponding acoustoelectric voltage.

Therefore, the two relaxation mechanisms available are intervalley scattering and spatial redistribution. Since the spatial redistribution time is known, this experiment (as will be shown) determines the intervalley scattering time.

In intervalley scattering, the electron changes its valley but not its position in r space, and in spatial redistribution, it changes its position but not its valley. Instead of a single traveling potential, we now have four potentials each corresponding to a single valley.



Traveling potentials, $V^{(\alpha)}$, with electron densities, n_{α} , for the intermediate frequency case. (The curved arrows indicate the two relaxation mechanisms, and ii' is the backward slope of the potential.) The net average force for the electrons in each class is in the direction of wave propagation.

Fig. 2. Pictorial description of acoustoelectric effect in many-valley semiconductor (symmetric four-class system).

Furthermore, we are able to overcome space charge problems. In the absence of the shear wave, the valleys are equally populated with n_0 electrons per unit volume in each, and the total density of electrons $n(x)$ at any position along the crystal is $4n_0$. In the presence of the shear wave, the electrons tend toward an equilibrium which favors regions of lower potential and valleys of lower energy. The electrons can now get behind, however, without upsetting space charge neutrality.

The reason is that lifting the valley degeneracy causes redistribution among the valleys, but does not affect the distribution in r space. Similarly, spatial redistribution will no longer produce space charge inequalities, since electrons in valleys seeing opposite deformation potentials will diffuse in opposite directions. Consequently, as many electrons as diffuse toward the low potential regions in one valley, diffuse away from the high potential regions in the opposite valley. (See Fig. 2.) Any deviations from a uniform electron density are damped out in a time characterized by the dielectric relaxation time which is short compared to the period of the acoustic wave (Sec. E). Therefore, at any position along the crystal $n(x)$ will still equal $4n_0$.

D. DERIVATION OF ACOUSTOELECTRIC VOLTAGE

We will derive here the case for a symmetric four-class system, and show that it gives the same result as the symmetric two-class

system used by W.S.W. (See beginning of Sec. C for nomenclature.)

If we have a shear wave traveling along a [100] axis, and polarized in a [010] axis, the only nonzero component of the strain tensor referred to the usual cubic axes is $u_{xy} = u_{12}$. Now, if the wave is still traveling along [100], but is polarized in an arbitrary direction $[\alpha\beta]$, in the rotated system only $u'_{12} = u$ is nonzero. Relating back to original cubic system and using the transformation law of second rank tensors $u_{ij} = \sum_{\rho,\sigma} R_{i\rho} R_{j\sigma} u'_{\rho\sigma}$ we get $u_{12} = \alpha u$ and

$u_{13} = -\beta u$ where

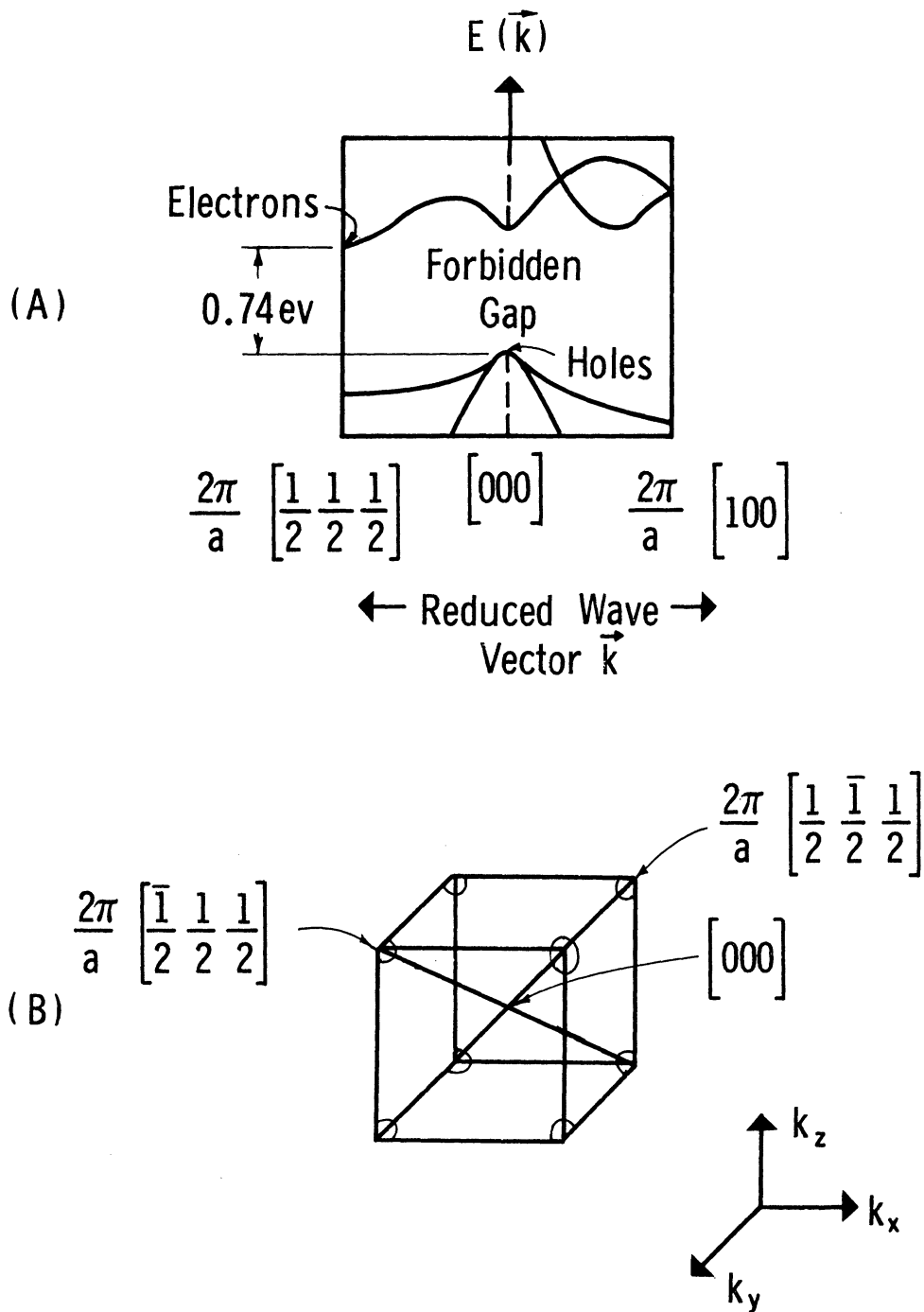
$$R_{ij} = \begin{pmatrix} 1 & 0 & 0 \\ 0 & \alpha & \beta \\ 0 & -\beta & \alpha \end{pmatrix}$$

Using the deformation potential as defined by Herring (13), the contribution to the potential energy due to a strain for an electron in the α 'th valley is

$$V^{(\alpha)} = \left[\Xi_d \delta_{ij} + \Xi_u K_i^{(\alpha)} K_j^{(\alpha)} \right] u_{ij} \quad (2.1)$$

The gradient of $V^{(\alpha)}$ (i.e., the force) is longitudinal in character, and will couple the shear wave to longitudinal currents. Ξ_d and Ξ_u are the dilation and uniaxial deformation potential constants, and $K_i^{(\alpha)}$ and $K_j^{(\alpha)}$ are the i 'th and j 'th components of a unit vector from the center of the zone to the α 'th valley.

As previously discussed, we have four valleys in germanium at the positions $[111]$, $[\bar{1}11]$, $[1\bar{1}1]$, and $[\bar{1}\bar{1}1]$. (See Fig. 3B.) Although



The schematic representation of the energy bands, (A), (41, p. 304), and the location of the valleys (B). A constant energy ellipsoid in the neighborhood of each of the valleys is also shown.

Fig. 3. Energy band structure of germanium.

the Brillouin zone has a shape which is not cubic, the cube illustrates the relevant properties and is used for simplicity. The unit vectors

lie along the [111] axes, and are

$$\vec{K}^{(1)} = \frac{1}{\sqrt{3}} [\hat{i} + \hat{j} + \hat{k}]; \quad K_1^{(1)} = \frac{1}{\sqrt{3}} \text{ etc}$$

$$\vec{K}^{(2)} = \frac{1}{\sqrt{3}} [-\hat{i} + \hat{j} + \hat{k}]; \quad K_1^{(2)} = -\frac{1}{\sqrt{3}}$$

$$\vec{K}^{(3)} = \frac{1}{\sqrt{3}} [\hat{i} - \hat{j} + \hat{k}]$$

$$\vec{K}^{(4)} = \frac{1}{\sqrt{3}} [-\hat{i} - \hat{j} + \hat{k}]$$

(2.2)

and

$$V^{(1)} = \frac{1}{3} \Xi_u u_{12} + \frac{1}{3} \Xi_u u_{13} = \frac{1}{3} (\alpha - \beta) \Xi_u u = A^{(1)} u$$

$$V^{(2)} = -\frac{1}{3} \Xi_u u_{12} - \frac{1}{3} \Xi_u u_{13} = -\frac{1}{3} (\alpha - \beta) \Xi_u u = -A^{(1)} u$$

$$V^{(3)} = \frac{1}{3} \Xi_u (\alpha + \beta) u = A^{(3)} u \quad (2.3)$$

$$V^{(4)} = -\frac{1}{3} \Xi_u (\alpha + \beta) u = -A^{(3)} u$$

So that $V^{(1)} = -V^{(2)}$ and $V^{(3)} = -V^{(4)}$. Since originally, all valleys had extremal energy E_0 , the extremal energy of the α 'th valley is now $E_0 + V^{(\alpha)}$. The original valley degeneracy is completely destroyed in a symmetric pairwise manner, i.e., a symmetric four-class system.

Following W.S.W., we define a "field strength" of the elastic wave $\Phi = \Phi_0 e^{ikx - i\omega t}$ such that $1/2 \operatorname{Re}(\Phi \Phi^*)$ is equal to the elastic energy density. We also introduce a quantity "q" which W.S.W. called the "acoustic charge". It is defined as $1/\sqrt{2}$ times the deformation potential in a strain of unit energy density. This enables us to write the local potential experienced by an electron in the form $V^{(\alpha)} = q^{(\alpha)} \Phi$.

Furthermore, the average acoustic power flow is

$$S = \frac{1}{2} \operatorname{Re}(\Phi \Phi^*) C$$

where C is the velocity of a shear wave traveling in a [100] direction.

The elastic energy density for a cubic crystal (15, p. 91) is

$$\begin{aligned} \frac{1}{2} \operatorname{Re}(\Phi^* \Phi) &= \frac{1}{2} C_{11} (u_{11}^2 + u_{22}^2 + u_{33}^2) \\ &+ C_{12} (u_{11} u_{22} + u_{11} u_{33} + u_{22} u_{33}) \\ &+ \frac{1}{2} C_{44} (u_{12}^2 + u_{13}^2 + u_{23}^2) \end{aligned}$$

where C_{11} , C_{12} , and C_{44} are the non-zero elastic constants.

For our case, the energy density reduces to:

$$\frac{1}{2} \text{Re}(\Phi^* \Phi) = \frac{1}{2} C_{44} (u_{12}^2 + u_{13}^2) = \frac{1}{2} C_{44} u$$

so that for a strain of unit energy density, we get

$$u = \sqrt{\frac{2}{C_{44}}} \quad \text{and} \quad q^{(\alpha)} = \frac{1}{\sqrt{2}} V^{(\alpha)}$$

which yields

$$q^{(\alpha)} = \frac{1}{\sqrt{2}} A^{(\alpha)} u = \frac{A^{(\alpha)}}{\sqrt{C_{44}}}$$

where the $A^{(\alpha)}$ are given by Eq. (2.3), or

$$q^{(1)} = \frac{1}{3} \frac{\Xi u}{\sqrt{C_{44}}} (\alpha - \beta) = (\alpha - \beta) q$$

$$q^{(2)} = -(\alpha - \beta) q$$

$$q^{(3)} = (\alpha + \beta) q$$

$$q^{(4)} = -(\alpha + \beta) q$$

(2.4)

where

$$q = \frac{1}{3} \frac{\Xi u}{\sqrt{C_{44}}}$$

The i 'th type of particle therefore experiences a local potential

$$V^{(i)} = q^{(i)} \phi.$$

We now calculate the bunching that occurs as a result of the [100] - [00 β] acoustic wave using the approach of W.S.W. It is a macroscopic approach, which is valid when the sound wave length is much greater than the electron's mean free path.

The continuity equation for the i 'th valley is

$$\frac{\partial n_i}{\partial t} + \frac{\partial j_i}{\partial x} = P_i \quad ; \quad \begin{aligned} n_i &= n_i(x - ct) \\ j_i &= j_i(x - ct) \end{aligned} \quad (2.5)$$

where P_i is the net rate of intervalley scattering which produces particles of type i . It will be discussed below.

The particle current density for the i 'th valley is

$$j_i = -D \left[\frac{\partial n_i}{\partial x} + \frac{q^{(i)} n_i}{kT} \frac{\partial \bar{\Phi}}{\partial x} \right] \quad (2.6)$$

where the first term is the ordinary diffusion term due to concentration gradients and the second is the conductivity current set up by the force field $q^{(i)} \partial \phi / \partial x$ accompanying the acoustic wave. We have used the relations $\sigma^{(i)} = n_i \mu = n_i D / kT$ where $\sigma^{(i)}$ is the conductivity of the i 'th valley, and D and μ are the directionally averaged diffusion constant and mobility ordinarily encountered. The fact that the mobility, which is a tensor quantity for a single valley, can be replaced by its directionally averaged value for particle motion along a [100] direction is explained in Appendix A.

We will discuss the continuity Eq. (2.5) in order to derive P_i (the net rate of intervalley scattering). To repeat, the physical situation is that the shear wave produces a spatially variable traveling potential and also shifts the relative energy of the valleys at the acoustic frequency. The electron distribution n_i attempts to relax to its thermal equilibrium distribution. We mean by the thermal equilibrium distribution the distribution which would be attained in the presence of the shear wave if the electrons were capable of instantaneous relaxation.

If we consider a fixed volume of the crystal, and we want to find how the density of type i particles changes with time (dn_i/dt) when the equilibrium distribution is upset, we would say that it can "relax" due to particles flowing into the volume from outside ($\partial j_i/\partial x$) and by production of particles within the volume (P_i). In other words, one gets the standard form of a continuity equation where $\partial j_i/\partial x$ is related to spatial redistribution and P_i to intervalley scattering.

P_i (the net rate of production of type i particles) is described by the equation

$$P_i = \left\{ R(j \rightarrow i) n_j - R(i \rightarrow j) n_i \right\} + \left\{ R(k \rightarrow i) n_k - R(i \rightarrow k) n_i \right\} + \left\{ R(l \rightarrow i) n_l - R(i \rightarrow l) n_i \right\} \quad (2.7)$$

so that $R(j \rightarrow i)n_j$ is the total rate at which electrons leave valley j for i , and $R(i \rightarrow j)n_i$ is the reverse rate. $R(j \rightarrow i)$ is the probability per unit time that an electron in valley j will make a transition to valley i , and n_j is the instantaneous density of electrons in j .

The first bracket, therefore, gives the net rate of production of type i particles due to the fact that the total transition rate from i to j is not equal to the reverse rate. That is, there are net transitions.

In thermal equilibrium $P_i = 0$, and each bracket must separately be equal to zero. This gives for the first bracket

$$R(j \rightarrow i) n_j^0 = R(i \rightarrow j) n_i^0$$

where n_i^0 and n_j^0 are the equilibrium densities of particles in valleys i and j and

$$n_i^0 = n_0 \exp\left[-\frac{q^{(i)}\Phi}{kT}\right] = n_0 \left[1 - \frac{q^{(i)}\Phi}{kT}\right]$$

since at equilibrium the electrons would populate the valleys according to a Boltzmann distribution, n_0 is the equilibrium density of electrons in each valley in the absence of strain, and we consider only the case of $q^{(i)}\Phi \ll kT$.

This yields

$$R(j \rightarrow i) = R(i \rightarrow j) \exp\left[\frac{(q^{(j)} - q^{(i)})\Phi}{kT}\right]$$

or

$$R(j \rightarrow i) = R(i \rightarrow j) \left[1 + (g^{(j)} - g^{(i)}) \frac{\Phi}{kT} \right] \quad (2.8)$$

Since the valleys are driven at the acoustic frequency, and the distribution of electrons among the valleys takes a finite time to reach equilibrium, n_i and n_j will not necessarily be equal to n_i^0 and n_j^0 . The electrons "relax" toward equilibrium with "relaxation times" given by $1/R(i \rightarrow j)$ and $1/R(j \rightarrow i)$.

Still considering only the first bracket, and using Eq. (2.8), we get

$$P_i = R(i \rightarrow j) \left[n_j - n_i + n_j (g^{(j)} - g^{(i)}) \frac{\Phi}{kT} \right]$$

We expect the n_i 's to perform a small sinusoidal variation around n_0 (the equilibrium value in the absence of strain):

$$n_i = n_0 + \delta n_i \exp(i k x - i \omega t) \quad (2.9)$$

where δn_i is assumed to be of order $q^{(i)} \Phi / kT$.

To first order

$$P_i = R(i \rightarrow j) \left[(\delta n_j - \delta n_i) + n_0 (q^{(j)} - q^{(i)}) \frac{\Phi_0}{kT} \right] e^{i(kx - \omega t)} \quad (2.10)$$

We now want to relate $R(i \rightarrow j)$ to R_0 , where R_0 is the probability per unit time for an intervalley transition to occur between any pair of valleys (e.g., i to j or k to l) in the absence of strain.

We assume

$$R(i \rightarrow j) = R_0 \left[1 + \text{order } \frac{q \Phi}{kT} \right]$$

Therefore, to first order, we can replace $R(i \rightarrow j)$ by R_0 in (2.10).

Performing the same manipulations for other two brackets, (2.7) can be written

$$P_i = R_0 \left\{ \begin{aligned} & \left[(\delta n_j - \delta n_i) + n_0 (q^{(j)} - q^{(i)}) \frac{\Phi_0}{kT} \right] \\ & + \left[(\delta n_k - \delta n_i) + n_0 (q^{(k)} - q^{(i)}) \frac{\Phi_0}{kT} \right] \\ & + \left[(\delta n_l - \delta n_i) + n_0 (q^{(l)} - q^{(i)}) \frac{\Phi_0}{kT} \right] \end{aligned} \right\} e^{i(kx - \omega t)}$$

which reduces to

$$P_i = R_0 \left\{ \begin{aligned} & (\delta n_j + \delta n_k + \delta n_l - 3\delta n_i) \\ & + n_0 (q^{(j)} + q^{(k)} + q^{(l)} - 3q^{(i)}) \frac{\Phi_0}{kT} \end{aligned} \right\} e^{i(kx - \omega t)} \quad (2.11)$$

We require that $\sum_{\alpha} \delta n_{\alpha} = 0$ since the total density of electron $n(x) = 4n_0$ does not change. This condition yields

$$\delta n_j + \delta n_k + \delta n_l - 3\delta n_i = -4\delta n_i$$

which is substituted into (2.11). We want to make one further change in (2.11); R_0 was defined as the probability per unit time that an intervalley transition will take place between any pair of valleys, so that the total probability for transitions from i to j , i to k , and i to l will be $3R_0 = R_{iv}$. R_{iv} is therefore the total probability per unit time for an electron to leave a valley. In other words, it is the intervalley scattering rate per electron.

Finally,

$$P_i = \frac{R_{iv}}{3} \left[-4\delta n_i - n_0 (3q^{(j)} - q^{(k)} - q^{(l)}) \frac{\Phi_0}{kT} \right] e^{i(kx - \omega t)} \quad (2.12)$$

For $i = 1$, using the values for the $q^{(\alpha)}$ in Eq. (2.4), we get

$$P_1 = \frac{-4}{3} R_{iv} \left[n_0 (\alpha - \beta) \frac{q \Phi_0}{kT} + \delta n_1 \right] e^{i(kx - \omega t)}$$

This is the form which we want for the P_i 's, and we can now return to the solution of Eqs. (2.5 and 2.6).

The continuity equation becomes

$$\frac{\partial n_1}{\partial t} + \frac{\partial j_1}{\partial x} = -\frac{4}{3} R_{iv} \left[n_0 (\alpha - \beta) \frac{q \Phi_0}{k T} + \delta n_1 \right] e^{i(kx - \omega t)} \quad (2.13)$$

and taking derivative of the current equation

$$\frac{\partial j_1}{\partial x} = ik j_1 = Dk^2 \left[\delta n_1 + n_0 (\alpha - \beta) \frac{q \Phi_0}{k T} \right] e^{i(kx - \omega t)} \quad (2.14)$$

Substituting (2.14) into (2.13) and using $\partial n_1 / \partial t = -i\omega \delta n_1$, we obtain

$$\delta n_1 \left[-i\omega + Dk^2 + \frac{4}{3} R_{iv} \right] = -n_0 \left[Dk^2 + \frac{4}{3} R_{iv} \right] (\alpha - \beta) \frac{q \Phi_0}{k T}$$

We define

$$\frac{1}{\tau_r} = \frac{4}{3} R_{iv} + Dk^2$$

so that

$$\delta n_1 = \frac{-n_0 (\alpha - \beta)}{1 - i\omega \tau_r} \frac{q \Phi_0}{k T}$$

where the total relaxation time τ_r is composed of the intervalley scattering time $1/R_{iv}$ and spatial redistribution time $1/Dk^2$ as previously discussed. $1/Dk^2$ is the time it takes an electron to diffuse a distance equal to a wavelength divided by 2π .

Finally

$$n_1 = n_0 \left[1 - (\alpha - \beta) \frac{q \Phi_0}{kT} \frac{e^{i(kx - \omega t)}}{1 - i\omega \tau_r} \right] \quad (2.15)$$

and in similar fashion

$$n_2 = n_0 \left[1 + (\alpha - \beta) \frac{q \Phi_0}{kT} \frac{e^{i(kx - \omega t)}}{1 - i\omega \tau_r} \right]$$

$$n_3 = n_0 \left[1 - (\alpha + \beta) \frac{q \Phi_0}{kT} \frac{e^{i(kx - \omega t)}}{1 - i\omega \tau_r} \right] \quad (2.15)$$

$$n_4 = n_0 \left[1 + (\alpha + \beta) \frac{q \Phi_0}{kT} \frac{e^{i(kx - \omega t)}}{1 - i\omega \tau_r} \right]$$

To find the average or dc force exerted by the wave on an electron, in i th valley, we find the local force $-q^{(i)} \partial \Phi / \partial X$, weight it with the electron distribution, average over a wavelength, and divide by the average electron distribution:

$$\bar{F}_i = \frac{\frac{1}{2} \operatorname{Re} \left(-q^{(i)} \frac{\partial \Phi}{\partial X} n_i^* \right)}{n_0} \quad (2.16)$$

From (2.4), (2.15) and (2.16) we get

$$\bar{F}_1 = \bar{F}_2 = (\alpha - \beta)^2 \left[\frac{q^2 S}{c^2 kT} \frac{\omega^2 \tau_r}{1 + \omega^2 \tau_r^2} \right] \quad (2.17)$$

and

$$\bar{F}_3 = \bar{F}_4 = (\alpha + \beta)^2 \left[\frac{g^2 S}{c^2 k T} \quad \frac{\omega^2 \tau_r}{1 + \omega^2 \tau_r^2} \right] \quad (2.18)$$

so that \bar{F}_i is the average force exerted by the acoustic wave on the i 'th type of electron and $S = 1/2 \operatorname{Re}(\Phi_0^* \Phi_0)$ is the average acoustic power density.

We now want to find the average electric field which is set up by the shear wave due to electrons being dragged to the back of the crystal. We are working with open circuit conditions, and the force associated with the electric field builds up until it is equal and opposite to the acoustic force, in order to satisfy the condition that there is no net current flow.

To find the average electric field, we first calculate the total short circuit current which would flow under the action of the acoustic wave. The total current j_A is the sum of the currents of the individual valleys, and the conductivity of the i 'th valley for [100] particle motion, averaged over a wavelength, is one-quarter of the total conductivity (see Appendix A).

The current for an individual valley is given by $j^{(i)} = \frac{\bar{\sigma}^{(i)}}{e} \bar{F}_i$; taking the time average of Eq. (2.6), substituting from Eqs. (2.17) and (2.18) with $\bar{\sigma}_i = n_0 D / kT$,

employing
$$j_A = \sum_i j^{(i)} \quad \text{and} \quad \sigma = \sum \sigma^{(i)} = \frac{4n_0 D}{kT}$$

we get

$$j_A = \frac{g}{e} \left[\frac{\bar{F}_1 + \bar{F}_3}{2} \right]$$

This is the total current which would flow under short circuit conditions.

For open circuit conditions, we require that $j_A + j_E = 0$ where $j_E = -\sigma \bar{E}$ is the total current set up by the opposing electric force; which yields

$$\bar{E} = \frac{(\bar{F}_1 + \bar{F}_3)}{2e}$$

or

$$e \bar{E} = \frac{q^2 S}{c^2 k T} \frac{\omega^2 \tau_r}{1 + \omega^2 \tau_r^2} \quad (2.19)$$

This is the result obtained by W.S.W., which we have arrived at with considerably more work. It does however show that the symmetric four-class system gives the same result as the two-class system, and perhaps also justifies the form of P_i which W.S.W. arrived at by intuition. We should also mention that in deriving the form for P_i we kept only the lowest order in $q\Phi/kT$, which, since $e\bar{E}$ was found to be linear in the power under our experimental conditions, is valid.

E. SPACE CHARGE

In order to show how space charge can diminish the acoustoelectric effect, we will calculate the effect for a simple single valley semiconductor (e.g., InSb) first neglecting and then considering space charge.

When we neglect space charge, we get from the current equation

$$j = -D \left[\frac{\partial n}{\partial x} + n \frac{q}{kT} \frac{\partial \Phi}{\partial x} \right]$$

and from the continuity equation

$$\frac{\partial n}{\partial t} + \frac{\partial j}{\partial x} = 0$$

that

$$n = n_0 \left[1 - \frac{q \Phi_0}{kT} \frac{e^{i(kx - \omega t)}}{1 - i\omega \tau_D} \right]$$

where $\tau_D = 1/Dk^2$, the spatial redistribution time, is the only relaxation mechanism available.

$$\overline{F} = \frac{\frac{1}{2} \operatorname{Re} \left(-q \frac{\partial \Phi}{\partial x} n^* \right)}{n_0} = \frac{q^2 S}{c^2 kT} \frac{\omega^2 \tau_D}{1 + \omega^2 \tau_D^2}$$

This is what we would get for n-type germanium if τ_D were much faster than the intervalley scattering time as previously mentioned.

Then

$$\frac{1}{\tau_r} = \frac{4}{3} R_{iv} + \frac{1}{\tau_D} \approx \frac{1}{\tau_D}$$

and when substituted into (2.19) gives the above result.

If we now include space charge, we have also to solve Poisson's equation

$$\frac{\partial^2 V_{sc}}{\partial x^2} = -\frac{4\pi e^2}{K} (n - n_0)$$

where $(n - n_0)$ is the periodic electron density modulation caused by the sound wave. Since n_0 is the equilibrium density of free electrons which is equal to the density of positive donors, this then represents the periodic deviation from charge neutrality. V_{sc} is the space charge potential, and the total electron potential is

$$V_T = V_{sc} + q\Phi \quad ; \quad \begin{aligned} V_T &= V_T(x - ct) \\ V_{sc} &= V_{sc}(x - ct) \end{aligned}$$

Again solving the current equation

$$j = -D \left[\frac{\partial n}{\partial x} + \frac{n}{kT} \left(q \frac{\partial \Phi}{\partial x} + \frac{\partial V_{sc}}{\partial x} \right) \right]$$

and continuity equation, we get for the instantaneous electron distribution

$$n = n_0 \left[1 - \frac{q\Phi_0}{kT} \frac{e^{i(kx - \omega t)}}{1 + \left(\frac{\lambda}{L_D}\right)^2 - i\omega\tau_D} \right]$$

where $\lambda = 1/k$ is the acoustic wavelength divided by 2π , and L_D is the Debye length

$$L_D = \left[\frac{\kappa \kappa^T}{4\pi n_0 e^2} \right]^{\frac{1}{2}}$$

The total electron potential is then

$$V_T = \frac{q \bar{\Phi}_0 (1 - i\omega \tau_D)}{1 + \left(\frac{\lambda}{L_D}\right)^2 - i\omega \tau_D} e^{i(\kappa x - \omega t)}$$

and

$$\bar{F} = \frac{1}{2} \operatorname{Re} \left(-\frac{\partial V_T}{\partial x} n^* \right) = \frac{q^2 S}{c^2 \kappa^T} \frac{\omega^2 \tau_D}{\left[1 + \left(\frac{\lambda}{L_D}\right)^2 \right]^2 + \omega^2 \tau_D^2}$$

Now, at 60 mc/sec

$$\left(\frac{\lambda}{L_D}\right)^2 \approx 10^2 \text{ to } 10^5$$

depending on temperature and doping and

$$\omega^2 \tau_D^2 < 1$$

so that space charge effects drastically reduces the acoustoelectric effect.

The reason for this is that for

$$\left(\frac{\lambda}{L_D}\right)^2 \gg 1$$

$$V_{sc} \approx -q \bar{\Phi}$$

and the total electron potential approaches zero. Physically, the

Debye length is the distance over which one can maintain a nonuniform potential. If this distance is small compared to a wavelength, enough electrons instantaneously regroup in such a manner as to screen the deformation potential. The total potential approaches a uniform value, and consequently there is no force on the remaining electrons. This regrouping takes place via transport in an electron field characterized by the dielectric relaxation time $\kappa/4\pi\sigma$. Potential and space charge inequalities are damped out in a dielectric relaxation time, which is very short compared to the period of the wave.

F. ATTENUATION AND RADIATION PRESSURE (16)

The attenuation of the ultrasonic wave due to the interaction with conduction electrons will be equal to the average rate that the wave loses energy to an electron times the total number of electrons. The average rate at which the wave loses energy to the i th type of electron is

$$\frac{\overline{dW}_i}{\overline{dt}} = \frac{1}{2} \operatorname{Re} \left(\frac{F_i j_i^* - q^{(i)} \Phi \left(\frac{\partial n_i^*}{\partial t} + \frac{\partial j_i^*}{\partial x} \right)}{n_0} \right)$$

The first term is the local force $F_i = -q^{(i)} \partial\Phi/\partial X$ times the local current which is the ordinary Joule heat loss. The second term is the energy lost to disappearing particles. Since all quantities go as $\exp(ikx - i\omega t)$

$$\frac{d\bar{W}_i}{dt} = \frac{\frac{1}{2} \operatorname{Re} \left(-c\omega g^{(i)} \Phi n_i^* \right)}{n_0}$$

or

$$\frac{d\bar{W}_i}{dt} = \frac{c \left(-g^{(i)} \frac{\partial \Phi}{\partial x} n_i^* \right)}{n_0} = c \bar{F}_i$$

which is c times the average momentum loss (acoustoelectric force) to the i 'th type particle. Averaging over all valleys, and multiplying by the total number of electrons, gives $(4n_0)c\bar{F} = N_0c\bar{F}$. $4n_0 = N_0$ is density of electrons cm^{-3} , and \bar{F} is the average acoustoelectric force. Thus the attenuation due to the free carriers per unit power density is

$$\alpha = \frac{N_0 c \bar{F}}{S} \left(\frac{\text{nepers}}{\text{cm}} \right) = \frac{N_0 c e \bar{E}}{S}$$

where S is power density.

For typical values, we have

$$\begin{aligned} N_0 &\approx 10^{15} \text{ cm}^{-3} & S &\approx 1 \frac{\text{watt}}{\text{cm}^2} \\ c &\approx 3 \times 10^5 \frac{\text{cm}}{\text{sec}} & \bar{E} &\approx 25 \frac{\text{mV}}{\text{cm}} \end{aligned}$$

So that

$$\alpha \approx 1.5 \times 10^{-3} \frac{\text{nepers}}{\text{cm}} \approx 2 \times 10^{-4} \frac{\text{dB}}{\text{cm}}$$

and a logarithmic decrement of

$$\delta = \alpha \lambda \approx 7.5 \times 10^{-6} \quad \text{at } 60 \text{ MC}$$

The attenuation in the acoustic power over the length of 5 cm due to free electrons will be

$$S = S_0 e^{-\alpha x} \approx .99 S_0$$

The power density at the far end of the crystal is still 99% of its original value. This represents a negligible loss for our purposes.

Radiation Pressure

The acoustoelectric effect is the result of the loss of momentum by the wave to the electrons. This momentum transfer is directed along the direction of propagation of the wave, and is the average force (i.e., the acoustoelectric force) exerted by the wave on an absorber (i.e., a free electron). In analogy to electromagnetic waves, we can say that the wave exerts a radiation pressure on an absorber which is simply the acoustoelectric force.

CHAPTER III

EXPERIMENTAL EQUIPMENT AND PROCEDURE

A. GENERAL

The experimental arrangement used here is similar to that previously used by W.S.W.

The acoustic wave is generated by driving a quartz transducer, usually at 60 mc, which is acoustically coupled to the germanium. The wave is absorbed at the far end of the crystal (approximately 5 cm long) by means of an indium absorber, and a voltage is set up along the crystal. The acoustoelectric voltage is in principle dc, but the rf was amplitude modulated in order to produce an audio component (Appendix B). Aside from the fact that small audio voltages are easier to amplify and detect than dc, the reason for audio is that a thermal gradient of a few hundredths of a degree Kelvin per cm will produce a dc thermoelectric voltage which is often comparable to or larger than the acoustoelectric voltage. Gradients of this order exist even in the absence of acoustic power, and in our method of acoustic power measurement (see below), thermal gradients of several tenths of a degree Kelvin are produced.

The audio component of the acoustoelectric voltage is measured at three contacts along the crystal spaced about 1 cm apart. The dc thermoelectric voltage, produced by the dissipation of the

acoustic energy in the absorber, is measured at the same contacts as the acoustoelectric voltage.

The rf driving the quartz transducer was around 20 v, which produced an acoustic power density of around 0.5 w/cm^2 . Depending on the temperature and the resistivity of the germanium, the acoustoelectric voltage ranged from less than $1 \text{ } \mu\text{v/cm}$ to over $100 \text{ } \mu\text{v/cm}$, usually being less than $20 \text{ } \mu\text{v/cm}$. The main experimental problems were eliminating pickup and producing good crystals. The rf can easily be picked up and demodulated at metal-semiconductor contacts or at circuit nonlinearities such as the input stages of the low level amplifier, which when overdriven produce a large spurious signals at the audiofrequency. To prevent this required special sample and sample holder design, ohmic metal-to-semiconductor contacts down to the lowest temperatures used, doubly shielded cables, careful grounding, etc. The test used for checking the pickup level was to replace the transducer by a piece of mica of equivalent size and thickness. Since the impedance of a heavily loaded quartz crystal is approximately its geometrical capacitance, the mica reproduces the rf configuration without producing any acoustoelectric voltage. On all crystals on which final data were taken, the total spurious signal at liquid nitrogen temperature was slightly less than $1 \text{ } \mu\text{v}$, which means a 1:1 signal to noise ratio at 110 to 120°K. This is the reason for discontinuing the experiment at 100°K, and for less consistency in the data at high temperatures.

B. SAMPLES AND TRANSDUCER

Final data were taken on five different resistivity samples of antimony-doped germanium. The resistivity range was 0.2 ohm-cm with $8.3 \times 10^{15} \text{ cm}^{-3}$ donors to 10 ohm-cm with $1.5 \times 10^{14} \text{ cm}^{-3}$ donors.

The single crystals were doped and grown in a [100] direction by the Western Electric Company. They were grown from intrinsic raw material with unknown contamination levels of about 10^{13} cm^{-3} (quite possibly arsenic) which is probably as good as can be achieved without special efforts. All crystals were then doped only with antimony to the final donor concentration.

The front face, or driving end of each crystal, was oriented in a [100] direction by standard Back Laue Reflection Techniques (17, Chap. 8), since a crystal grown in a [100] direction can be several degrees off axis. Two crystals were oriented with all faces in a [100] direction, and one was oriented with the side faces in [011] directions, in order to check on the independence on orientation of the side faces. The final dimensions of the crystals were approximately 0.54 cm by 0.54 cm and 4.5 to 5 cm long. The samples were not etched, and the final lapping was 400 Carborundum grit ($\approx 35 \mu$).

Achieving low resistance ground contacts and ohmic signal contacts was of utmost importance in this experiment. This is necessitated by the fact that the ground contact serves as a return path to ground for the rf current which drives the transducer. Any current

which flows through the crystal produces an rf voltage which can be demodulated by non-ohmic contacts. Furthermore, rf chokes were placed on the sample holder, close to the signal contacts, in order to present a high impedance to the rf.

A layer of gold containing 0.6% antimony about $10,000\text{\AA}$ thick was deposited on the germanium in a high vacuum evaporator. A mask covered the germanium so that only the ground contact and the signal contacts were exposed. The gold-antimony combination is then alloyed to the germanium by heating in a carbon boat to approximately 425°C , a temperature between the gold-germanium eutectic point and the temperature where copper contamination of the germanium becomes serious. (Copper in germanium is a deep lying acceptor which can compensate up to three donors (i.e., trap three electrons). It diffuses rapidly into germanium at temperatures above 500°C , so that the resistivity of n-type germanium can be appreciably increased (18).) This temperature was maintained for several minutes, and then slowly lowered, in order to achieve a semiequilibrium process which results in uniform regrowth layers. The indium absorber is then soldered on the back end of the crystal, and finally a fresh layer of gold is evaporated onto the ground and signal contacts. A heater, in the form of a miniature 1 K resistor, is thermally anchored to the absorber. Copper wires (0.004 in.) were attached to the signal contacts with air drying silver paste. (See Fig. 4.)

The presence of the antimony serves to give a high donor con-

centration at the surface, which along with a relatively rough surface, greatly diminishes hole injection, and helps produce ohmic contacts (19, Chap. 14). The fresh layer of gold on top of the alloyed layer gives a low contact resistance. The contacts were ohmic up to a minimum current of 40 ma at liquid nitrogen temperature.

In preliminary work, large differences in acoustoelectric voltage occurred between the upper and lower sections of the crystal. That is, the voltage measured between the top and middle contact could be 50% larger than the corresponding voltage between the middle and bottom contacts. It was finally discovered that this discrepancy was due to imperfect contact between the indium and the germanium, caused by an oxidizing film which formed during soldering. The discrepancy became greater at lower temperatures, because of different thermal expansion rates of the two materials. This was probably due to a nonuniform absorption of the acoustic wave, which altered the acoustoelectric field in an irregular manner. Final data were taken on crystals where the discrepancy was less than 10%, and usually less than 5%.

The quartz transducers were Y cut to operate in a fundamental shear mode of 20 mc. They were usually operated in their third harmonic. The dimensions were 0.51 cm x 0.51 cm and 0.01 cm thick. The acoustic bond between the quartz and the germanium was made by a thin layer of Nonaq stopcock grease, which solidifies near 200°K. It pro-

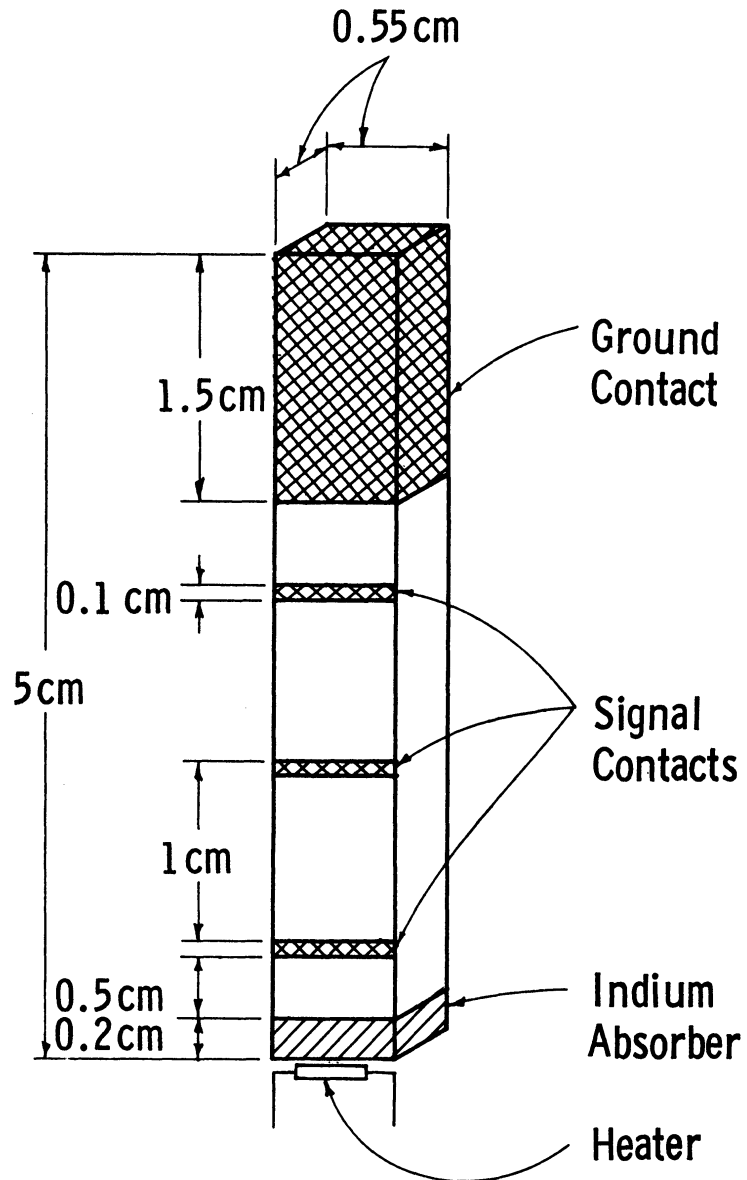


Fig. 4. Typical germanium sample.

vided good shear wave coupling over our entire temperature range.

The side of the transducer facing away from the germanium was plated with a thin layer of gold in order to produce a uniform charge distribution and uniform excitation. The transducer was held against the germanium by a brass plug on a spring loaded teflon plunger.

C. SAMPLE HOLDER

The samples were held in a two-chamber copper enclosure, to which was attached a copper can containing charcoal. (see Figs. 5 and 6.) The holder was suspended into a conventional double Dewar system by a stainless steel tube of 0.5 in. O.D. and 30 cm long. The tube also served as the outer conductor for the rf input, the inner conductor being a tightly stretched .008 in. copper wire. The tube was attached to the sample holder by means of a BNC connector. The massive copper sample holder and charcoal-filled can gave the system good thermal stability.

The two-chamber construction was designed in order to shield the signal leads from the rf at the driving end. The germanium crystals were held in cantilever fashion at the ground contact, securely locked into the notch between the two chambers with a corrugated phosphor-bronze spring. This provided good electrical and thermal contact between the germanium and the holder. The fact that the crystal was thermally isolated, except at the ground contact, enabled the absorbed power to produce a thermal gradient along the crystal (approximately

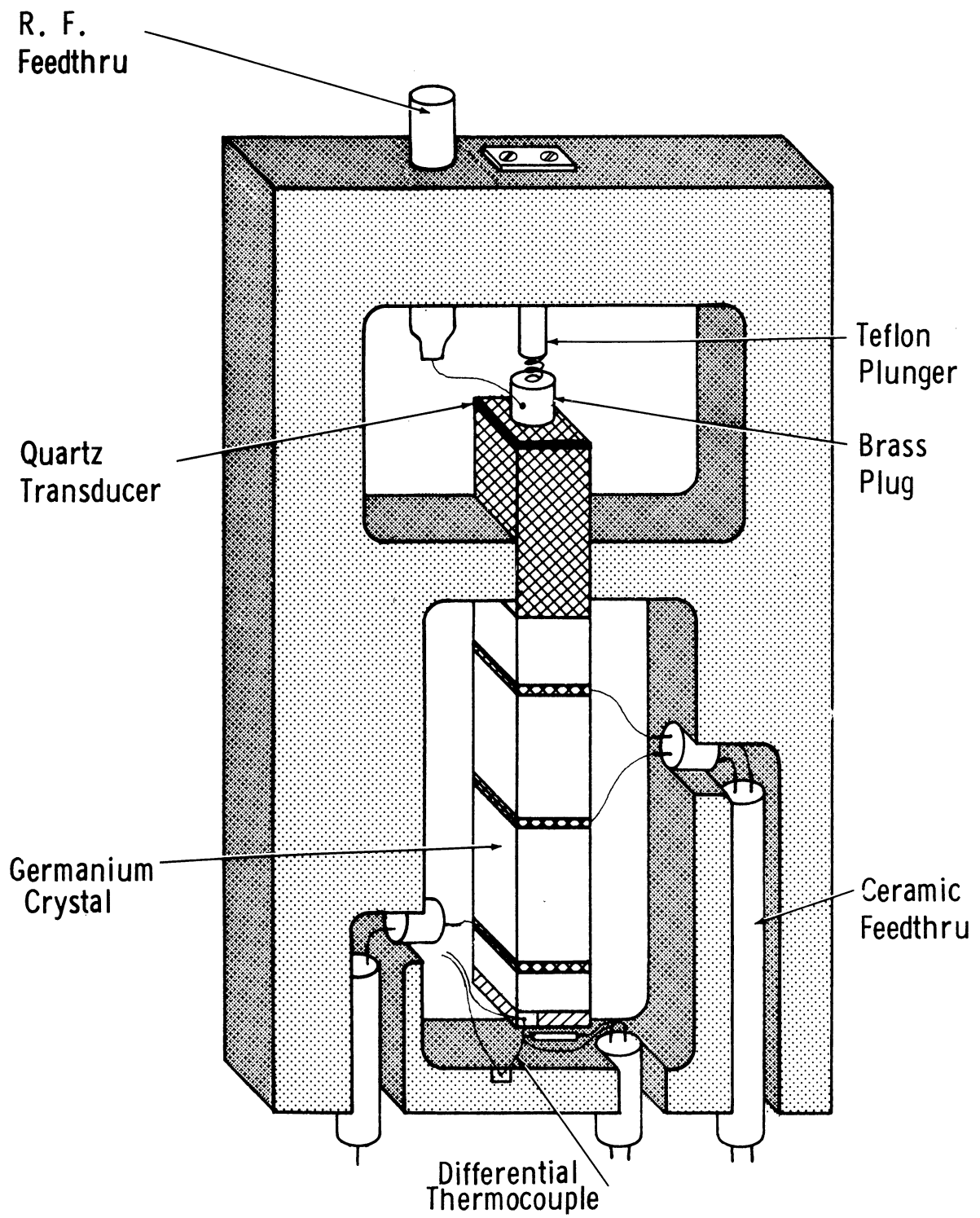


Fig. 5. Sample holder with mounted crystal.

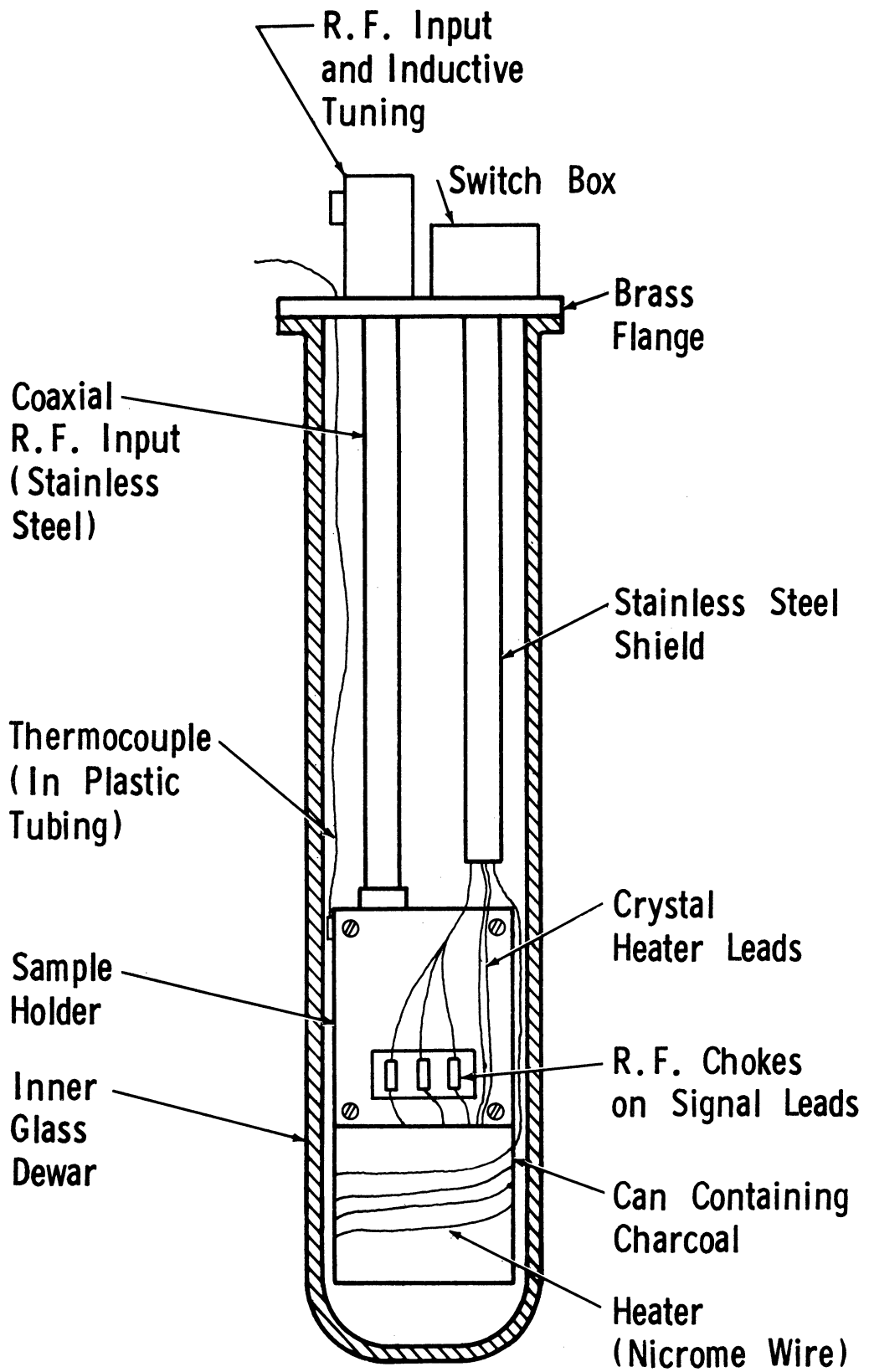


Fig. 6. Layout of Dewar.

0.3°K/cm), which was necessary for our method of power measurements.

All signal leads and heater leads were 0.004 in. or 0.005 in. copper wire in order to minimize heat leaks. They were brought out of the Dewar by means of a second stainless steel tube. Two copper-constantan thermocouples were used; one to measure the temperature of the sample holder, and the other to measure the temperature differences between the crystal and the holder. The first thermocouple, which measured the absolute temperature, consisted of three constantan wires in parallel and one copper wire. It was firmly secured to the sample holder in a position where it was free from mechanical disturbances, and was calibrated several times, in situ, at the boiling points of liquid helium (4.2°K), liquid nitrogen (77.4°K), and liquid oxygen (90.2°K). The extra constantan wires and the freedom from mechanical disturbances were necessary in order to cut down inhomogenieties and possible crimping or stresses which would change the thermocouple calibration (20, p 134). It was calibrated in place in order to reproduce the thermal gradients that would exist in practice, and was recalibrated several times during the course of the experiment. Only minor adjustments were necessary after each recalibration. The temperature was interpolated between calibration points by means of a table prepared by the National Bureau of Standards (21).

The second thermocouple was of the differential type. A constantan wire was thermally anchored to but electrically insulated from both the absorber and the sample holder by means of nail polish and

cigarette paper. A 0.003 in. copper wire was soldered to each end of the constantan. This enabled us to measure the total temperature difference between the crystal and sample holder due both to the heating caused by the absorbed power and to the finite thermal resistance at the ground contact.

Helium was used as the refrigerant in the temperature range of 10° to 80°K. Nitrogen was used from 70°K* to 120°K. The system had good thermal stability and could stay within 0.5°K of any desired temperature for the two or three minutes necessary for data taking. The temperature was raised by means of a heater wound around the charcoal-filled can.

D. ELECTRICAL EQUIPMENT

The block diagram of the electrical equipment is shown in Fig. 7. An rf oscillator, of the plate coupled Hartley type, drives a tuned power amplifier which is plate modulated at 10 kc. The rf unit would work at either 60 mc or 20 mc by changing the inductors in the tuned circuits. The final tank circuit was inductively coupled to a short output cable. Since the cables and transducer present a capacitive load, a small variable inductor, placed on the flange on the Dewar, was used to tune for maximum power transfer. Another pickup coil was connected directly to the plates of a Dumont oscilloscope in order to measure and monitor the modulation percentage.

The signal leads are used both for the acoustoelectric voltage

*obtained by pumping on the nitrogen

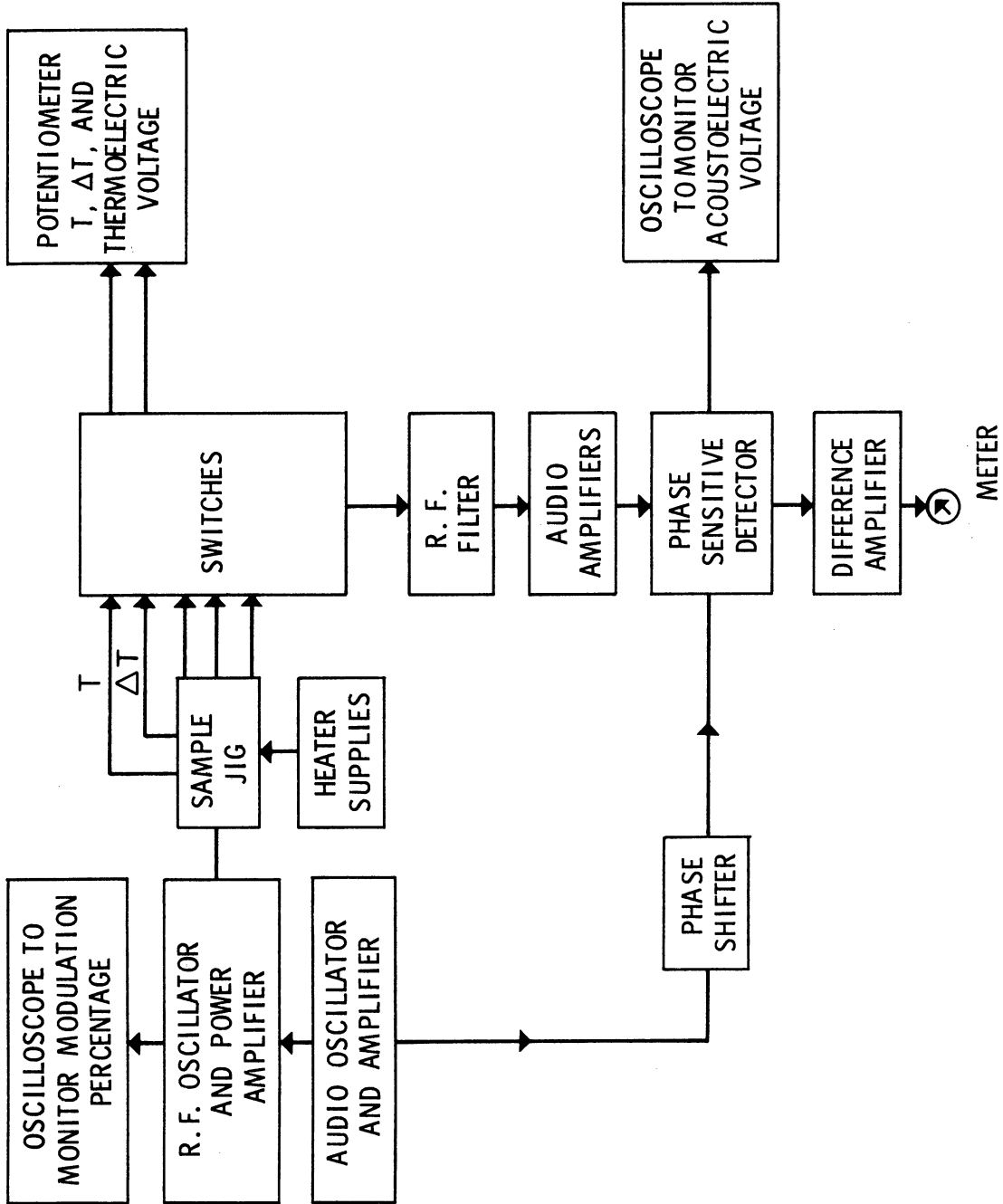


Fig. 7. Block diagram of electrical system.

and thermoelectric voltage, and provision was made for switching between them. When used for acoustoelectric voltage, the leads go to a type 122A Tektronix amplifier (maximum gain of 1000) used in differential gain position. This automatically gives the voltage between any two contacts, and subtracts out any pickup common to both. It then goes to a transistor amplifier (maximum gain of four), and an emitter follower which drives a phase sensitive detector. The output of the detector goes to a difference amplifier, used as a voltmeter, which serves as the output indicator. The maximum sensitivity of the system was $0.5 \mu\text{v}$. The signal leads, when used to measure thermoelectric voltages, are connected pairwise to a Rubicon type B precision potentiometer. The same potentiometer is used to measure the temperature and the differential temperature through another set of switches.

E. EXPERIMENTAL PROCEDURE

Data were taken in the temperature range of 10°K to 120°K . A convenient modulation percentage was chosen depending on the amount of power absorbed and the magnitude of the acoustoelectric signal. When running the two high resistivity crystals, it was necessary to change the amplification factor several times in the temperature range of 10°K to 80°K .

The procedure used in taking data was to stabilize the system at a particular temperature, measure the temperature, the acousto-

electric voltage between the three sets of terminals, and the thermoelectric voltage due to the absorbed power alternating between the top and middle contacts and the middle and bottom contacts. The rf was then unplugged, and the thermoelectric voltage was reproduced by running dc through the miniature resistor anchored to the absorber. Knowing the voltage and current through the resistor, gave directly the absorbed acoustic power. The temperature was remeasured, the dc turned off and the rf was reconnected. After allowing the system to return to equilibrium, the differential temperature was measured. (It was usually around 1° or 2°K .) The temperature was then raised 2 or 3°K by the heater on the copper can, the heater was turned down, and the system allowed to stabilize at the new temperature.

The modulation percentage was measured approximately every ten degrees, by photographing the modulation trapezoid with a Polaroid scope camera. Amplification factors were measured before and after each run, and the phase sensitive detector was calibrated after each run.

F. RESISTIVITY MEASUREMENT

The resistivity of each crystal was measured between 10°K and room temperature in order to find the number of ionized and neutral donors at each temperature. The method used was a standard one for measuring resistivity of semiconductors and insulators (22, p 34).

Direct current of 100 to 500 ma, depending on the resistivity

of the crystals, was run between the absorber and the ground contact, both of which served as equipotential surfaces. The voltage was measured between the same contacts as the acoustoelectric voltage, and the standard formula $\rho = \frac{V}{I} \frac{A}{L}$ gave the resistivity. A potentiometer was used to measure the voltage in order to eliminate the effect of contact resistance. The effect of thermal gradients due to the crystal hanging in the cantilever manner were corrected for by using both current polarities, or by measuring the voltage with and without current. Joule heating of the crystal represented a negligible error.

The mobility of n germanium as a function of temperature and resistivity is known from the work of Debye and Conwell (23). Since $\frac{1}{\rho} = ne\mu$, we have the number of free electrons which are equal to the number of ionized donors at each temperature. The number of neutral donors is the saturation donor concentration minus the number of ionized donors.

CHAPTER IV

RESULTS

A. REDUCTION OF THE DATA

The intervalley scattering rate is calculated for each crystal as a function of temperature from the observed audio component of the acoustoelectric voltage (see Appendix A). All quantities except R_{iv} in the formula for the acoustoelectric voltage (2.19) are either previously known (q and Dk^{2*}) or are measured (power, modulation percentage, frequency, etc.). This then determines the absolute value for R_{iv} since

$$\frac{1}{\epsilon_r} = \frac{4}{3} R_{iv} + Dk^2$$

The intervalley scattering rate R_{iv} is plotted as a function of temperature for five antimony-doped germanium crystals in Fig. 8. The data was fit by attributing the intervalley scattering rate to phonons and to impurities. It is seen from the data that all rates approach a common line at higher temperatures, particularly the purer crystals. This is the phonon line previously found by W.S.W. At low temperatures, the rates for different crystals are distinctly different since impurity effects dominate. It is impossible to fit the data in this range without attributing the rate to both ionized

*D is known from mobility data (23).

and neutral impurities. Following W.S.W.

$$R_{iv}(T) = R_{\text{phonons}}(T) + R_{\text{ionized donors}}(T) + R_{\text{neutral donors}}(T) \quad (4.1)$$

The total intervalley scattering rate is due to three independent rates, and

$$R_{\text{ionized donors}}(T) = N_+(T) \langle G_I v \rangle = N_+(T) A(T) \quad (4.2)$$

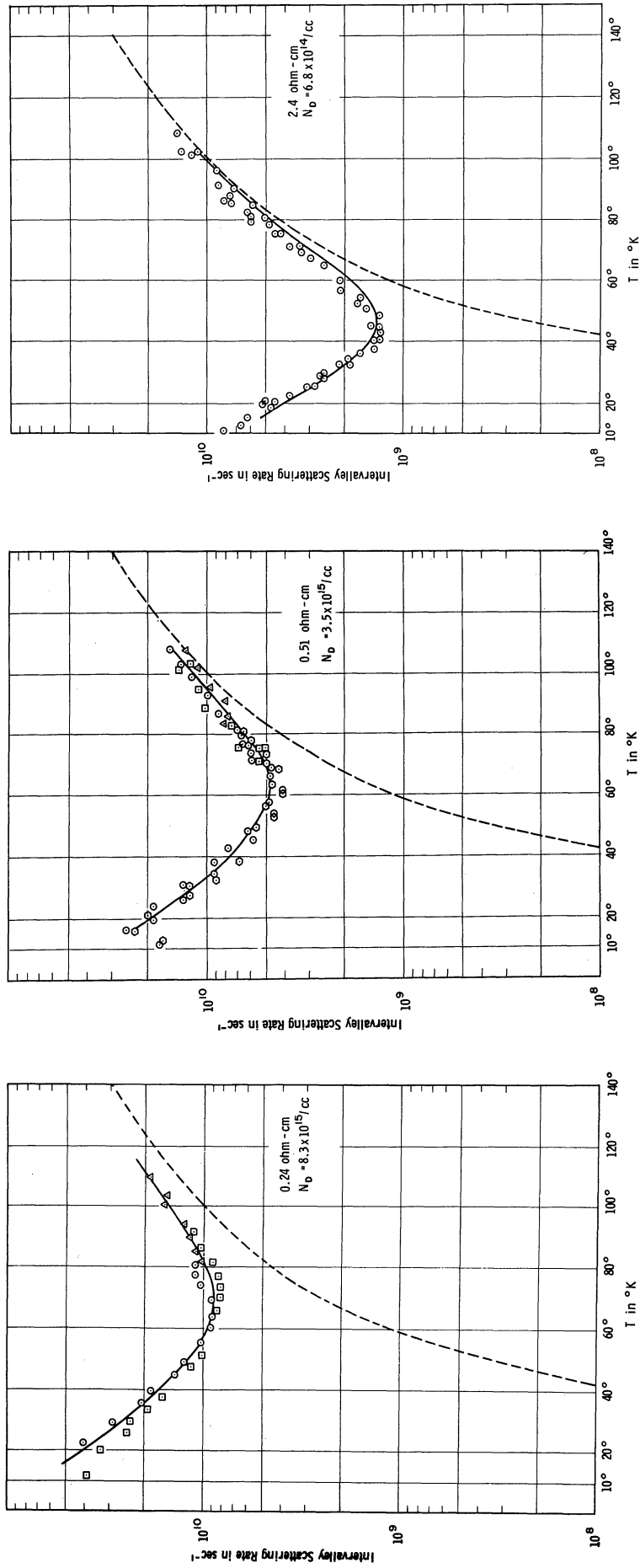
$$R_{\text{neutral donors}}(T) = N_0(T) \langle G_N v \rangle = N_0(T) B(T) \quad (4.3)$$

where N_+ and N_0 are the densities of ionized and neutral donors for a particular crystal at the temperature T . See Fig. 9. $A(T)$ and $B(T)$ are the intervalley scattering rates per electron per ionized and per neutral donor. They are equal to the Boltzman average of an effective cross section times a velocity.

The phonon curve was previously determined, and agrees well with the high temperature data in this experiment. We have, therefore, subtracted off the phonon contribution from the total rate.

$$R_{\text{impurities}}(T) = R_{iv}(T) - R_{\text{phonon}}(T) \quad (4.4)$$

The impurity rates R_{imp} were fit for the five crystals with the two parameters $A(T)$ and $B(T)$ by the method of least squares. The fit was performed in order to give the least percentage error



The dashed lines are the phonon contribution. The solid lines are the results of the least squares fit. N_D is the total donor concentration which is equal to $N^+ + N_0$.

Fig. 8. Intervalley scattering rates as a function of temperature for antimony-doped germanium.

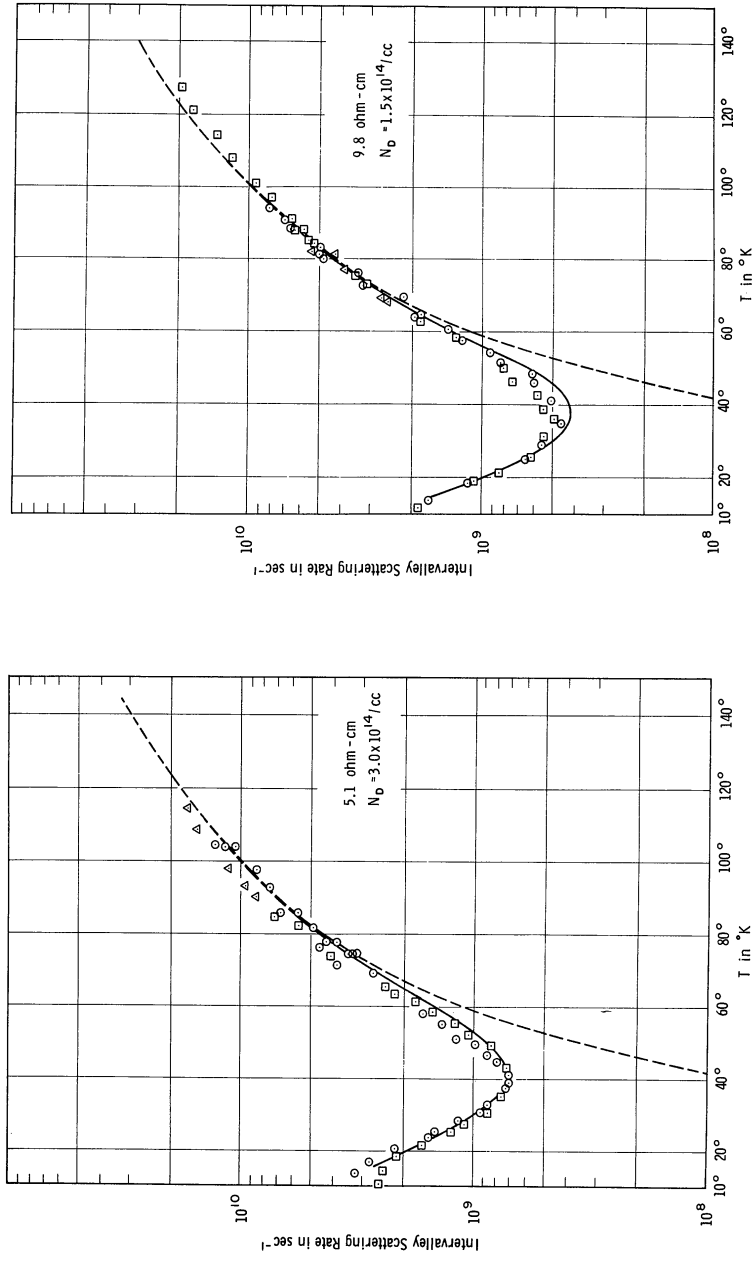


Fig. 8. (Concluded)

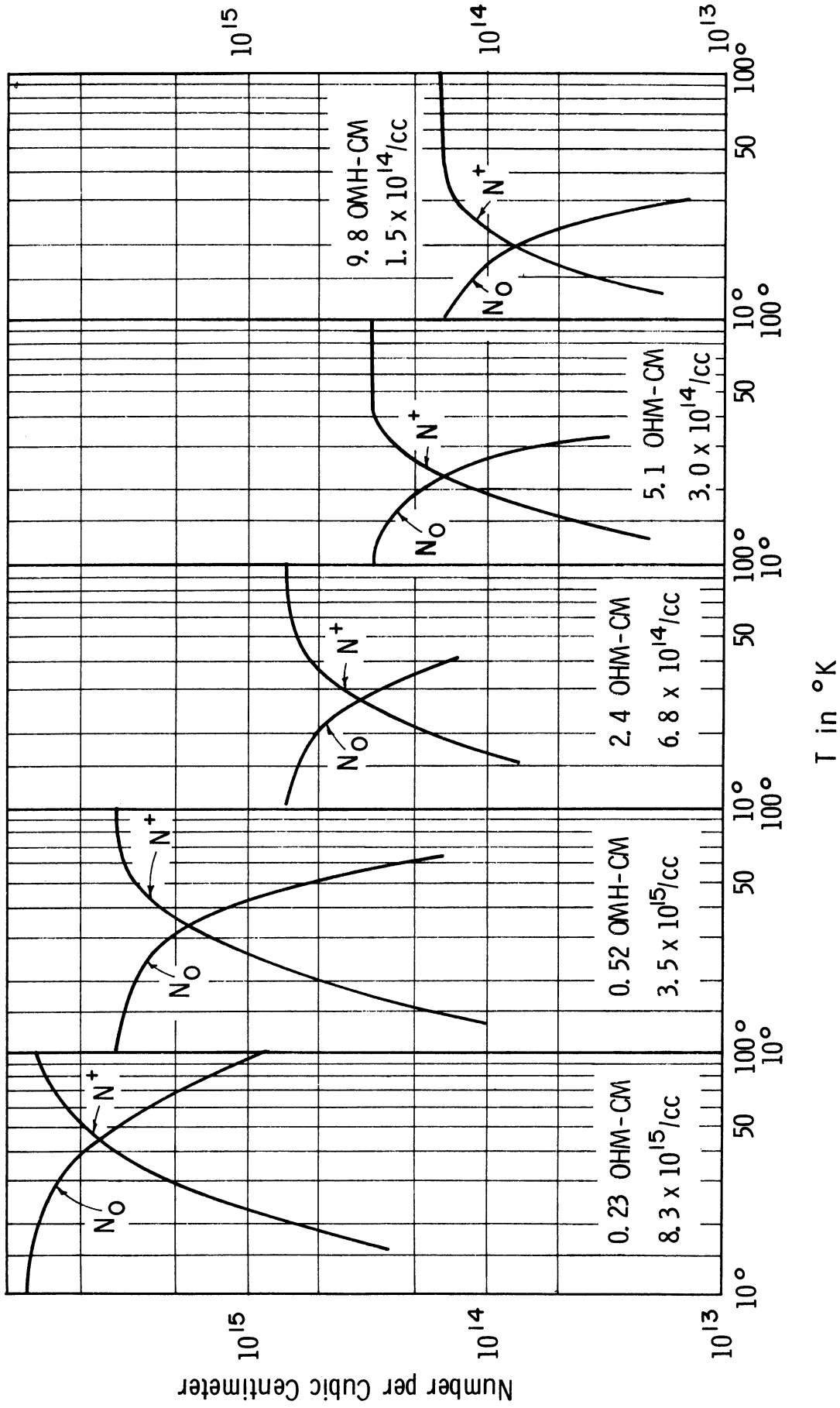


Fig. 9. Ionized and neutral donor concentrations as a function of temperature.

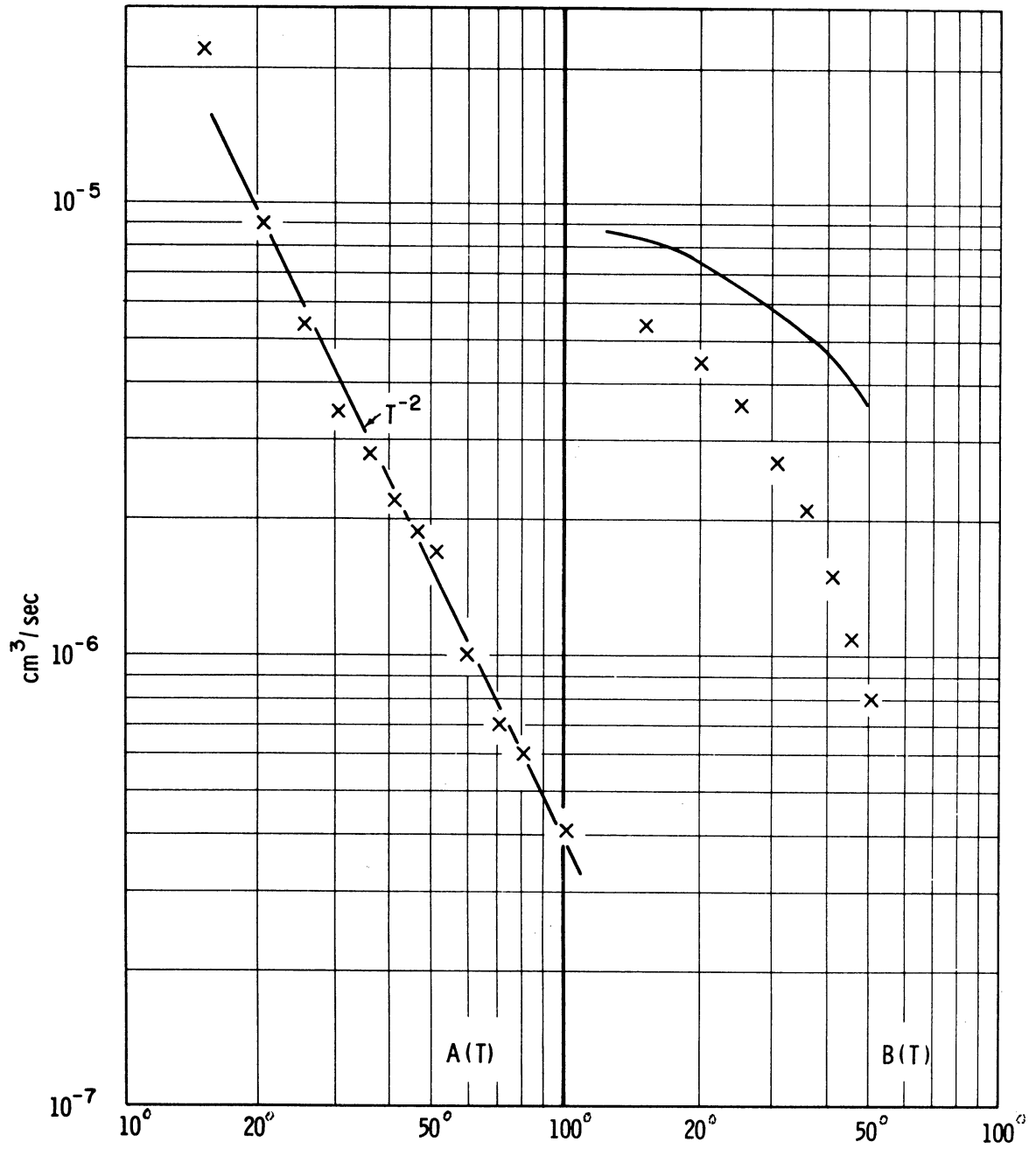
in each crystal. This was done by weighting all crystals equally, and by normalizing the impurity contribution to the intervalley scattering rate. The normalization was necessary in order to give equal weight to crystals whose rates at certain temperatures differed by a factor of 50. The results of the least squares fit are shown in Fig. 8 as the solid lines and in Fig. 10 as the \underline{x} 's.

The check that we used for impurity concentrations was to calculate $\frac{N_+^2}{N_0}$ from our measured values for N_+ and N_0 (Chap. III, Sec. F and Fig. 9). It can be shown (with obvious modifications in the derivation of (24, p 30)) that $\frac{N_+^2}{N_0} = N_c e^{-\frac{E_0}{kT}}$ where $N_c = \left(\frac{m^*kT}{2\pi\hbar^2}\right)^{3/2}$ is an effective density of states in the conduction band, and E_0 the donor ionization energy. Since $\frac{N_+^2}{N_0}$ is independent of doping, the consistency of the impurity concentrations can be checked. The consistency was good, the only disagreement being in the 0.5 ohm-cm crystal. A shift of the order of 5% in the number of ionized and neutral donors at each temperature would bring this crystal into agreement.

Furthermore, the slope of

$$\frac{\ln \left(\frac{N_+^2 T^{-3/2}}{N_0} \right)}{T^{-1}} \text{ is } - \frac{E_0}{k}$$

This gives us a check on possible contamination or compensation of the crystals, since E_0 for antimony in germanium is known to be 9.6 mev. $\frac{N_+^2}{N_0} T^{-3/2}$ is plotted against $\frac{1}{T}$ in Fig. 11, where we have aver-



$A(T)$ is the intervalley scattering rate per ionized antimony donor and $B(T)$ per neutral antimony donor. The solid line for $B(T)$ represents the theoretical fit. (See p 113.)

Fig. 10. $A(T)$ and $B(T)$ for antimony-doped germanium.

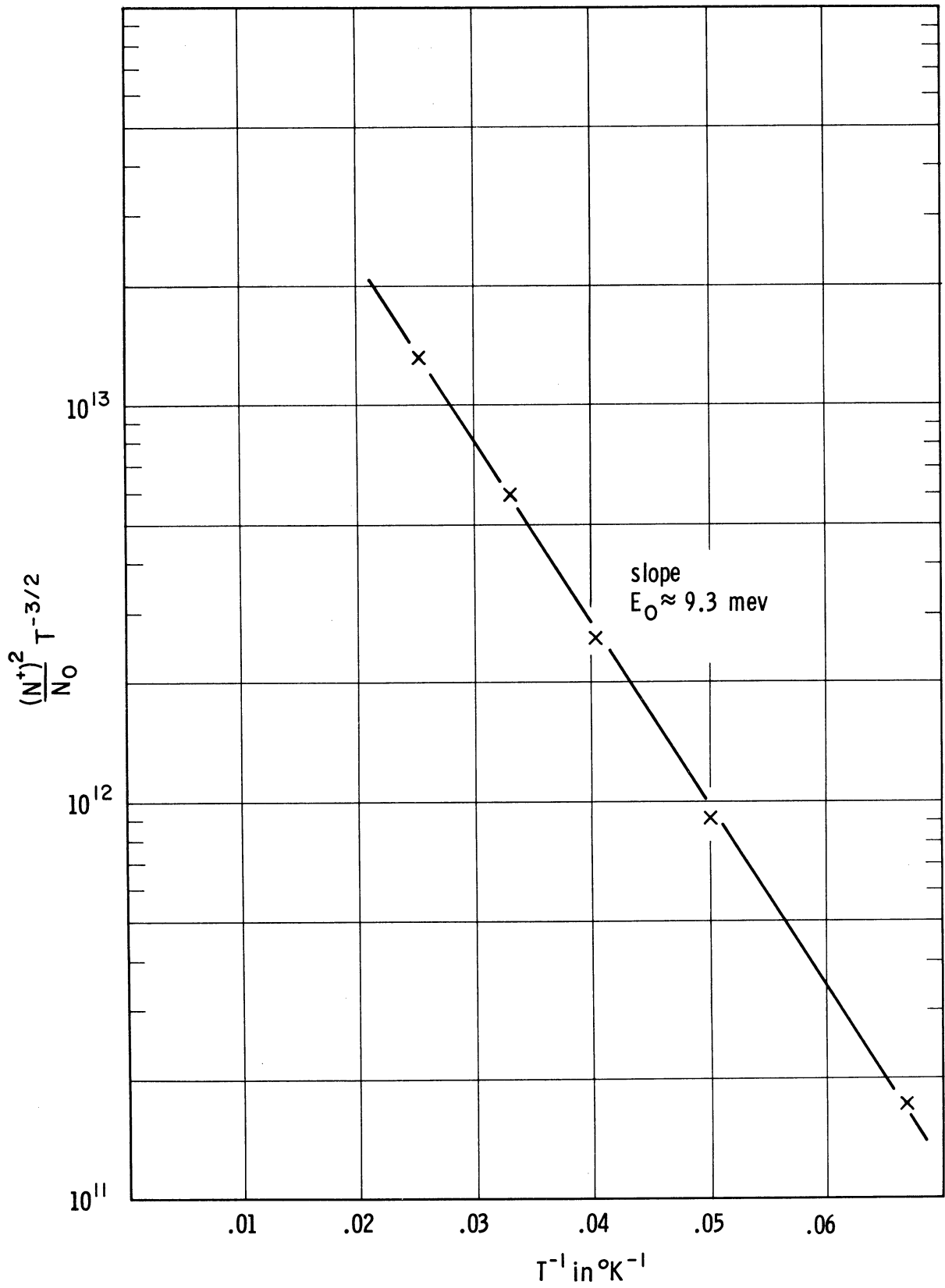


Fig. 11. Plot of $\frac{(N^+)^2}{N_0} T^{-3/2}$.

aged $\frac{N_+^2}{N_0}$ over all crystals. A least squares fit to a straight line gives $E_0 = 9.3$ mev. The value of N_c obtained was consistent with an effective mass equal to $\approx 0.23 m_0$.

B. ESTIMATES OF ERROR

The quantities needed for the absolute measurement of the intervalley scattering rate are modulation percentage, absorbed power, radio frequency, amplification factors, sensitivity of phase sensitive detector, area of crystal, and the temperature. The error in these quantities we believe to be random.

There is the possibility of systematic errors such as pickup, electrical leakage, heat leakage, reverse heating, distance between contacts, imperfect absorption of the sound wave, acoustic beam spreading, and ultrasonic attenuation. There is also the possibility of error in determining the number of ionized and neutral donors at each temperature. These errors will be discussed below.

The two parameters $A(T)$ and $B(T)$ could have been determined from two crystals with donor concentrations differing by a factor of two or three. We have fit five crystals with donor concentrations differing by more than a factor of 50. The internal consistency of these crystals (the percentage deviation of the average experimental value from the least squares fit) is within 10%. This means that despite the large number of quantities needed (few of which can be measured better than 5%) the random errors give an overall statisti-

cal error of less than 10%.

The major possibilities of serious error would be systematic errors such as reverse heating, heat leakage, and beam spreading which could give an almost constant percentage error in the measured intervalley rate for each crystal. These would not affect either the internal consistency or the reproducibility of the data, since they would shift the parameters $A(T)$ and $B(T)$ by this percentage. The possibility of a major error due to something of this nature should be small.

We will now try to explain the reasons for our confidence in the data. The data for each crystal is a conglomeration of data from several separate runs. Usually, the crystal was entirely remade before the second helium run. That is, the old leads, ground contact, and absorber were removed, and new ones were attached. Various runs were made with power densities and modulation percentages differing by almost a factor of two. Final data was taken over a several month period during which the amplifiers and phase sensitive detector were calibrated many times, and the thermocouple calibration checked three or four times. The thermocouple calibration is believed accurate to $\pm 1^\circ\text{K}$. The reproducibility of data for a particular crystal was always within 15%.

One possible systematic error is the measurement of the distance between contacts. The contacts were slightly less than 1 mm wide,

and the distance between centers was about 1.2 cm. The length that we used was the distance between centers rather than the closest distance between contacts. Room temperature resistivity measurements using the distance between centers agreed to within 3 or 4% of the average resistivity quoted by the Western Electric Company. The resistivity was measured both before and after heating the crystal to attach the leads. This gave us another check for possible contamination, and no significant disagreement occurred. The distance between centers could be measured to about 0.05 cm out of approximately 1.2 cm. We would not expect an error of over 5% due to this factor.

Several of the systematic errors are believed to be somewhat random. That is, they would differ from run to run, and would have different effects for different crystals and at different temperatures. Pickup, both external and due to rectification at metal-semiconductor contacts, is of this nature. Pickup of either type would be considerably more serious for the 0.2 ohm-cm crystal than for the 10 ohm-cm, since the maximum observed signal for the 0.2 ohm-cm was about 6 $\mu\text{v}/\text{cm}$ and for the 10 ohm-cm it was as high as 150 $\mu\text{v}/\text{cm}$ near 20°K. If pickup were significant in the 15° to 100°K range, one would expect a considerably worse internal consistency.

Nonuniform acoustic absorption would also be of this type. Remaking the crystals, and resoldering the absorbers would tend to show

if there was any serious discrepancy due to nonuniform absorption or rectification. If nonuniform absorption were a serious factor, it should show up in poor reproducibility of data taken before and after remaking the crystal and in the internal consistency between crystals.

Another error of this form is electrical leakage. Surface leakage can be minimized by initially cleaning the crystals well, and keeping them clean. Leakage was considered negligible except in the region below 15°K , where it may have been a factor in the poor internal consistency and reproducibility.

The above "random" systematic errors would also tend to show up in discrepancies between the two sections of the crystals. Requiring the intervalley scattering rates measured between the top and middle contacts and the middle and bottom contacts to agree within several percent further eliminates serious errors.

Pickup was the major problem above 80°K , since the level could not be reduced much below $1\mu\text{v}/\text{cm}$. This is the reason for more scatter in the high temperature data, and for discontinuing the experiment at 100°K .

We would expect a total error due to these causes to be around 5% in the 15°K to 80°K range and around 10% from 80°K to 100°K .

There is also an indeterminacy in the impurity concentrations. From the room temperature resistivity, we determined the saturation number of donors from a graph by Prince (51). Resistivity was then

measured as a function of temperature for each crystal, and mobility values taken from Debye and Conwell (23). The number of ionized donor follows from $\frac{1}{\rho} = ne\mu$, $n = N_+$. Judging by the consistency of $\frac{N_+^2}{N_0}$ as mentioned in Chap. IV, Sec. A, we would expect an error of less than 10%.

Finally, we reach the systematic errors which would not appreciably affect either the reproducibility or internal consistency. Reverse heating arises from the I^2R losses when rf current flows through the transducer to ground. The R represents an effective contact resistance. Reverse heating was estimated by the thermoelectric voltage generated when the mica is present rather than the quartz. Since, in this case, there is no acoustic wave generation and no heating of the absorber, any thermal gradient produced arises from the I^2R loss. No correction was necessary. In the experiment of W.S.W., this factor represented a 5 or 10% correction. Perhaps the reason is that they drove an unplated surface of germanium with its relatively high contact resistance, while in our case we had a low resistivity of a gold plated surface. They did not have to plate their front surface because their ground contact region was of considerably higher conductivity than the active region of their crystal. RF flowed to ground in their crystals through the entire driving end instead of just through a thin layer of gold.

Heat leakage was also a cause of a small error. As previously

mentioned, it was necessary to have high thermal impedance between the crystal and the holder except at the ground contact. If all of the dissipation of acoustic power took place at the absorber, it would not be necessary to have perfect thermal isolation. For in this case, since power is measured by the substitution method, the same heat loss would be reproduced by means of the heater, and no error would ensue. If, however, there is some distributed loss of acoustic power due to ultrasonic attenuation and beam spreading, we can only perfectly reproduce this loss in cases of complete thermal isolation, as will be explained below. In any event, heat leaks are due to thermal conductance of the leads. The radiation loss between the crystal and the holder will be negligible because of their small temperature difference (20, p 191). A rough calculation shows that thermal conductance can account for a loss of 5 mw per lead (equal to 15mw) when the holder is at 20°K (20, p 196). This would represent a loss of around 5% of the input power, most of which will be reproduced by the heater.

The last causes of error that we wish to discuss are attenuation and beam spreading. Both factors can lead to an absorption and a scattering of the ultrasonic wave, with the energy lost by absorption being converted into heat. Aside from attenuation by the conduction electrons, other possible loss mechanisms are scattering and absorption due to defects, dislocations, boundaries, etc. Boundary effects would be due to beam spreading. The loss due

to scattering will show up as a discrepancy between the two sections of the crystal. In other words, any deviation of the ultrasonic beam from a [100] transverse wave will mean a diminishing of the acoustoelectric voltage without a proportional reduction in power density. This would mean a higher acoustoelectric voltage at the top section of the crystal, but the same power density in both sections. This error has already been taken into account when discussing imperfect absorption of the sound wave, since we cannot determine how much discrepancy is due to scattering and how much to imperfect absorption.

We would now like to show that if we had complete thermal isolation except at the ground contact, no loss would occur as the result of distributed absorption of the ultrasonic wave. Assuming thermal isolation, heat current flows only to the ground contact, and the heat current passing through any unit area is simply proportional to the acoustic power flowing through the same area. In other words, the heat current is the same regardless of where the power is dissipated, as required by the conservation of energy (conversion of acoustic energy into heat). If $J(x)$ is the heat current in cal/sec cm², at some distance x along the crystal and $S(x)$ is the acoustic power density in watts/cm², then $J(x) = AS(x)$. A is the reciprocal of the mechanical equivalent of heat i.e., 0.24 cal/joule. The acoustoelectric force is $eE(x) = BS(x)$, and in the

interval x_1 to x_2 ,

$$eV_{AE} = \int_{x_1}^{x_2} eE(x) dx = \frac{B}{A} \int_{x_1}^{x_2} J(x) dx$$

The acoustoelectric voltage measured in the two sections of the crystal will be determined by the heat current in that region, regardless of the location of the heat sources. This heat current would be exactly reproduced by the heater, leaving invariant the calculated intervalley scattering rates. The acoustoelectric voltage and the power density were always higher by around 10% in the top section of the crystal than the bottom. It is only when, for instance, the acoustoelectric voltage is 15% higher in the top section and the power density by only 10%, that the discrepancies discussed before will enter.

When, however, there are heat leaks, the heat current will be partly lost through these leaks. The heater can only reproduce that part of the distributed heat current which flows through the ground contact. It will reproduce all of the heat current which is formed at the absorber. If we had considerable distributed absorption along with excessive heat leaks, it would again show up in the discrepancy between the two sections.

It is also worth noting that data on the 5 ohm-cm crystal was taken at both 60 and 20 mc.

$$\bar{E} = K \frac{q^2 \omega^2 \tau_r}{1 + \omega^2 \tau_r^2} \quad \text{where} \quad \frac{1}{\tau_r} = \frac{4}{3} R_{iv} + \frac{\omega^2}{c^2} D$$

At 20 mc, the spatial redistribution rate $\frac{\omega^2}{c^2} D$ is slow compared to R_{iv} and the $\omega^2 \tau_r^2$ term in the denominator is negligible. We have therefore two linearly independent equations for the same crystal which gave substantially the same calculated value for R_{iv} . Alternatively, we can instead eliminate R_{iv} from the above equations and calculate a value of q^2 . Reasonable agreement between the calculated value and the value we used corresponding to a deformation potential

$$\bar{\epsilon}_u = 16.6 \text{ ev or } q^2 = 1.17 \times 10^{-47} \frac{\text{ml}^5}{\text{t}^2} \text{ (MKS units) where}$$

$$q = \frac{1}{3} \frac{\bar{\epsilon}_u}{\sqrt{C_{44}}}$$

provides a further check on possible systematic errors. If there were serious systematic errors, we could use the calculated value of $\bar{\epsilon}_u$, instead of the accepted value,* and we would still be correct in our values for $A(T)$ and $B(T)$. However, at $\approx 40^\circ\text{K}$ where $\bar{E}(60 \text{ mc})$ deviates most from a simple proportionality to ω^2 , we get $q^2 = 1.21 \times 10^{-47} \text{ MKS}$, $\bar{\epsilon}_u = 16.9 \text{ ev}$. This is within experimental error of the accepted value.

The last comment we will make is the agreement of the high tem-

*Accepted values of $\bar{\epsilon}_u$ range from 16 ev to 19 ev (1,25,26), with part of the possible discrepancy due to a temperature dependence of $\bar{\epsilon}_u$ (25).

perature data for the high resistivity crystals with the phonon line previously determined by W.S.W.

Summing up, we would expect a statistical error of less than 10%, and an error in impurity concentrations of around 10%. We also expect three errors of around 5%, one due to pickup and imperfect absorber, another due to uncertainty in the distance between contacts, and the last due to a combination of heat leakage and ultrasonic attenuation. Since these errors are independent, $A(T)$ and $B(T)$ should be reliable to around $\pm 15\%$ in the temperature range 15°K to 80°K, and probably around $\pm 20\%$ from 80°K to 100°K.

CHAPTER V

INTERPRETATION OF INTERVALLEY SCATTERING RATES

A. PRELIMINARY REMARKS

We wish to discuss the problem of donor induced intervalley transitions, and how different donors will affect this transition rate. Straightforward calculations of intervalley scattering rates due to the shielded Coulomb field of a donor gives results which are several orders of magnitude too small. The reason is that an intervalley transition involves a large momentum change, and the shielded Coulomb field is too weak to provide this kick.

Intervalley scattering, as will be shown, depends on the detailed structure of the donor. The structure of donor states in germanium is a topic of considerable interest, and there exists an excellent review article on this subject by Kohn (10). Since we cannot discuss donor induced intervalley scattering without some knowledge of donor states, we will give a concise introduction to this subject based primarily on the article by Kohn.

For the sake of completeness, we should mention phonon induced intervalley scattering, which predominates at high temperatures. A $< 100 >$ phonon is necessary to induce an intervalley transition between any pair of valleys. In the simple model proposed by Herring (13) and used by W.S.W. (1), only one phonon energy is considered,

and the actual phonon energy determined will be a weighted average of several possible phonons. The "intervalley phonon" determined by W.S.W. agrees well with the present experiment and corresponds to the two degenerate $\langle 100 \rangle$ phonons determined by Brockhouse et al., (42), from neutron diffraction experiments. The phonon energies in units of $\frac{h\nu}{k}$, correspond to a temperature of 310°K , and are the longitudinal acoustic and longitudinal optical phonons. The lower energy $\langle 100 \rangle$ phonons (transverse acoustic) are symmetry forbidden according to group theoretical arguments of Lax and Hopfield (38).

B. THEORY OF DONOR STATES IN GERMANIUM

A donor, with five electrons in its outer shell, enters substitutionally into the germanium lattice. It forms covalent bonds with four germanium atoms, and its extra electron is weakly bound. We can picture the donor as a closed shell with a single positive charge, giving rise to a Coulomb potential $\frac{e}{K\epsilon}$. The dielectric constant K enters because of polarization of the host lattice, and at distances far from the donor where this approximation is valid, K is taken as the static dielectric constant for germanium. An electron bound by this weak Coulomb field would in general be expected to execute large orbits, because of its small effective mass (approximately 0.2 free electron) and the shielded nature of the potential.

The Schroedinger equation for an electron in a crystal in the field of a donor is

$$\left\{ -\frac{\hbar^2}{2m_0} \nabla^2 + V(r) - \frac{e^2}{Kr} \right\} \Psi(r) = E \Psi(r) \quad (5.1)$$

where $V(r)$ is the periodic crystalline potential. In the effective mass approximation, the equation becomes

$$\left\{ -\frac{\hbar^2}{2m_t} \left(\frac{\partial^2}{\partial x^2} + \frac{\partial^2}{\partial y^2} \right) - \frac{\hbar^2}{2m_l} \frac{\partial^2}{\partial z^2} - \frac{e^2}{Kr} \right\} F(r) = E F(r) \quad (5.2)$$

where m_l and m_t are respectively the effective masses along the symmetry axis of the valley and normal to the axis. Even though $m_l \approx 20 m_t$, we will for illustrative purposes assume an isotropic effective mass $m^* = (m_t^2 m_l)^{1/3} \approx 0.2 m_0$ where m_0 is the free electron mass.

With this further approximation, the equation is

$$\left\{ -\frac{\hbar^2}{2m^*} \nabla^2 - \frac{e^2}{Kr} \right\} F(r) = E F(r) \quad (5.3)$$

This is the hydrogen equation with m_0 replaced by m^* and e^2 replaced by e^2/K . The $F(r)$ are hydrogen-like envelope functions.

If the assumption of isotropic mass is not made, the equation must be solved by variational methods, and the $F(r)$ will not be spherically symmetric for S-states, but will instead be compressed in the heavy mass direction. In either case, the states are labeled with the usual hydrogen notation 1s, 2p, etc.

The validity of the effective-mass approximation, where we have incorporated the crystalline potential into an effective mass is discussed by Kohn (10, p 274 ff). The basic assumptions are that $\frac{e^2}{Kr}$ varies slowly with respect to a lattice constant, and that the electron energy, in the neighborhood of a conduction band minimum be a continuous, differentiable function of crystal momentum i.e.,

$$\mathcal{E}(\underline{P}) = \frac{(P_x - P_{x_0})^2}{2m_t} + \frac{(P_y - P_{y_0})^2}{2m_t} + \frac{(P_z - P_{z_0})^2}{2m_l}$$

where P_{x_0} , P_{y_0} , P_{z_0} are the crystal momenta at the energy minimum. The symmetry axis of the constant-energy ellipsoids is taken as the z axis. The wave function for an electron bound to the donor would be

$$\Psi(\underline{k}, \underline{r}) = \psi(\underline{k}, \underline{r}) F(\underline{r})$$

where $\psi(\underline{k}, \underline{r})$ is a Bloch wave function and $\underline{k} = \underline{P}_0/\hbar$ is the wave vector at the energy minimum.

$$\psi(\underline{k}, \underline{r}) = u(\underline{k}, \underline{r}) e^{i \underline{k} \cdot \underline{r}}$$

where $u(\underline{k}, \underline{r})$ has the translational symmetry of the crystal. It varies rapidly over a unit cell, and approaches the atomic wave function in the neighborhood of a nucleus. The envelope $F(\underline{r})$ must change slowly over a lattice spacing, since this is equivalent to

requiring $\frac{e^2}{Kr}$ to change slowly over this distance. The wave function $\Psi(\underline{k}, \underline{r})$ is a physically plausible result since a free electron in a crystal is described by a Bloch function, and an electron weakly bound to a donor is then a Bloch function slowly modulated by a hydrogen like envelope.

In this approximation, the eigenvalues E_n for "S" like states are

$$E_n = \frac{1}{n^2} \left[\frac{e^4 m^*}{2 \hbar^2 K^2} \right]$$

The ground state is $E_0 = \frac{1}{K^2} \frac{m^*}{m_0} E_H$ and the donor "Bohr radius" $a_D = \frac{K m_0}{m^*} a_H$, where E_H and a_H are the ground state energy and Bohr radius for the hydrogen atom. Since K for germanium is around 16, and $m^*/m_0 \approx 0.2$, $E_0 \approx 10.5$ meV, $a_D \approx 40a_0$ and $F_{1s} = \left(\frac{1}{\pi a_D^3} \right)^{1/2} e^{-r/a_D}$.

A variational calculation using the following trial function

$$F_{1s} = \left(\frac{1}{\pi a^2 b} \right)^{1/2} \exp \left(- \sqrt{\frac{x^2 + y^2}{a^2} + \frac{z^2}{b^2}} \right)$$

gives $a \approx 64.5a_0$, $b \approx 22.7a_0$, and $E_0^* = 9.2$ meV. We now take the effective radius $a^* = (a^2 b)^{1/3} \approx 46a_0$. Since E_0^* is the donor ionization energy which is known experimentally to be 12.7 meV for arsenic and 9.6 meV for antimony, corrections to effective mass theory will be required.

Since, however, we have four equivalent valleys, we will have a four-fold degenerate solution to the effective mass equation (omitting spin degeneracy). The solutions are therefore

$$\Psi^{(j)}(\mathbf{r}) = \sum_{i=1}^4 \alpha_i^{(j)} \psi(\mathbf{k}_i, \mathbf{r}) F_i(\mathbf{r}) = \sum_{i=1}^4 \alpha_i^{(j)} u(\mathbf{k}_i, \mathbf{r}) F_i(\mathbf{r}) e^{i\mathbf{k}_i \cdot \mathbf{r}}$$

where i labels the valleys, and i and j run from one to four. Each $\psi(\mathbf{k}_i, \mathbf{r}) F_i(\mathbf{r})$ is composed of momentum states from the extremal region of a single valley. The $u(\mathbf{k}_i, \mathbf{r})$ are chosen to be equal at any lattice site, in particular at the donor nucleus $\mathbf{r} = 0$. The $\alpha_i^{(j)}$ are numerical coefficients, and in the limit of the validity of the effective mass approximation, we set $\alpha_i^{(j)} = \delta_{ij}$. We have four decoupled solutions, each belonging to a single valley, and no mechanism for transitions between valleys exists. Valley is, therefore, a good "quantum number."

The presence of a donor, representing a local positive charge, destroys the perfect translational symmetry of the lattice. In particular, bound electrons whose orbits penetrate into the central cell and possibly into the donor core, due to the breakdown of dielectric shielding in the immediate vicinity of the donor, will see a potential that is rapidly varying with respect to a lattice constant. This is a violation of the effective mass approximation, and it will give rise to a splitting of the original four fold degenerate levels into a singlet and a triplet. The magnitude of this splitting is a measure of the change in the polarization energy of the lattice as the electron penetrates into the central impurity cell. This splitting will be greatest for the deepest penetrating orbits (i.e., low

lying S states) and is called the "valley-orbit" splitting. It represents the breakdown of the effective mass approximation.

The exact form of the central cell potential is not known. It can, however, be taken into account by adding to the original Hamiltonian

$$H_0 = -\frac{\hbar^2}{2m_t} \left\{ \frac{\partial^2}{\partial x^2} + \frac{\partial^2}{\partial y^2} \right\} - \frac{\hbar^2}{2m_l} \frac{\partial^2}{\partial z^2} - \frac{e^2}{Kr}$$

a perturbation $U(r)$ which is large only in or near the central impurity cell. We take (27)

$$H_{ij} = \int_0^\infty \Psi_i^*(r) [H_0 + U(r)] \Psi_j(r) dr = \begin{cases} -E_0^* \Delta & ; i=j \\ -\Delta & ; i \neq j \end{cases} \quad (5.4)$$

where the $\Psi_\alpha(r)$ are the single valley wave functions.

The modified Hamiltonian in matrix notation is

$$H_{ij} = \begin{bmatrix} -E_0^* \Delta & -\Delta & -\Delta & -\Delta \\ -\Delta & -E_0^* \Delta & -\Delta & -\Delta \\ -\Delta & -\Delta & -E_0^* \Delta & -\Delta \\ -\Delta & -\Delta & -\Delta & -E_0^* \Delta \end{bmatrix} \quad (5.5)$$

In this new representation, the original four-fold degenerate levels have been split into a singlet and a triplet. (A small splitting would exist, however, even for $U(r) = 0$.) The singlet energy is $E_s = -E_0^* 4\Delta$ and the triplet is $E_T = -E_0^* \Delta$. The negative sign has been chosen for the matrix elements Δ since it is known that the singlet lies lowest in arsenic and phosphorus-doped germanium (50), and is

probably also lowest for antimony-doped germanium.

The wave functions are again written

$$\Psi^{(2)}(\underline{r}) = \sum_{i=1}^4 \alpha_i^{(2)} \psi(\underline{k}_i, \underline{r}) F_i(\underline{r})$$

but the eigenstates of this Hamiltonian, instead of the previous single valley states are linear combinations of them.

$$\Psi^{(S)}(\underline{r}) = \frac{1}{2} [\Psi_1 + \Psi_2 + \Psi_3 + \Psi_4] = \frac{1}{2} \begin{pmatrix} 1 \\ 1 \\ 1 \\ 1 \end{pmatrix} \quad (5.6a)$$

where $\Psi_1 = \psi(\underline{k}_1, \underline{r}) F_1(\underline{r})$, etc.

The singlet is the totally symmetric combination of the four valleys. The triplets $\Psi^{(T)}$ are

$$\begin{aligned} \Psi(\pi_1) &= \frac{1}{2} [\Psi_1 - \Psi_2 + \Psi_3 - \Psi_4] \\ \Psi(\pi_2) &= \frac{1}{2} [\Psi_1 - \Psi_2 - \Psi_3 + \Psi_4] \\ \Psi(\pi_3) &= \frac{1}{2} [\Psi_1 + \Psi_2 - \Psi_3 - \Psi_4] \end{aligned} \quad (5.6b)$$

An electron, bound to a donor, is no longer in a single valley, but in some linear combination of valleys. Valley is, therefore, no longer a good "quantum number."

The quantity " 4Δ " is the valley-orbit splitting. The ground state splittings have been measured for the common Group V impurities.

The results are

$$\text{Arsenic} \quad 4\Delta = 4.1 \text{ meV} \quad (25, 29, 30)$$

$$\text{Phosphorus} \quad 4\Delta = 3.0 \text{ meV} \quad (29, 30)$$

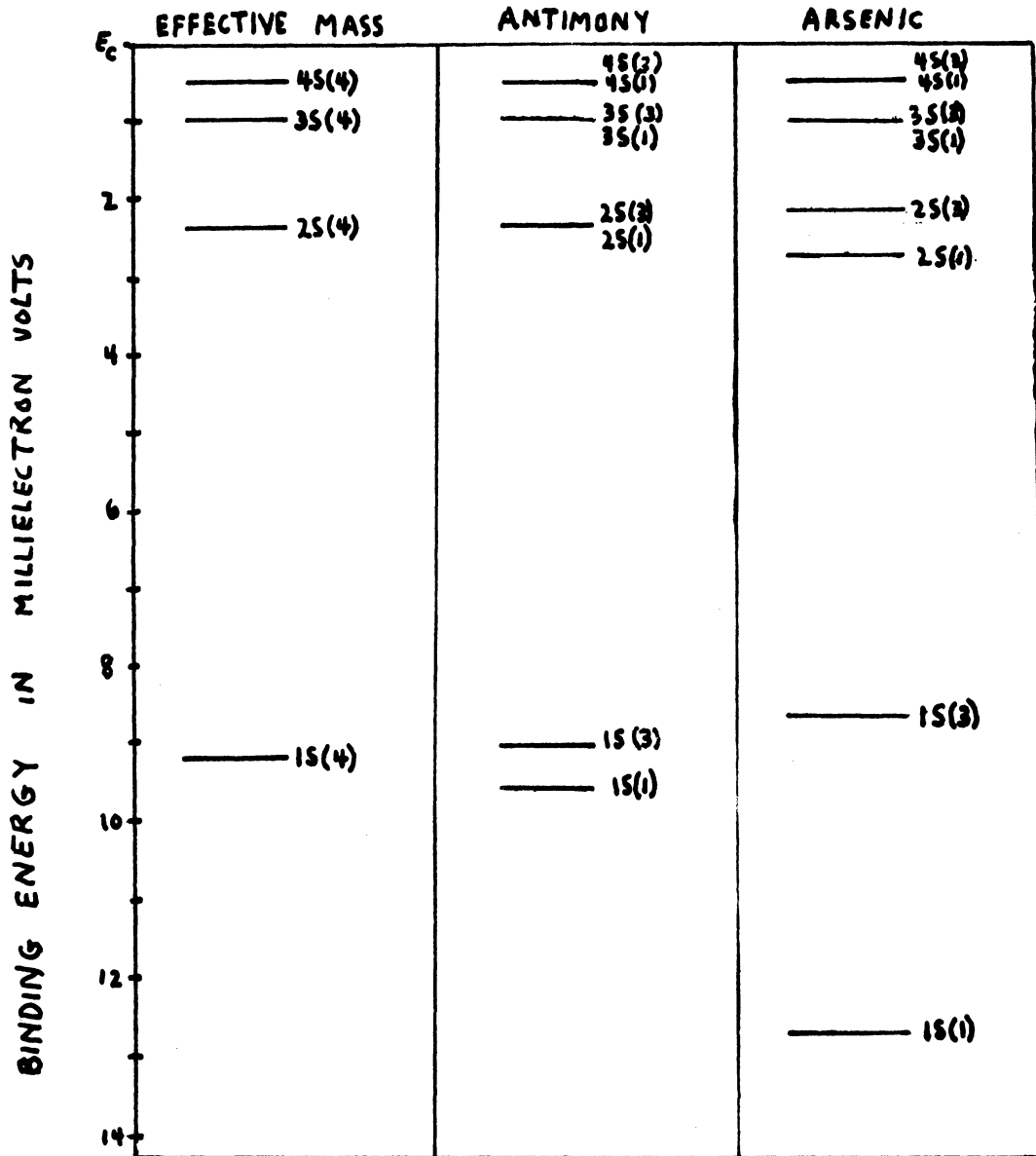
$$\text{Antimony} \quad 4\Delta = 0.6 \text{ meV} \quad (31, 32)$$

The valley-orbit splitting is around one-third of the donor ionization energy in arsenic, and only approximately one-fifteenth of the ionization energy in antimony. These two donors provide the extremes for studying the effect of the valley-orbit splitting on the intervalley scattering rate. (See Fig. 12).

C. INTRODUCTION TO THE IONIZED DONOR PROBLEM

We mentioned in our preliminary remarks that the shielded Coulomb field of a donor was too weak to produce appreciable intervalley scattering. This will be shown in Sec. D.

Two mechanisms have been proposed for ionized arsenic donors. The first is direct transitions caused by the central cell potential, for which, to make the calculations tractable, we pick a delta function located at the donor site (Sec. D). This model is due to Price (11), and predicts an intervalley scattering rate which depends on the square of the valley-orbit splitting. The other mechanism is a compound capture re-emission process (Sec. E). An electron is captured into an excited state of the donor, from which it may be directly re-emitted, or it may cascade among the various excited states before re-emission. Its subsequent re-emission may, in either case, take place into a valley different from the original one. According to Koenig (12) this process, which was first proposed by W. S. W., should be linearly dependent on the valley-orbit splitting.



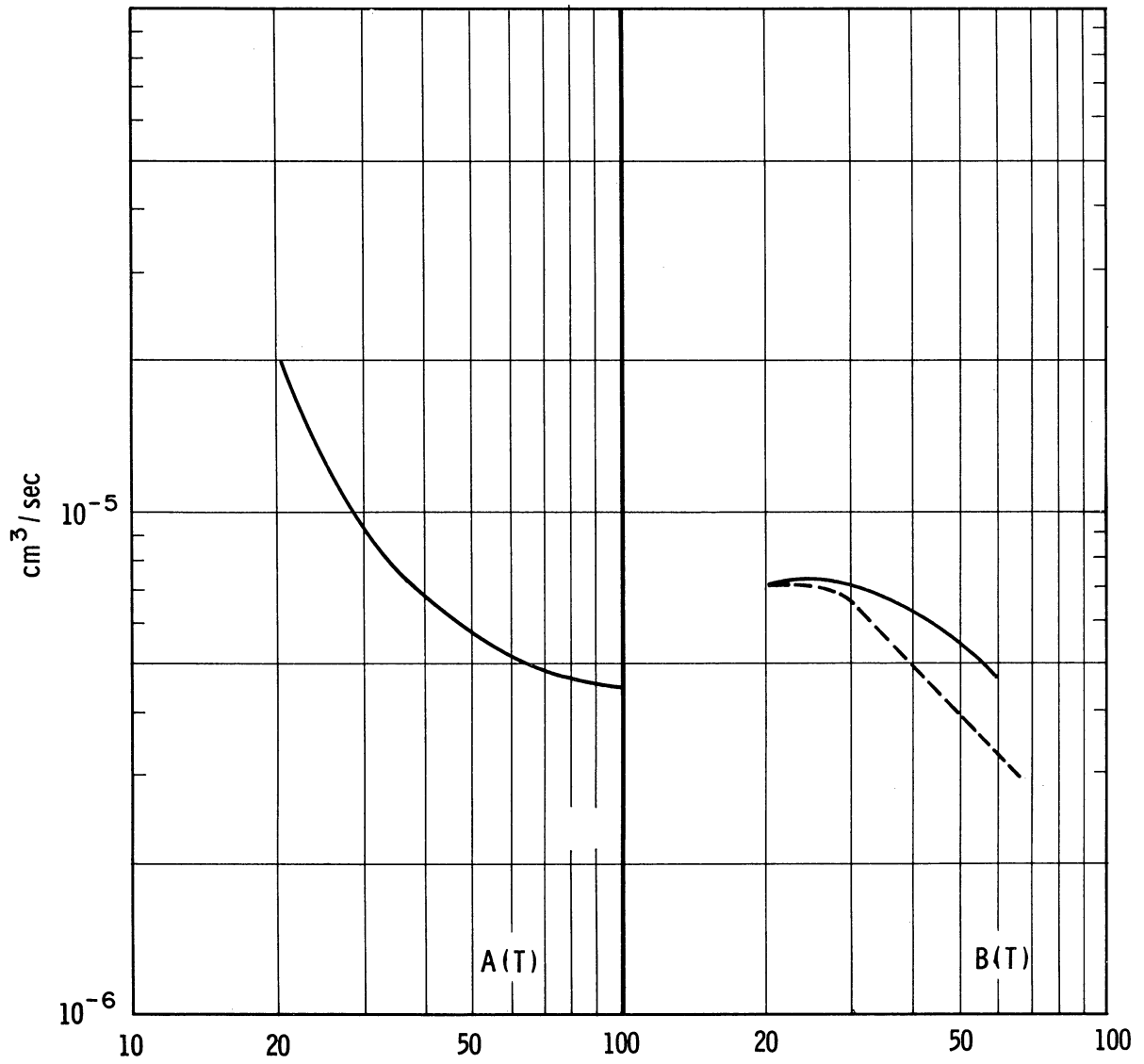
The numbers in parentheses are the degeneracy of the "S" like states, spin degeneracy being omitted. The centers of gravity of the excited states are taken at the effective mass value.

Fig. 12. Theoretical spectrum and corrected spectra for energy levels of donors in germanium (S states only).

The compound capture re-emission process is not readily calculable, but it appears feasible that the total intervalley rate due to ionized arsenic could be fit by adding to the direct scattering by the delta function the contribution from the compound capture process.

For antimony, however, the situation is somewhat different. Since its ground state valley-orbit splitting has been measured to be one-seventh that of arsenic, we would have expected the rate per ionized antimony to be considerably smaller than that for arsenic. This is not, however, what has been observed. At 20°K (cf Fig. 10 and 13), the rate per ionized antimony donor is one-half that per ionized arsenic. At 100°K, the factor has become one-tenth. The temperature dependence of the scattering rates are, therefore, distinctly different. The rate per ionized antimony donor follows a simple temperature dependence, while the rate for arsenic is such as to indicate that both above mentioned mechanisms contribute. For antimony, however, the sum contribution from these mechanisms does not appear to be large enough to fit the observed rate. (Secs. D and E.)

The valley-orbit splitting, as previously discussed, depends on the central cell potential. To the author's knowledge, these potentials are not known analytically, and the valley-orbit splittings for the various donors in germanium have not been successfully



The solid lines are the results obtained by W.S.W. for arsenic-doped germanium. The dashed line for $B(T)$ is the theoretical fit.

Fig 13. $A(T)$ and $B(T)$ for arsenic-doped germanium (1).

calculated. The matrix elements $-\Delta$ used in the last section were chosen so that they would give the measured valley-orbit splitting. We will show in Appendix C that we can adjust the magnitude of a delta function to obtain the observed splittings. There is no unique potential for obtaining this splitting, and apparently no good reason why the splitting for arsenic should be appreciably larger than for antimony. In fact, arsenic, which has the largest valley-orbit splitting of the Group V donors, is right next to germanium in the periodic table. One might, therefore, guess that arsenic would "fit" better into the germanium lattice than would antimony and phosphorus. However, although radii of the donors vary monotonically as one descends column V of the periodic table, the valley-orbit splittings do not (33).

The compound capture re-emission process turns out to depend predominantly on the excited states, with only negligible contribution from the ground state. The valley-orbit splittings of the excited states have not been measured, but we have calculated them using hydrogenic wave functions and assuming a delta function for the central cell potential (Appendix C). It might be possible to find a potential which would give the measured difference for the valley-orbit splitting of the ground states of arsenic and antimony donors, but would give less disparity in the excited states. However, this is somewhat speculative, and we will conclude by saying

that the subject of the valley-orbit splittings is not a closed one.

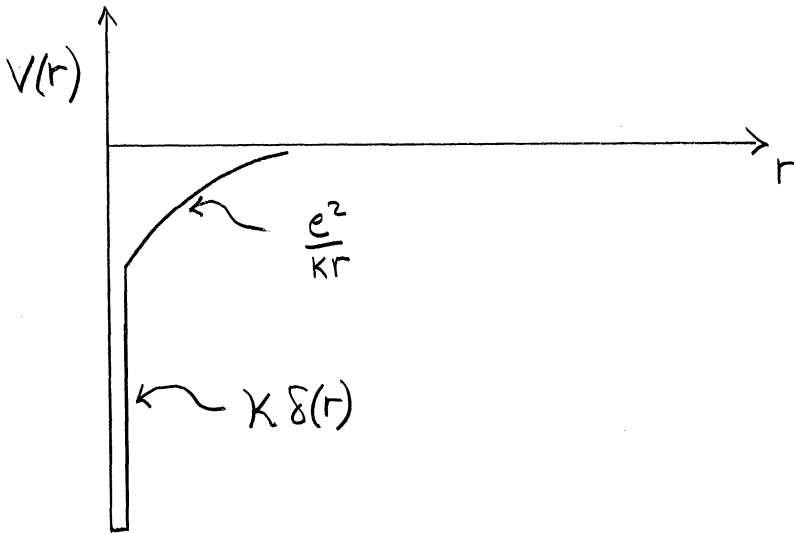
D. IONIZED IMPURITY SCATTERING-DIRECT

We first wish to discuss direct intervalley scattering by the potential field of an ionized donor. As is shown in Appendix C, the donor potential can be written

$$V(r) = -\frac{e^2}{kr} + \kappa \delta(r) \quad (5.7)$$

where

$$\kappa = -\frac{(4\Delta)}{4|\psi(0)|^2} = -\frac{\Delta\pi a^*{}^3}{|u(k,0)|^2}$$



Following the notation of Landau and Lifshitz (34, p 410 ff)

for the scattering amplitude in Born approximation

$$f_1(\theta) = \frac{m}{2\pi\hbar^2} \int_0^\infty u^*(k_1, r) e^{-ik_1 \cdot r} \left(\frac{e^2}{kr}\right) u(k_2, r) e^{ik_2 \cdot r} dr$$

The periodic part of the Bloch functions are given an appropriate average, and can be removed from the integral

$$\begin{aligned}
 f(\theta) &= \frac{m}{2i\hbar^2} \left| \overline{u^*(\underline{k}_1, r) u(\underline{k}_2, r)} \right| \int_0^a e^{-i\underline{k}_1 \cdot \underline{r}} \left(\frac{e^2}{Kr} \right) e^{i\underline{k}_2 \cdot \underline{r}} d\underline{r} \\
 &= \frac{4m}{\hbar^2} \left(\frac{e^2}{2Ka^*} \right) \frac{\left| \overline{u^*(\underline{k}_1, r) u(\underline{k}_2, r)} \right|}{|\underline{k}_1 - \underline{k}_2|^2} \quad (5.8)
 \end{aligned}$$

For an intervalley scattering process, $|\underline{k}_1 - \underline{k}_2|$ is of order $\frac{2\pi}{C}$ where "C" is a lattice constant. That is, the Coulomb field must supply momentum components of $\approx \frac{2\pi}{C}$, which means the electron must penetrate into the central cell.

The cross section is

$$\begin{aligned}
 \sigma &= 3 \int \sigma(\theta) d\Omega = 3 \int |f(\theta)|^2 d\Omega \\
 \sigma &\approx 3.5 \times 10^{-5} \left| \overline{u^*(\underline{k}_1, r) u(\underline{k}_2, r)} \right| a^{*2} \quad \text{c.g.s}
 \end{aligned}$$

The factor of three enters because of the three possible final valleys.

Now, the experimental cross sections are of order a^{*2} , so that direct scattering by a Coulomb potential is several orders of magnitude too small. Furthermore, the factor $\left| \overline{u^*(\underline{k}_1, r) u(\underline{k}_2, r)} \right|$ is nearly unity for $|\underline{k}_1| \approx |\underline{k}_2|$ i.e., an intravalley process, but is consider-

ably less than unity for an intervalley process. We conclude, therefore, that direct scattering by means of the shielded Coulomb field of a donor ion makes a negligible contribution to the intervalley scattering rate. This is opposed to intravalley scattering where scattering by the Coulomb field is the dominant mechanism, since intravalley scattering requires only a small momentum change (35).

The possibility of direct scattering by a sharply peaked potential was pointed out by Price (11). In unpublished work, he has been able to fit W.S.W. data for ionized arsenic impurities in the region above 45°K with only a delta function scatterer.* Below 45°K, the difference between the experimental and the calculated value increases rapidly. We have sketched Price's work below with several minor modifications.

$$f_2(\theta) = \frac{m}{2\pi\hbar^2} \int_0^\infty u^*(k_1, r) e^{-ik_1 \cdot r} [K \delta(r)] u(k_2, r) e^{ik_2 \cdot r} dr$$

$$= \frac{m}{2\pi\hbar^2} K |u(k, 0)|^2$$

$$f_2(\theta) = \frac{m}{2\pi\hbar^2} \pi \Delta a^{*3} \quad (5.9)$$

*The reason why a delta function should produce appreciable scattering is discussed by Bohm (36, p 538).

We have used plane waves where we should have been using Coulomb functions. This is particularly true at the origin where the plane wave approximation is poorest. Since we are only interested in the electron wave function at the origin, we can use an enhancement factor which is the ratio of the squared modulus of an attractive Coulomb wave function to a plane wave at the origin. According to Landau and Lifshitz (34, p 422) this factor is

$$R = \frac{2\pi}{\delta k a^*} \left[1 - \exp\left(-\frac{2\pi}{\delta k a^*}\right) \right]^{-1} \quad (5.10)$$

$\hbar\delta k$ is the electron's thermal momentum and

$$\delta k a^* = \sqrt{\left(\frac{2m^*}{\hbar^2} E\right) \left(\frac{e^2}{2k E_0^*}\right)^2} = \sqrt{\frac{E}{E_0^*}}$$

where

$$E_0^* = \frac{e^2}{2k a^*} \quad \text{and} \quad E = \frac{\hbar^2 \delta k^2}{2m^*}$$

is the thermal energy; E_0^* is the effective mass ionization energy.

(According to Price, this is the correct energy to use.)

Since we are working at temperatures where $E_0^* > E$, we can omit the exponential in the enhancement factor, so that

$$R = 2\pi \sqrt{\frac{E_0^*}{E}} \quad (5.11)$$

and the Born approximation scattering amplitude becomes

$$f_2(\theta) = \frac{\pi m^* \Delta a^{*3}}{\hbar^2} \sqrt{\frac{E_0^*}{E}} \quad (5.12)$$

and

$$\sigma = 3 \int |f_2(\theta)|^2 d\Omega = 12\pi |f_2(\theta)|^2$$

since $f_2(\theta)$ is isotropic and the factor of three is again for the three possible final valleys. Therefore the total intervalley scattering cross section for this process is

$$\sigma = \frac{12\pi^3 m^{*2}}{\hbar^4} \left[\Delta^2 a^{*6} \frac{E_0^*}{E} \right] \quad (5.13)$$

$A(T)$ (the intervalley scattering rate per donor due to the delta function) is the thermal average of σv given by

$$\langle \sigma v \rangle = \frac{\int_0^\infty E^{\frac{1}{2}} \exp\left(-\frac{E}{kT}\right) \sigma v dE}{\int_0^\infty E^{\frac{1}{2}} \exp\left(-\frac{E}{kT}\right) dE}$$

The thermal average of v/E is given by

$$\left\langle \frac{v}{E} \right\rangle = 2 \sqrt{\frac{2}{\pi m^* k T}}$$

consequently

$$A(T) = \frac{24 m^{*3/2} \pi^{5/2}}{\hbar^4} \Delta^2 a^{*6} E_0^* \sqrt{\frac{2}{kT}} \quad (5.14)$$

with a $T^{-1/2}$ temperature dependence. Using effective mass values for $a^*(46^\circ\text{A})$ and $E_0^*(9.2 \text{ meV})$ and with $m^* = 2 \times 10^{-28} \text{ gm}$, $4\Delta = 4.1 \text{ meV}$ for arsenic, and 0.6 meV for antimony, we get

$$A(T) \approx 4.0 \times 10^{-6} \left(\frac{100}{T} \right)^{\frac{1}{2}} \frac{\text{cm}^3}{\text{sec}} \quad (5.15)$$

for arsenic and

$$A(T) \approx 8.5 \times 10^{-8} \left(\frac{100}{T} \right)^{\frac{1}{2}} \frac{\text{cm}^3}{\text{sec}} \quad (5.16)$$

for antimony. For arsenic at 50°K, $A(T) \approx 5.6 \times 10^{-6} \text{ cm}^3/\text{sec}$ which is exactly the experimental value from W.S.W. For temperatures above 50°K, $A(T)$ has the right temperature dependence. Below 50°K, however, the experimental value is greater than the calculated value and this difference increases rapidly with decreasing temperature.

For antimony, $A(T)$ is considerably smaller than the experimental value over the entire temperature range, and has the wrong temperature dependence.

Direct scattering by the delta function can account for the observed rates at temperatures above 50°K for arsenic. (However, we feel that, in a correct theory, $A(T)$ due to the above process would make a sizable contribution for temperatures above 50°K; but not the entire contribution.) At lower temperatures for ionized arsenic donors, and for the entire temperature range for ionized antimony, some other process must be operative.

E. IONIZED DONORS-COMPOUND CAPTURE RE-EMISSION PROCESS

The second process that we wish to describe is the capture of an electron into an excited state of a donor, and its subsequent re-emission at a later time into a valley which may differ from the original. The initial capture process is related to the "giant trap" mechanism of Lax (37). Lax describes how an electron, moving in the vicinity of an ionized donor, can dissipate approximately kT of energy in order to be initially captured into an excited state of binding energy U . He considered recombination processes where the thermal density of carriers was disturbed by means of impact ionization due to a pulsed external electric field, and the measured quantity (39,47) was the recombination time in which the electron density returned to thermal equilibrium. From this recombination time, cross sections were calculated. The electron was assumed to diffuse or cascade up and down the energy scale (the various excited states) and is either captured into the ground state or escapes in a time short compared to the measured recombination time. In other words, the individual jumping times among the excited states and between an excited state and a continuum state is short compared to the eventual recombination time. The diffusion up and down the ladder takes place by absorption and emission of phonons (phonon processes are considerably faster than photon processes), and if the electron reaches an excited state of binding en-

ergy kT below the conduction band, there will be few phonons available that can scatter it back. Lax describes this by means of a sticking probability $P(U)$ where $P(U) \approx 1$ for $U > kT$ and considerably less than 1 for $U < kT$. The total cross section is the sum of all states j of $\sum_j \sigma_c(j)P(U_j)$ where $\sigma_c(j)$ is the capture cross section for the j 'th state. It turns out that only s-states contribute appreciably to the total cross section (40).

We are dealing with a thermal equilibrium process, and we need the capture to last for only a finite time. As an electron is captured, another electron is emitted from a different donor so that the thermal equilibrium density is maintained. Analogously to Lax's sticking probability, Ascarelli and Rodriguez (40) have calculated thermal emission rates for temperatures below 10°K . States having sticking probability close to one will have long thermal emission times (small thermal emission rates) while small sticking probability implies short emission times. They also state a formula for the rate of cascading (transition rate) between any two low lying excited states.

We have calculated the thermal emission rates for the first four excited states ($j = 2$ to 5) for temperatures of 25°K , 50°K , and 100°K , modifying the calculation of Ascarelli and Rodriguez to fit our temperature range. We have also calculated transition rates between several low lying excited states. Our calculations

are discussed in Appendix D and are listed in Tables I and II.

The crucial quantity in determining the intervalley scattering rate for a given state is the product of its valley-orbit splitting and the average time an electron spends there. This is why a difference between antimony and arsenic donors would be expected (due to the difference in valley-orbit splitting); states which would be most effective in inducing intervalley transitions are those in which an electron spends just enough time to make an intervalley transition, and is shortly thereafter re-emitted into the continuum. For the ground state the electron is there too long, and for high lying excited states it is not there long enough. We will now attempt to put this in a more quantitative form.

As shown in Chap. V, Sec. B, the singlet and triplet wave functions for an electron bound to a donor are

$$\Psi_S = \frac{1}{2} [\Psi_1 + \Psi_2 + \Psi_3 + \Psi_4] \quad (5.6a)$$

$$\Psi_{T_1} = \frac{1}{2} [\Psi_1 - \Psi_2 + \Psi_3 - \Psi_4] \quad (5.6b)$$

$$\Psi_{T_2} = \frac{1}{2} [\Psi_1 - \Psi_2 - \Psi_3 + \Psi_4]$$

$$\Psi_{T_3} = \frac{1}{2} [\Psi_1 + \Psi_2 - \Psi_3 - \Psi_4]$$

and $E_S = -E_0^* - 4\Delta$; $E_T = -E_0^*$

where $\psi_i = \psi_i(kr)F(r)$ are the single valley wave functions.

To consider a specific process, let an electron belonging to valley 1 be captured by a donor at $t = 0$, and we follow the electrons wave function in time.

At $t = 0$, its wave function is

$$\psi_1 = \frac{1}{2} \left[\psi_S + \psi_{T_1} + \psi_{T_2} + \psi_{T_3} \right]$$

and at a later time t

$$\begin{aligned} \psi_1(t) &= \frac{1}{2} \left[\psi_S e^{-i \frac{E_S}{\hbar} t} + (\psi_{T_1} + \psi_{T_2} + \psi_{T_3}) e^{-i \frac{E_T}{\hbar} t} \right] \\ &= \frac{1}{2} e^{+i \frac{E_S^*}{\hbar} t} \left[\psi_S e^{+i \frac{4\Delta}{\hbar} t} + (\psi_{T_1} + \psi_{T_2} + \psi_{T_3}) \right] \end{aligned}$$

since ψ_S and the ψ_T 's are the solutions to

$$H \begin{Bmatrix} \psi_S \\ \psi_T \end{Bmatrix} = (H_0 + U(r)) \begin{Bmatrix} \psi_S \\ \psi_T \end{Bmatrix} = i\hbar \frac{\partial}{\partial t} \begin{Bmatrix} \psi_S \\ \psi_T \end{Bmatrix} = \begin{Bmatrix} E_S \psi_S \\ E_T \psi_T \end{Bmatrix}$$

and therefore

$$\psi_S(\pi) = \psi_S(0) e^{i \left(\frac{E_S^* + 4\Delta}{\hbar} \right) t}$$

etc.

Because the singlet and triplet have different energies, they change their phase differently in time. Consequently, at a later time the electron will be in a different linear combination of singlet and triplet corresponding to a different valley or, in general,

combination of valleys. If we, therefore, give this process time to work, we have a finite probability for an intervalley transition.

Substituting back for the single valley functions and defining $\nu = \frac{4\Delta}{\hbar}$, we get

$$\begin{aligned}\Psi_1(t) &= \frac{1}{4} e^{i\frac{E}{\hbar}t} \left[(\Psi_1 + \Psi_2 + \Psi_3 + \Psi_4) e^{i\frac{\nu}{2}t} + (3\Psi_1 - \Psi_2 - \Psi_3 - \Psi_4) \right] \\ &= e^{i\frac{E}{\hbar}t} \left[\frac{1}{4} (3 + e^{i\nu t}) \Psi_1 + \frac{1}{4} (e^{i\nu t} - 1) (\Psi_2 + \Psi_3 + \Psi_4) \right]\end{aligned}$$

The probability that the electron will have made a transition from valley 1 to some other valley at time t is three times the square of the coefficient of one of the other valley functions.

$$\text{Probability} = \frac{3}{16} |e^{i\nu t} - 1|^2 = \frac{3}{8} (1 - \cos \nu t)$$

The transitions occur at a rate $\nu = \frac{4\Delta}{\hbar}$ having a maximum probability of $3/4$ and a time average of $3/8$. However, the probability of making a transition at time t must be weighted by the probability that the electron has not left a particular level before time t .

This probability will be of the form $\exp(-t/\bar{\tau}_j)$, where $\bar{\tau}_j$ is the average time that an electron spends in the j 'th level. $\bar{\tau}_j$ depends on the rate of emission into the continuum or conduction band (thermal ionization rate) and on the transition rate to all other bound

states:

$$\frac{1}{\bar{\tau}_j} = \beta_j + \sum_{j' \neq j} W_{j \rightarrow j'}$$

where β_j is the thermal ionization rate and $W_{j \rightarrow j'}$ is the transition rate from bound state j to bound state j' .

The probability, therefore, that an electron leaving a level at time t will leave in a different valley is

$$\frac{3}{8} \left[1 - \cos \nu_j t \right] \exp \left(-t / \bar{\tau}_j \right)$$

The subscript on the ν indicates the valley-orbit splitting of the j 'th level as described in Appendix C.

The time average probability is

$$P(\nu_j, \bar{\tau}_j) = \frac{\frac{3}{8} \int_0^{\infty} dt \left[1 - \cos \nu_j t \right] \exp(-t/\bar{\tau}_j)}{\int_0^{\infty} dt \exp(-t/\bar{\tau}_j)} = \frac{3}{8} \frac{\nu_j^2 \bar{\tau}_j^2}{1 + \nu_j^2 \bar{\tau}_j^2} \quad (5.17)$$

The total rate of transitions due to a level j is

$$\left[\beta_j + \sum_{j' \neq j} W_{j \rightarrow j'} \right] P(\nu_j, \bar{\tau}_j) = \frac{3}{8} \frac{\nu_j^2 \bar{\tau}_j^2}{1 + \nu_j^2 \bar{\tau}_j^2}$$

since this is the total rate of leaving a level times the probability of an intervalley transition occurring. This rate is a maximum for $\nu_j \bar{\tau}_j = 1$ or equivalently

$$\nu_j = \beta_j + \sum_{j' \neq j} W_{j \rightarrow j'}$$

and is equal to $3/16 \nu_j$. A state is most effective therefore when the rate at which intervalley transitions occur (ν_j) is equal to the

rate at which electrons leave ($\beta_j + \sum_{j'} w_{j \rightarrow j'}$), so that the electron spends just enough time to make a transition.

This means that if we have a state for which

$$\nu_j \approx \beta_j + \sum_{j' \neq j} w_{j \rightarrow j'}$$

the resulting intervalley transition rate is $\approx 3/16 \nu_j$ while for other states the rate is correspondingly less than the maximum. Of

this rate, the fraction $\frac{\beta_j}{\beta_j + \sum_{j' \neq j} w_{j \rightarrow j'}}$ is directly observable,

and the remainder $\frac{\sum w_{j \rightarrow j'}}{\beta_j + \sum w_{j \rightarrow j'}}$ is observable when the electron

is emitted from some other state. (We only observe a transition when the electron is re-emitted into the conduction band.)

We would now like to explain, in a little more detail, what W.S.W. called the compound capture re-emission process. An electron is captured into a state j having a capture cross section $\sigma_c(j)$. It may be directly re-emitted (this probability is $\frac{\beta_j}{\beta_j + \sum w_{j \rightarrow j'}}$) or it may make transitions up and down the energy scale (the probability for any such transition is $\frac{w_{j \rightarrow j'}}{\beta_j + \sum w_{j \rightarrow j'}}$). What has to

be determined is the intervalley scattering rate due to every possible sequence of events weighted by its probability of occurrence. The total rate is then the sum of all these weighted individual rates. One limit which can be

calculated is the complete omission of internal transitions (this implies that

$$\beta_j \gg \sum_{j' \neq j} w_{j \rightarrow j'}$$

which we know to be incorrect). See Tables I and II. The other limit consists of assuming that there is a considerable amount of cascading down to the first excited state and the ground state, where the characteristic rates ν_j of making an intervalley transition are large. The electron then cascades back up the energy scale where it is re-emitted into the continuum. We will now calculate these limits.

In order to maintain the thermal equilibrium density of carriers, the number of electrons bound to donors in level j times the thermal emission rate from that level must be equal to the number of free electrons times the capture rate of that level:

$$N_0^j \beta_j = n \left(N_+ \langle \sigma_c(j) v \rangle \right) \quad (5.18)$$

The capture rate is the number of ionized donors N_+ times a thermal average of the capture cross section and electron velocity, and n is the number of free electrons. N_0^j is the number of neutral donors in which the electron is bound in level j , and β_j is its thermal emission rate.

Now, we multiply both sides of the above equation by $S(j)$, where $S(j)$ is the total probability that an emitted electron has undergone an intervalley transition. $A_j(T)$ (the intervalley scat-

tering rate per ionized donor due to the j 'th level) is $\langle \sigma_c(j)V \rangle S(j)$, since this is $\langle \sigma_{iv}V \rangle$ where σ_{iv} is the effective intervalley scattering cross section; so that

$$A_j(T) = \frac{N_0^i \beta_j S(j)}{n N_+} \quad (5.19)$$

and the total ionized donor contribution is

$$A(T) = \sum_j A_j(T)$$

We have that

$$N_0^i = \frac{g_j \exp\left(\frac{E_F - \epsilon_j}{kT}\right)}{\sum_i g_i \exp\left(\frac{E_F - \epsilon_i}{kT}\right)} \frac{N_D}{1 + \sum_i \frac{1}{g_i} \exp\left(\frac{\epsilon_i - E_F}{kT}\right)} \quad (5.20)$$

where N_D is the concentration of donors, g_j is the degeneracy of the j 'th level (for s states $g = 8$ because of the two-fold spin and the four-fold valley degeneracy), and E_F and ϵ_j are the Fermi energy and the energy of the j 'th donor state.

The first factor in the above expression is the fraction of electrons which are bound in level j , and the second is the total number of neutral donors at temperature T .

This reduces to

$$N_0^i = N_D \frac{g_j \exp\left(\frac{E_F - \epsilon_j}{kT}\right)}{1 + \sum_i g_i \exp\left(\frac{E_F - \epsilon_i}{kT}\right)} \quad (5.21)$$

Furthermore,

$$N_+ = \frac{N_D}{1 + \sum_i g_i \exp\left(\frac{E_F - \epsilon_i}{kT}\right)} \quad (5.22)$$

and

$$n = g_j N_c \exp\left(\frac{E_F - E_c}{kT}\right) \quad (5.23)$$

so that

$$g_j N_c \exp\left(\frac{E_F}{kT}\right) = n \exp\left(\frac{E_c}{kT}\right)$$

where E_c is the conduction band edge energy, and the density of states factor is given by

$$N_c = \left(\frac{m^* k T}{2\pi \hbar^2}\right)^{3/2} *$$

(see, for example, 41, p 284 ff).

After some reduction, we get

$$A_j(T) = \frac{\beta_j S(j) \exp\left(\frac{E_c - \epsilon_j}{kT}\right)}{N_c}$$

and defining $E_c - \epsilon_j = E_j$, the ionization energy of the j 'th state
 $= \frac{E_0^*}{j^2}$, the final result is

$$A_j(T) = \beta_j S_j \left[\frac{2\pi \hbar^2}{m^* k T}\right]^{3/2} \exp\left(\frac{E_0^*}{j^2 k T}\right) \quad (5.24)$$

*Contrary to convention, we do not include the degeneracy in the definition of N_c .

The problem now is to calculate $S(j)$, the average probability that an electron emitted from level j will have made an intervalley transition. This probability must include the effect of electrons emitted from level j which have reached the states $j = 1$ or 2 and have cascaded up to j . To actually find $S(j)$, we must follow the path of many electrons from capture into j or some other excited state, until eventual re-emission from j into the continuum. This suggests a Monte Carlo type of calculation which we have not attempted.

In the limit of $\beta_j \gg \sum_{j' \neq j} w_{j \rightarrow j'}$, the dominant process will be direct re-emission from the same level into which capture occurred. The probability of the electron having changed valleys upon emission from j is

$$P(\nu_j, \bar{\nu}_j) = \frac{3}{8} \frac{\nu_j^2 \bar{\nu}_j^2}{1 + \nu_j^2 \bar{\nu}_j^2}$$

so that for $\beta_j \gg \sum w_{j \rightarrow j'}$, this reduces to

$$P(\nu_j, \bar{\nu}_j) = S(j) = \frac{3}{8} \frac{\nu_j^2 / \beta_j^2}{1 + \nu_j^2 / \beta_j^2}$$

This approximation is not very satisfactory, as can be easily seen from Tables I and II. For example, an electron captured into $j = 4$ has an appreciable probability of making a transition to $j = 3$. Continuing down the energy scale $w_{3 \rightarrow 2}$ is comparable to β_3 .

In the limit, however, of neglecting cascading, we have simply

that

$$A_j(T) = \frac{3}{8} \frac{v_j^2 / \beta_j}{1 + v_j^2 / \beta_j} \left[\frac{2\pi h^2}{m^* k T} \right]^{3/2} \exp\left(\frac{E_0^*}{j^2 k T}\right) \quad (5.25)$$

TABLE I

THERMAL EMISSION RATES

 β_j (sec⁻¹)

(Calculated from (D.11) to (D.14))

	<u>25°K</u>	<u>50°K</u>	<u>100°K</u>
β_2	5.2×10^9	1.0×10^{10}	2.1×10^{10}
β_3	6.2×10^{10}	1.2×10^{11}	2.5×10^{11}
β_4	3.5×10^{11}	7.0×10^{11}	1.4×10^{12}
β_5	6.3×10^{11}	1.3×10^{12}	2.5×10^{12}

TABLE II

INTERNAL TRANSITION RATES

 $w_{j \rightarrow j'}$ (sec⁻¹)

(Calculated from (D.17) and (D.18))

25°K

$$\begin{aligned} w_{1 \rightarrow 2} &= 1.6 \times 10^7 \\ w_{1 \rightarrow 3} &= 8.0 \times 10^5 \\ w_{1 \rightarrow 4} &= 2.0 \times 10^5 \end{aligned}$$

50°K

$$\begin{aligned} w_{1 \rightarrow 2} &= 1.0 \times 10^8 & w_{5 \rightarrow 1} &= 6.1 \times 10^6 \\ w_{1 \rightarrow 3} &= 6.7 \times 10^6 & w_{4 \rightarrow 1} &= 1.7 \times 10^7 \\ w_{1 \rightarrow 4} &= 1.6 \times 10^6 & w_{3 \rightarrow 1} &= 5.5 \times 10^6 \\ & & w_{2 \rightarrow 1} &= 5.3 \times 10^8 \\ w_{5 \rightarrow 2} &= 1.3 \times 10^9 & w_{5 \rightarrow 3} &= 1.2 \times 10^{11} \\ w_{4 \rightarrow 2} &= 5.5 \times 10^9 & w_{4 \rightarrow 3} &= 2.7 \times 10^{12} \\ w_{3 \rightarrow 2} &= 9.8 \times 10^{10} & & \end{aligned}$$

The results obtained from (5.25) for antimony-doped germanium using the values for β_j in Table I and ν_j in Table III are given below in Table IV and compared with the experimental value.

TABLE III
CHARACTERISTIC RATE OF
CHANGING VALLEYS ν_j (sec⁻¹)

<u>Antimony</u>		<u>Arsenic</u>	
ν_1	$= 9.1 \times 10^{11}$	ν_1	$= 6.3 \times 10^{12}$
ν_2	$= 1.1 \times 10^{11}$	ν_2	$= 7.8 \times 10^{11}$
ν_3	$= 3.4 \times 10^{10}$	ν_3	$= 2.3 \times 10^{11}$
ν_4	$= 1.4 \times 10^{10}$	ν_4	$= 9.8 \times 10^{10}$
ν_5	$= 7.3 \times 10^9$	ν_5	$= 5.0 \times 10^{10}$

$\nu_j = \frac{4\Delta_j}{\hbar}$, where $4\Delta_j$ is the valley-orbit splitting of the j'th state. From Eq. (C.11), $4\Delta_j = \frac{4\Delta}{j^3}$, where 4Δ is the valley-orbit splitting of the ground state = 0.6 meV for antimony and 4.1 meV for arsenic.

TABLE IV
COMPOUND CAPTURE PROCESS FOR ANTIMONY
(A(T) in cm³/sec)

	<u>25°K</u>	<u>50°K</u>	<u>100°K</u>
Observed Value	5.5×10^{-6}	1.7×10^{-6}	4.2×10^{-7}
A ₂	1.9×10^{-7}	7.2×10^{-8}	4.2×10^{-8}
A ₃	3.1×10^{-7}	5.3×10^{-8}	8.8×10^{-9}
A ₄	1.0×10^{-8}	1.5×10^{-9}	2.6×10^{-10}
Total	5.1×10^{-7}	1.4×10^{-7}	5.1×10^{-8}

For comparison, we have also calculated A(T) from (5.25) for arsenic at 25°K. The contribution from this process is 1.7×10^{-6} cm³/sec which when added to the delta function contribution (8.0×10^{-6} cm³/sec)

Eq. (5.15) gives for the total rate $9.7 \times 10^{-6} \text{ cm}^3/\text{sec}$. The observed value from W.S.W. is $1.3 \times 10^{-5} \text{ cm}^3/\text{sec}$.

We have omitted the ground state from the above mostly because our approximation for calculating β_j is not valid for $j = 1$. It seems clear, however, that its thermal emission rate should be quite small, since a phonon of energy greater than kT is necessary to liberate the electron, whereas for other states the opposite is true. In the limit $\nu_j \gg \beta_j$, the direct rate reduces to $3/8 \beta_j$, so that the ground state would be negligible.

It is seen that this limit is approximately an order of magnitude too small for antimony, and even adding the delta function contribution ($\approx 8.5 \times 10^{-8} \left(\frac{100}{T}\right)^{1/2}$) helps only at the high temperature end.

In the other limit, cascading is significant, and we assume that at least one level attains close to its maximum possible rate. This occurs for $\beta_j + \sum_{j' \neq j} w_{j \rightarrow j'} = \nu_j$, and the rate is $3/16 \nu_j$. From

Tables I, II, and III, it appears that the only plausible candidate is $j = 2$. For higher states β_j is already greater than ν_j , so that including internal transitions, these states are less effective than in the previous limit. For $j = 1$, it appears that

$\beta_1 + \sum_{j' \neq 1} w_{1 \rightarrow j'}$ is too small in comparison to ν_1 for this state to

achieve maximum effectiveness. There should, however, be some con-

tribution from this state.

We now assume that $A(T)$ can be written (cf 5.24)

$$A_j(T) = \left[\beta_j + \sum_{j' \neq j} w_{j \rightarrow j'} \right] S(j) \left[\frac{2\pi^2 \hbar^2}{m^* k T} \right]^{3/2} \exp\left(\frac{E_0^*}{j^2 k T} \right) \quad (5.26)$$

and the state $j = 2$ attains its maximum possible rate. Therefore,

$$\left[\beta_2 + \sum_{j' \neq 2} w_{2 \rightarrow j'} \right] S(2) \approx \frac{3}{16} \nu_2$$

For $j = 1$,

$$\left[\beta_1 + \sum_{j' \neq 1} w_{1 \rightarrow j'} \right] S(1) = f \nu_1$$

where "f" is an adjustable fraction allowing us to match the experimental data.

$$f \nu_1 = \frac{3}{8} \frac{\nu_1^2 \bar{\tau}_1}{1 + \nu_1^2 \bar{\tau}_1^2} \approx \frac{3}{8} \left[\beta_1 + \sum w_{1 \rightarrow j'} \right]$$

for

$$\nu_1 \gg \frac{1}{\bar{\tau}_1} = \left[\beta_1 + \sum w_{1 \rightarrow j'} \right]$$

For 25°K , $A_2 \approx 2.1 \times 10^{-6} \text{cm}^3/\text{sec}$, which means A_1 should contribute $\approx 3.3 \times 10^{-6} \text{cm}^3/\text{sec}$. This gives $f \approx \frac{1}{670}$. At first sight, this might appear reasonable, but it implies more than 10^9 transitions per second from the ground state. From Table II, however this appears much too large.

At 50°K, $A_2 \approx 4.2 \times 10^{-7} \text{ cm}^3/\text{sec}$, so that A_1 must contribute $\approx 1.2 \times 10^{-6} \text{ cm}^3/\text{sec}$. f is then approximately $\frac{1}{90}$, so that more than 10^{10} transitions per second from the ground state are required. This also does not appear to be reasonable.

The above overestimates the actual situation. First, because we would not expect $j = 2$ to attain its maximum rate, but, at best, something close to it.

Furthermore, some of the electrons making transitions from $j = 1$ or 2 to a higher state, may return to these states before re-emission into the continuum.

For ionized arsenic, the $j = 2$ and $j = 3$ states would be expected to contribute to the intervalley scattering rate, and no contribution would be required from the ground state. It appears reasonable, then, that the contribution from the compound capture process added to the rate due to direct scattering by the central cell potential could fit the experimental data.

F. CONCLUDING REMARKS ON IONIZED DONORS

It might be advantageous to specifically point out in detail the difference of $A(T)$ for antimony and arsenic. (See Figs. 10 and 13.) At 20°K, the rate per ionized arsenic donor is roughly twice that of antimony. The rate for antimony follows a simple temperature dependence of approximately T^{-2} which means the effective intervalley scattering cross section σ_{iV} goes as $T^{-2.5}$

$(A(T) = \langle \sigma_{iv} V \rangle)$. The rate for arsenic which initially falls rapidly, levels off with approximately a $T^{-0.5}$ dependence. This leveling is presumably due to direct intervalley scattering by the central cell potential (Sec. C). The rate for antimony and part of the rate for arsenic were believed to be due to the compound capture re-emission process. The maximum difference between the two donors occurs at the highest temperature measured (100°K), and is about a factor of 10. Here, the rate for antimony should begin to level off due to the onset of direct scattering; however, we cannot determine this from our data.

It may be worth mentioning that recombination cross sections (39,47), briefly discussed in Sec. E, follow approximately a $T^{-2.5}$ temperature dependence. These cross sections have been measured up to 10°K, and an extrapolation to 20°K gives a result considerably smaller than the effective intervalley cross section. W.S.W. originally conjectured that the discrepancy could be attributed to higher excited states being effective for intervalley scattering than for recombination. The initial capture of the electron in both processes takes place by means of the "giant trap" mechanism (37). The fact that higher excited states are effective for intervalley scattering is to some degree true, but only the first two states can possibly make a sizeable contribution in antimony, and only the first three for arsenic. (Higher states have maximum

intervalley scattering rates which are too small to contribute significantly.) States which are effective for recombination have binding energy greater than kT , which means only the ground state for temperatures above 30°K .

The form of the giant trap mechanism has been obscured by the method used to calculate thermal ionization rates. The "giant trap" describes the thermal capture rate (inverse of thermal ionization) and can also include the impact capture or recombination rate which will be briefly discussed below.

It would be comforting, therefore, if the giant trap mechanism which is reasonably successful in explaining recombination cross sections could also explain the compound capture re-emission contribution to the intervalley scattering rate, taking into account that more states are effective. However, as we discussed in the previous section, the compound capture process according to our calculations cannot explain the experimentally observed rates for antimony. It is capable, in principle, of explaining the rates for arsenic. Whether it actually does fit the observed data cannot be determined from our calculations. Furthermore, the direct scattering contribution complicates the problem for arsenic, since it must first be subtracted in order to determine the compound capture contribution.

It has been stated by Ascarelli and Rodriguez (40) that when

an electron is emitted by a donor, the emission may occur (with appreciable probability) into a random valley. This would mean that the maximum rate for each state would depend on its thermal emission rate β_j , and not appreciably on its characteristic rate of changing valleys ν_j (i.e., the valley-orbit splitting). This would be true if the phonon necessary for thermal ionization were of comparable energy to an intervalley phonon. This does not appear to be the case, and we are not convinced of the validity of their statement. If this were true, however, we would have a process which was independent of the valley-orbit splitting. This, plus the contribution from the compound capture and the delta function process could then possibly explain the observed rates.

It has been suggested by Koenig (12) that perhaps impact ionization and its inverse process, impact recombination (Auger Effect), might play an important role in the intervalley scattering process. The reasoning is that if impact ionization rates were significant, the number of electrons leaving the ground state per second would be considerably larger than the rate due to thermal emission which we calculated in Sec. E. This would then increase the contribution of the ground state to the intervalley scattering rate, since we found that the ground state was ineffective because the rate at which electron left was too slow. In order to maintain thermal equilibrium concentrations, the rate of impact ioni-

zation must equal the rate of electron capture by impact recombination (i.e., electron-electron collisions in the vicinity of an ionized donor in which one electron removes the excess energy so that the other is readily captured).

This would mean that instead of our previous rate equation (Eq. (4.1)) for intervalley scattering, the rate per electron due to impurities would be

$$R_{imp} = N_+ A(T) + N_0 B(T) + N_+^2 C(T) \quad (5.27)$$

where $N_+^2 C(T)$ is the rate per electron due to impact recombination, and $N_+ C(T)$ is the rate per electron per ionized donor.

This can be seen as follows: this rate must be proportional to the rate of impact recombination times the probability of an intervalley transition occurring. The rate of impact recombination is proportional to the probability that two electrons will collide in the vicinity of an ionized donor with the proper energy losing collision; that is, to the square of the electron concentration times the density of ionized donors. The total rate of intervalley transition occurring is $N_+^3 C(T)$, where $C(T)$ is the temperature dependent proportionality factor giving both the probability of initial capture and the ensuing intervalley transition probability. (As an electron is captured via impact recombination, another electron is released as a result of impact ionization in order to maintain ther-

mal equilibrium concentrations.) Since we have defined R_{imp} as the intervalley scattering rate per electron, R_{imp} due to impact recombination is $N_+^2 C(T)$. (In the limit of negligible compensation, the density of free electrons n equals the density of ionized donors N_+ .)

However, in the high temperature range where the number of neutral donors becomes small, $R_{\text{imp}} \propto N_+$, and in the low temperature range, the $N_0 B(T)$ term appears to be necessary. Since a good fit to the experimental data is possible without $N_+^2 C(T)$, we can only conclude that while there may be some contribution due to impact recombination, it is not the dominant mechanism.

G. NEUTRAL DONOR INDUCED INTERVALLEY TRANSITIONS

The scattering of electrons from neutral donors is similar to the scattering from atomic hydrogen. However, the only processes which we detect are those that lead to an intervalley scattering. This eliminates direct scattering by the combined field of the donor core and the bound electron, since the resulting rates will be of the same order as for direct scattering by ionized donors. We can, however, have the delta function type scattering.

The process with which we will be primarily concerned (it is the only significant contribution for antimony-doped germanium) is exchange scattering by means of the Coulomb field of the core and the bound electron.

Only those exchange processes are detected in which a change

of valley results. This will be $3/4$ of the total exchange cross section. One way to visualize this process is to say that since the bound electron is a linear combination of valleys, it has a finite probability at any instant to be found in any one of the four valleys. The incoming electron belongs to a specific valley and if the exchange occurs when the bound electron is in a valley other than the valley of the incoming electron, an intervalley transition has taken place. Since the bound electron, on the average, will be $3/4$ of the time in a valley different from that of the incoming, the intervalley scattering cross section for neutral antimony donors should be just $3/4$ of the total exchange cross section.

We have tried to calculate the exchange cross section in first-order Born approximation. In a simplified two-valley representation the wave function for the bound electron is

$$\Psi \approx \left[\frac{e^{i\vec{K}_\alpha \cdot \vec{r}} + e^{i\vec{K}_\beta \cdot \vec{r}}}{\sqrt{2}} \right] e^{-\frac{r}{a^*}} ; \vec{K}_\alpha \text{ and } \vec{K}_\beta$$

are the extremum or valley minima wave vectors. We have taken plane wave trial functions for the free electron. For a specific example, if electron 1 is incoming and belongs to valley α , then $\vec{k}_1 = \vec{K}_\alpha + \vec{\delta k}$, where $\vec{\delta k}$ is the thermal momentum; and if electron 2 is emitted into valley β with $\vec{k}_2 = \vec{K}_\beta + \vec{\delta k}$, an intervalley transition has occurred.

The scattering amplitude is (43, p 241 ff)

$$g(\theta) \approx \iint d\vec{r}_1 d\vec{r}_2 \left[e^{-i\vec{k}_1 \cdot \vec{r}_1} \left(\frac{e^{-i\vec{k}_\alpha \cdot \vec{r}_2} + e^{-i\vec{k}_\beta \cdot \vec{r}_2}}{\sqrt{2}} \right) e^{-\frac{r_1}{a^*}} \right. \\ \left. \times V(r_1, r_2) e^{i\vec{k}_2 \cdot \vec{r}_2} \left(\frac{e^{i\vec{k}_\alpha \cdot \vec{r}_1} + e^{i\vec{k}_\beta \cdot \vec{r}_1}}{\sqrt{2}} \right) e^{-\frac{r_2}{a^*}} \right] \quad (5.28)$$

and for this event

$$g(\theta) \approx \frac{1}{2} \iint d\vec{r}_1 d\vec{r}_2 \left[e^{-i(\vec{k}_1 - \vec{k}_\alpha) \cdot \vec{r}_1} e^{-\frac{r_1}{a^*}} V(r_1, r_2) \left(e^{i(\vec{k}_2 - \vec{k}_\beta) \cdot \vec{r}_2} \right) e^{-\frac{r_2}{a^*}} \right] \quad (5.29)$$

where the interaction potential is

$$V(r_1, r_2) = -\frac{e^2}{K r_1} + \frac{e^2}{K |\vec{r}_1 - \vec{r}_2|}$$

Now, matrix elements of this form will be of considerable magnitude. Unfortunately, putting in the normalization and density of states factor, the resulting cross section is two or three orders of magnitude too large.

The Born approximation is valid when the energy of the incoming electron is large compared to the binding energy of a state or to the potential from which we are calculating the scattering. In the above example, Born approximation would be valid for $\delta k a^* \gg 1$, which is opposite to the experimental situation. We did not, however, expect to be off three orders of magnitude. We have, therefore, tried to forget that we attempted this calculation. It is mentioned only because it illustrates the exchange process.

The scattering of electrons from antimony donors should be similar to scattering from hydrogen atoms, if we overlook the anisotropic effective mass. Since there have been many sophisticated calculations (in reasonable agreement with experiment) of scattering of slow electrons from hydrogen atoms (44), we have attempted to scale the hydrogen problem. The usual calculations are the partial wave phase shifts for the singlet and triplet states considering only incoming "S" waves. The singlet and triplet arise in processes involving identical spin 1/2 particles, since the total electronic wave function must be antisymmetric* (spin function times the space function). If $\Psi(r_1, r_2)$ is the space function of the two electron systems, we can equally write the wave function as $\Psi(r_2, r_1)$ and the total space function must be written $\Psi(r_1, r_2) \pm \Psi(r_2, r_1)$. The plus sign is symmetric with respect to interchange of electron 1 and 2, and the minus sign is antisymmetric. Since the two electron system has three symmetric spin functions and one antisymmetric spin function (Schiff, p 233), the minus sign must be given a statistical weight of three (triplet state), and the plus a statistical weight of one (singlet state).

Following Schiff (p 243) and Appendix E, the total differential cross section is written in terms of the scattering

*Actually, for a many-valley semiconductor, the total wave function must be antisymmetric in spin-valley times space functions. This does not, however, affect the exchange cross section. (See Appendix E.)

amplitudes

$$\sigma_{\text{total}}(\theta) = \frac{1}{4} |f(\theta) + g(\theta)|^2 + \frac{3}{4} |f(\theta) - g(\theta)|^2 \quad \text{Hydrogen} \quad (5.29)$$

$$\sigma_{\text{total}}(\theta) = \frac{7}{16} |f(\theta) + g(\theta)|^2 + \frac{9}{16} |f(\theta) - g(\theta)|^2 \quad \text{Donors} \quad (5.30)$$

where $f(\theta)$ is the scattering amplitude for direct scattering and $g(\theta)$ for exchange scattering.

$|f(\theta) + g(\theta)|^2 = \sigma_S(\theta)$ represents the singlet cross section resulting from the symmetric space function $\Psi(r_1, r_2) + \Psi(r_2, r_1)$ and $\sigma_T(\theta) = |f(\theta) - g(\theta)|^2$ represents the triplet cross section from the antisymmetric space function. The direct scattering cross section $\sigma_D(\theta)$ is $|f(\theta)|^2$ and the exchange cross section $\sigma_E(\theta)$ is $|g(\theta)|^2$.

The quantities which we have taken over from the hydrogen problem are the singlet partial wave phase shift δ_S and the triplet δ_T . The methods and results for such calculations are summarized in a recent review article (44), and we have used the results of Temkin (45) and Schwartz (46).

Still following Schiff (p 105) with obvious extensions, the cross sections are written in terms of the phase shifts (for "S" wave ($l=0$) only)

$$\sigma_S(\theta) = |f(\theta) + g(\theta)|^2 = \frac{1}{k^2} \left| e^{i\delta_S} \sin \delta_S \right|^2$$

$$\sigma_T(\theta) = |f(\theta) - g(\theta)|^2 = \frac{1}{k^2} \left| e^{i\delta_T} \sin \delta_T \right|^2$$

so that

$$f(\theta) + g(\theta) = \frac{1}{k} e^{i\delta_S} \sin \delta_S$$

$$f(\theta) - g(\theta) = \frac{1}{k} e^{i\delta_T} \sin \delta_T$$

$$\therefore f(\theta) = \frac{1}{2k} \left[e^{i\delta_S} \sin \delta_S + e^{i\delta_T} \sin \delta_T \right]$$

$$\therefore g(\theta) = \frac{1}{2k} \left[e^{i\delta_S} \sin \delta_S - e^{i\delta_T} \sin \delta_T \right]$$

The exchange cross section is

$$\sigma_E(\theta) = |g(\theta)|^2 = \frac{1}{4k^2} \left[\sin^2 \delta_S + \sin^2 \delta_T - 2 \sin \delta_S \sin \delta_T \cos(\delta_S - \delta_T) \right]$$

Since the differential cross section is spherically symmetric for incoming "S" waves

$$\sigma_E = 4\pi \sigma_E(\theta) = \frac{\pi b^2}{k^2 b^2} \left[\sin^2 \delta_S + \sin^2 \delta_T - 2 \sin \delta_S \sin \delta_T \cos(\delta_S - \delta_T) \right] \quad (5.30)$$

Scaling, in this problem, consists simply of replacing the hydrogen Bohr radius with the appropriate donor radius. The values δ_S and δ_T are listed in Table V, for values of $k^2 b^2$ up to 0.64.

(b for antimony $\approx 45\text{\AA}$). * This corresponds to a temperature of approximately 50°K , which is as high as our experimental determination. Also listed in this table is the temperature corresponding to each value of k^2b^2 , the exchange cross section, and $B(T)$ (the intervalley scattering rate per neutral donor), given by $B(T) = \frac{3}{4} \sigma_E V$ where $V = \sqrt{\frac{3kT}{m^*}}$ is the root mean square velocity. $B(T)$ for antimony is plotted against the experimental values in Fig. 10 (shown as the solid curve). This part of $B(T)$ also applies to arsenic donors, except that we will use the appropriate effective radius ($b \approx 39\text{\AA}$ *). The experimental values of $B(T)$ for arsenic obtained by W.S.W. are compared with the calculated values in Fig. 13.

TABLE V

NEUTRAL DONOR DATA

$\frac{E}{E_{\text{obs.}}} = k^2b^2$	δ_S (radians)	δ_T (radians)	$\sigma(\pi b^2)$	T	$B(T) \left(\frac{\text{cm}^3}{\text{sec}}\right)$
0.16	1.45	2.30	3.5	12°K	8.7
0.25	1.23	2.11	2.4	19°K	7.7
0.36	1.04	1.93	1.7	27°K	6.2
0.49	0.93	1.78	1.15	36.5°K	5.0
0.56	0.91	1.72	0.95	42°K	4.5
0.64	0.88	1.64	0.73	48°K	3.6

The radii are chosen from the asymptotic form of the envelope which for large values of r is $F(r) \sim e^{-r/b}$, where b is related to the effective mass radius by $b = a^ (E_{\text{eff. mass}}/E_{\text{obs.}})^{1/2}$ and $a^* = 46\text{\AA}$, $E_{\text{eff. mass}} = 9.2 \text{ meV}$, $E_{\text{obs.}} = 9.6 \text{ meV}$ for antimony and 12.7 meV for arsenic. See Kohn, p 291.

For arsenic, it may also be necessary to include the delta function scatterer. Similarly to the case for ionized arsenic, the delta function can cause direct intervalley transitions, and may also contribute to the exchange cross section. We have not, however, included the delta function.

Possible shortcomings of this calculation, other than those inherent in applying the hydrogen problem to donors (such as neglecting the anisotropy of the effective mass), are the inclusion of only "S" wave incoming angular momentum states, considering only elastic processes, and assuming all electrons bound to donors are in the ground state.

At low temperatures ($ka^* < 1$) according to Landau and Lifshitz (34 p. 404), the phase shift for the l th partial wave $\delta_l \approx (ka^*)^{2l+1}$, so that for low enough temperatures only $l = 0$ contributes. Furthermore, since the bound electron has zero angular momentum in the ground state, exchange processes for which the incoming electron has angular momentum other than zero should be less probable.

Inelastic collisions from the ground state can occur only if the incoming electron has sufficient energy to excite the bound electron. At temperatures we are working at, the only inelastic collisions possible are between the singlet and triplet of the ground state. Such inelastic exchange processes might be frequent for antimony but not for arsenic donors, and it is clearly not included in the hydrogen problem.

The percentage of electrons in the ground state will be determined by a Boltzman factor, assuming hydrogen-like excited states. At the highest temperature that neutral donor scattering rates have been measured ($T \approx 50^\circ\text{K}$) the approximate percentage in the ground state is 85%. We have neglected effects due to the relative populations (as a function of temperature) of the singlet and triplet components of the ground state.

APPENDIX A

MOBILITY AND CONDUCTIVITY IN A MANY-VALLEY SEMICONDUCTOR

We want to show that the mobility of an electron belonging to a specific $[111]$ valley is its spatially averaged value for motion in a $[100]$ direction. This will require preliminary remarks concerning mobility and conductivity in a many-valley semiconductor, which are based on a thorough treatment by Herring (13).

For germanium, the conductivity and mobility (due to carriers in all of the valleys) are isotropic. This follows from the fact that for cubic symmetry, the symmetric 2'nd rank conductivity and mobility tensors are $\sigma\delta_{ij}$ and $\mu\delta_{ij}$. That is, they are determined by a single scalar which is their directionally averaged value. If we consider, however, only the carriers belonging to one particular valley, the mobility in an arbitrary direction is not, in general, its spatially averaged value.

The mobility (for crystals which have isotropic effective mass) can be written in the form

$$\mu = \frac{e \tau(\epsilon)}{m^*} \quad (\text{A.1})$$

and the conductivity

$$\sigma = ne\mu \quad (\text{A.2})$$

This assumes that all scattering processes can be described in terms of a relaxation time, and that a total relaxation time exists. It is also assumed that $\tau(\epsilon)$ is a function only of the electron energy, and that it represents some appropriate average over the electron energy distribution.

For germanium, however, if we consider only carriers which belong to a particular valley, the mobility is a tensor because of the anisotropic effective mass. The principal axes of the mass tensor are the symmetry axis of the [111] valley and two mutually perpendicular axes normal to the symmetry axis. The principal values are m_l , m_t , and m_t (Chap. II, Sec. B).

In this set of axes, the mobility and conductivity are also diagonal. The mobility for a direction parallel to a symmetry axis is $\mu_l = \frac{e\tau(\epsilon)}{m_l}$ and for directions perpendicular to a symmetry axis is $\mu_t = \frac{e\tau(\epsilon)}{m_t}$. Since we have assumed that $\tau(\epsilon)$ is isotropic, then the mobility anisotropy ratio K for a single valley is

$$K = \frac{\mu_t}{\mu_l} = \frac{m_l}{m_t} \approx 20$$

That is, loosely speaking, the electron is more "mobile" in directions for which it has a smaller effective mass. In actual fact, $\tau(\epsilon)$ is not in general isotropic, and this reduces the anisotropy ratio (25).

The current in valley i is related to the electric field E by

the conductivity tensor of the valley, and the total current is the sum of the currents due to the individual valleys. The total conductivity tensor is the sum of the conductivity tensors of the individual valleys (i.e. $\sigma_{\alpha\beta} = \sum_i \sigma_{\alpha\beta}^{(i)}$ since $j_\alpha = \sum_i j_\alpha^{(i)} = \sum_\beta \left\{ \sum_i \sigma_{\alpha\beta}^{(i)} \right\} E_\beta$), and for a cubic crystal

$$\sigma = \frac{1}{3} \sum_\alpha \sigma_{\alpha\alpha} = \frac{4}{3} (2\sigma_t + \sigma_\ell) \quad (\text{A.3})$$

The overall mobility tensor is the average over all valleys of the single valley mobility tensors. So that

$$\mu_{\alpha\beta} = \frac{1}{4} \sum_i \mu_{\alpha\beta}^{(i)}$$

which for cubic symmetry becomes

$$\mu = \frac{1}{3} \sum_\alpha \mu_{\alpha\alpha} = \frac{1}{3} [\mu_\ell + 2\mu_t] \quad (\text{A.4})$$

σ and μ are the spatially averaged values of the conductivity and mobility tensors .

We will now show that for valleys along the [111] axes, the mobility of an electron along [100] is simply its spatially averaged value. This follows from the fact that since the valleys are symmetric with respect to a [100] axis, the mobility component along [100] averaged over all valleys is the same as the component in this direction from any one valley. Since the mobility averaged over all valleys is the same in all directions, i.e., its spatially

averaged value μ , the mobility component along [100] for any one valley is also equal to μ . The conductivity for any valley along [100] will be one-quarter of the total conductivity provided the electrons are evenly distributed among the valleys (i.e., in the absence of a symmetry destroying strain. For our case, the conductivity of a valley, averaged over an acoustic wavelength, will be one-quarter of the total conductivity.)

We want to briefly discuss the relaxation time $\tau(\epsilon)$. It will depend both on intravalley and intervalley scattering processes, and can be written in the form (13, 14, p 194)

$$\frac{1}{\tau(\epsilon)} \equiv \frac{1}{\tau^i} = \frac{1}{\tau^{ii}} + \sum_{j \neq i} \frac{1}{\tau^{ij}} \quad (\text{A.5})$$

where τ^{ii} is the relaxation time for intravalley scattering, and τ^{ij} is the relaxation time for scattering from $i \rightarrow j$ (i.e., $\frac{1}{R(i \rightarrow j)}$ from Eq. (2.7).

In the unstrained state, all τ^{ij} are equal, as are all τ^{ii} . In the presence of a symmetry destroying strain, the intravalley relaxation time does not change under the assumptions of the deformation potential model. That is, τ^{ii} depends only on the energy of the electron with respect to the extremal energy of the valley, and the valleys are shifted rigidly. However, as discussed in connection with Eq. (2.7), τ^{ij} is no longer equal to τ^{ji} .

This means that mobility will depend on the strain, and we could take this into account in Eq. (2.6). However, to lowest order in $\frac{q\Phi}{kT}$, we can still use its directionally averaged value.

APPENDIX B

THE USE OF MODULATED ACOUSTIC POWER

In the absence of modulation $\bar{E} = AS$ where $S = \frac{1}{2} \text{Re}(\Phi^* \Phi) C$. Now, if the rf is amplitude modulated $\Phi_m = \Phi(1+m \cos \omega_m t)$ where m is the modulation percentage, and ω_m is the modulation frequency ($\omega_m \approx 2\pi \times 10 \text{ KC}$).

$$\Phi_m^* \Phi_m = \Phi_0^* \Phi_0 \left(1 + 2m \cos \omega_m t + m^2 \cos^2 \omega_m t \right) \quad (\text{B.1})$$

$$V_{DC} = \frac{\bar{E}_{DC}}{L} = A'S \left(1 + \frac{m^2}{2} \right) = A'S'$$

$V_{AC} = \frac{\bar{E}_{AC}}{L} = A'S(4m)$ is the audio component at the modulation frequency. The audio component is taken as the peak to peak value because the amplifiers and phase sensitive detector were calibrated using an oscilloscope, where peak to peak values are the easiest quantity to measure. So that

$$V_{DC} = \frac{1 + \frac{m^2}{2}}{4m} V_{AC} = A'S' \quad (\text{B.2})$$

where V_{AC} is the measured audio component of the acoustoelectric voltage, and $S' = S(1 + \frac{m^2}{2})$ is the measured power density.

The thermoelectric voltage " V_S " produced by power dissipation in the absorber was usually considerably larger than the dc component of the acoustoelectric voltage. In cases where the dc component

could not be neglected, an addition to the measured power was made. Since the power is proportional to the thermoelectric voltage, the addition is

$$\frac{V_{DC}}{V_S} S' \quad (B.3)$$

i.e., since V_S and V_{DC} have opposite sign (p 6 and 24, p 40), the true thermoelectric voltage is $V_S + V_{DC}$. Therefore, the true power is

$$\left(1 + \frac{V_{DC}}{V_S}\right) S' \quad (B.4)$$

For n-type germanium, with the absorber at a temperature $+\Delta T$ with respect to the sample holder, the thermoelectric voltage was positive with respect to ground, while for the acoustoelectric voltage the absorber was negative.

The other point to be made is that while the dc component of the thermoelectric voltage is usually considerably larger than the dc component of the acoustoelectric voltage, for the audio components the opposite is true. Any audio temperature variations will be damped out as $\exp\left[-\sqrt{\frac{\omega_m}{2D}} X\right]$, where D is the heat diffusion constant = $\frac{K \text{ (thermal conductivity)}}{C \text{ (specific heat)}}$; K in $\frac{\text{cal}}{\text{cm sec deg}}$ and C in $\frac{\text{cal}}{\text{deg cm}^3}$ gives D in $\frac{\text{cm}^2}{\text{sec}}$.

From the heat flow equation

$$D \frac{\partial^2 T}{\partial X^2} = \frac{\partial T}{\partial t} \quad (B.5)$$

the ac solution at the modulation frequency

$$T(x, t) = T(x) e^{-i\omega_m t}$$

$$\therefore D \frac{\partial^2 T(x)}{\partial x^2} = -i\omega_m T(x)$$

$$\therefore T(x) = T_0 e^{i\sqrt{\frac{i\omega_m}{D}} x}$$

so that

$$T(x, t) = T_0 e^{-\sqrt{\frac{\omega_m}{2D}} x} \left(e^{i\sqrt{\frac{\omega_m}{2D}} x} - i\omega_m t \right) \quad (\text{B.6})$$

since $\sqrt{i} = \frac{1+i}{\sqrt{2}}$

Taking the absorber at $x = 0$, $T(0, t) = T_0 e^{-i\omega_m t}$. The ac temperature variation and the resulting ac thermoelectric voltage will be damped out for x several times $\sqrt{\frac{2D}{\omega_m}}$. The distance from the absorber to the bottom contact is approximately 0.5 cm.

We have calculated below some approximate values for the heat diffusion constant $D = \frac{K}{C}$ and the "damping length" $\sqrt{\frac{2D}{\omega_m}}$. Our values for the thermal conductivity K were obtained from Geballe and Hull (48), and for the specific heat from the American Institute of Physics Handbook (49 p 4-40).

$$\text{At } 10^\circ\text{K, } D(10) \approx 1600 \frac{\text{cm}^2}{\text{sec}}, \sqrt{\frac{2D}{\omega_m}} \approx 0.25 \text{ cm}$$

$$\text{At } 15^\circ\text{K, } D(15) \approx 400 \frac{\text{cm}^2}{\text{sec}}, \sqrt{\frac{2D}{\omega_m}} \approx 0.12 \text{ cm}$$

$$\text{At } 20^\circ\text{K, } D(20) \approx 150 \frac{\text{cm}^2}{\text{sec}}, \sqrt{\frac{2D}{\omega_m}} \approx 0.07 \text{ cm}$$

At 15°K , any ac temperature variation at the absorber will be down to e^{-4} of its original value at the bottom contact. At higher temperatures there will be negligible component of audio thermo-

electric voltages between any two terminals. Although corrections to the dc thermoelectric voltage due to the dc acoustoelectric voltage were often made, no corrections to the ac acoustoelectric voltage due to thermoelectric voltage were ever made.

APPENDIX C

DELTA FUNCTION REPRESENTATION OF VALLEY-ORBIT SPLITTING

The Hamiltonian for an electron in the field of a donor is

$$H = \left[-\frac{\hbar^2}{2m_t} \left(\frac{\partial^2}{\partial x^2} + \frac{\partial^2}{\partial y^2} \right) - \frac{\hbar^2}{2m_l} \frac{\partial^2}{\partial z^2} - \frac{e^2}{Kr} \right] + U(\vec{r}) \quad (C.1)$$

or

$$H_{ij} = H_0 \delta_{ij} + U_{ij}(\vec{r})$$

$U(\vec{r})$ is a potential which is significant only in or near the central impurity cell, and varies rapidly compared to a lattice spacing. Because of its short range, it will have approximately equal diagonal and off diagonal matrix elements. (This follows from Eq. (5.4) since the single valley wave functions are equal at the origin.)

Assuming a delta function representation for $U(r)$, we have

$$U_{ij}(\vec{r}) = K \delta(\vec{r}) \begin{bmatrix} | & | & | & | \\ | & | & | & | \\ | & | & | & | \\ | & | & | & | \end{bmatrix} \equiv K \delta(\vec{r}) \mathbb{I} \quad (C.2)$$

K must be determined in terms of the valley-orbit splitting of the particular donor, and $\delta(\vec{r})$ is located at the donor nucleus.

Using the eigenstates and eigenvalues in Chap. V, Sec. B.,

(5.6a and b)

$$H_{ij} \Psi_s = H_0 \delta_{ij} \Psi_s + K \delta(\vec{r}) \mathbb{I} \Psi_s = (-E_0^* - 4\Delta) \Psi_s \quad (C.3)$$

$$H_{ij} \Psi_T = H_0 \delta_{ij} \Psi_T + K \delta(\vec{r}) I \Psi_T = (-E_0^*) \Psi_T \quad (C.4)$$

where

$$\Psi_S = \frac{1}{2} \begin{bmatrix} \Psi_1 \\ \Psi_2 \\ \Psi_3 \\ \Psi_4 \end{bmatrix}; \quad \Psi_{T_1} = \frac{1}{2} \begin{bmatrix} \Psi_1 \\ \Psi_2 \\ \Psi_3 \\ \Psi_4 \end{bmatrix}; \quad H_0 \delta_{ij} = -E_0^* \begin{bmatrix} 1 & 0 & 0 & 0 \\ 0 & 1 & 0 & 0 \\ 0 & 0 & 1 & 0 \\ 0 & 0 & 0 & 1 \end{bmatrix}$$

For the singlet

$$\langle \Psi_S^* | H_0 \delta_{ij} | \Psi_S \rangle + K \langle \Psi_S^* | \delta(\vec{r}) I | \Psi_S \rangle = -E_0^* - 4\Delta \quad (C.5)$$

and

$$K \langle \Psi_S^* | \delta(\vec{r}) I | \Psi_S \rangle = -4\Delta \quad (C.6)$$

where

$$\langle \Psi_S^* | \delta(\vec{r}) I | \Psi_S \rangle = \frac{1}{4} \begin{bmatrix} 1 & 1 & 1 & 1 \end{bmatrix} \begin{bmatrix} 1 \\ 1 \\ 1 \\ 1 \end{bmatrix} |\Psi_1(0)|^2$$

so that $4K |\Psi_1(0)|^2 = -4\Delta$, since all single valley functions $\Psi_i(r)$ are equal at $r = 0$. Similarly for the triplet $K |\Psi_1(0)|^2 = 0$ so that $K = \frac{-(4\Delta)}{4} \frac{1}{|\Psi_1(0)|^2}$ where 4Δ is the valley-orbit splitting.

$$|\Psi_1(0)|^2 = |u(k,0)|^2 |F(0)|^2 = \frac{|u(k,0)|^2}{\pi a^{*3}} \quad (C.7)$$

and

$$K = \frac{-\Delta (\pi a^{*3})}{|u(k,0)|^2} \quad (C.8)$$

This is the Born approximation matrix element used for the delta function scatterer in Chap. V, Sec. C.

VALLEY-ORBIT SPLITTING OF EXCITED STATES

Using the same representation as above, the interaction energy H' for the n 'th "S" like state

$$H' \text{ (singlet)} = \langle \Psi_n^*(\vec{r}) | \chi \delta(\vec{r}) I | \Psi_n(\vec{r}) \rangle = -4\chi |F_n(0)|^2 |u(k,0)|^2 \quad (\text{C.8})$$

$$H' \text{ (triplet)} = \langle \Psi_n^*(\vec{r}) | \chi \delta(\vec{r}) I | \Psi_n(\vec{r}) \rangle = 0 \quad (\text{C.9})$$

$$\text{The total splitting} \quad H'_S - H'_T = -4\chi |F_n(0)|^2 |u(k,0)|^2 \quad (\text{C.10})$$

If we assume that the envelope functions are hydrogen-like, then

$$\text{near the origin} \quad F_{nl} \cong \frac{r^l}{n^{2+l}} \frac{z^{l+1}}{(2l+1)!} \frac{\sqrt{(n+l)!}}{\sqrt{(n-l-1)!}}$$

$$\text{and for } l=0, \quad F_{n0} \cong \frac{1}{n^2} \sqrt{\frac{n!}{(n-1)!}} = \frac{1}{n^{3/2}}$$

(Landau-Lifshitz p 124). Since the periodic part of the Bloch function* is the same for all donor excited states, we get simply that

*The periodic part of the Bloch functions are constructed for each band (i.e., valence or conduction band). They vary rapidly with r , but slowly with k within a given band. The donor excited states being modulated conduction band Bloch functions with a small range of k values, only the modulation envelope varies appreciably among the excited states.

$$4K |F_n(0)|^2 |u(k,0)|^2 = 4K \frac{|F_{10}(0)|^2}{n^3} |u(k,0)|^2 \quad (C.11)$$

$$= -\frac{4\Delta}{n^3}$$

APPENDIX D

THERMAL TRANSITION RATES

In Appendix A of their paper on "Recombination of Electrons and Donors in n-Type Germanium" (40), Ascarelli and Rodriguez have calculated thermal emission rates for temperatures below 10°K. We would like to extend these calculations to 100°K. They state the following formula for the "rate" (i.e., transition probability per unit time) that an electron in a bound state j is thermally excited to the continuum by means of phonon absorption.

$$\beta_j = \frac{\Xi^2 m^*}{(2\pi)^5 \rho \hbar^6 c_s^5} \int_{E_j}^{\infty} d(\hbar\omega) (\hbar\omega)^3 \bar{n}(\hbar\omega) K(\hbar\omega) \int d\Omega_q \int d\Omega_k |M(K, j)|^2 \quad (D.1)$$

In the above formula, Ξ is an appropriate deformation potential, c_s is the longitudinal velocity of sound, ρ the density of germanium, $\bar{n}(\hbar\omega)$ is the thermal distribution of phonons = $[\exp(\hbar\omega/kT) - 1]^{-1}$. $\hbar\omega$ and q are the phonon energy and wave vector, K is the electron wave vector, $|M(K, j)|$ is the matrix element governing the transition, and E_j is the binding energy of the j 'th bound state $E_j = E_0/j^2$.

The derivation below is based on a method used for ultrasonic attenuation (28, p 216). The transition probability per unit time is

$$\beta_j = \sum_{k, q} \left(\frac{2\pi i}{\hbar V} \right) \left| \langle \psi_k, n_q - 1 | H_1 | \psi_j, n_q \rangle \right|^2 \delta(E_k + E_j - \hbar \omega_q) \quad (\text{D.2})$$

$E_k = \frac{\hbar^2 k^2}{2m^*}$ is the kinetic energy of the emitted electron, and the sums are taken over the electron and phonon distributions. The delta function ensures conservation of energy.

H_1 (the electron-phonon interaction) in its simplest form is

$$H_1 = \sum_{\vec{r}} \vec{\nabla} \cdot \mathbf{s}(\vec{r}) \quad (\text{D.3})$$

This includes only longitudinal phonons. $\mathbf{s}(\vec{r})$ is the displacement of the atom from its equilibrium position, and is written in terms of phonon creation and destruction operators.

$$\mathbf{s}(\vec{r}) = \sqrt{\frac{\hbar}{2\rho V}} \hat{\mathbf{e}} \left[\frac{s}{\sqrt{\omega_q}} \exp(i\vec{q} \cdot \vec{r}) + \frac{s^\dagger}{\sqrt{\omega_q}} \exp(-i\vec{q} \cdot \vec{r}) \right] \quad (\text{D.4})$$

where $s(s^\dagger)$ are the phonon destruction (creation) operators, and $\hat{\mathbf{e}}$ is a unit polarization vector. s and s^\dagger act only on the phonon occupation number, and $\exp \pm i\vec{q} \cdot \vec{r}$ only on the electron coordinates.

We consider only the phonon destruction operator, since we are interested in absorption of a phonon by an electron

$$H_1 = \sum_{\vec{r}} \sqrt{\frac{\hbar}{2\rho V}} \frac{i|\vec{q}|}{\sqrt{\omega_q}} s \exp(i\vec{q} \cdot \vec{r}) \quad (\text{D.5})$$

$$\langle n_g - 1 | S | n_g \rangle = \sqrt{n_g} \quad (\text{D.6})$$

$$V^{-\frac{1}{2}} \langle \psi_k | e^{i\vec{q} \cdot \vec{r}} | \psi_j \rangle = M(k, j) \quad (\text{D.7})$$

ψ_k is the continuum function (plane waves or Coulomb Continuum functions) and ψ_j is the hydrogen-like envelope for the $j, l = 0$ state. j is used for the principal quantum number to avoid confusion with the phonon occupation number.

With

$$\sum_{\mathbf{k}} \rightarrow \frac{2V}{(2\pi)^3} \int d\vec{k}$$

i.e., the integral representation of the density of states for continuum, we get for the electron coordinates

$$\frac{2V}{(2\pi)^3} \int k^2 dk d\Omega_k |M(k, j)|^2 \delta(E_k + E_j - \hbar\omega_g) \quad (\text{D.8})$$

substituting

$$E_k = \frac{\hbar^2 k^2}{2m^*} \quad \text{and} \quad k^2 dk = \frac{m^*}{\hbar^2} \left(\frac{2m^* E_k}{\hbar^2} \right)^{\frac{1}{2}} dE_k$$

The result is

$$\frac{m^*}{\hbar^2} K \int d\Omega_K |M(K, j)|^2$$

with

$$K = \left(\frac{2m^*}{\hbar^2} \right)^{\frac{1}{2}} (\hbar\omega_q - E_j)^{\frac{1}{2}} j$$

setting

$$\sum_q \rightarrow \frac{V}{(2\pi)^3} \int d\vec{q} = \frac{V}{(2\pi)^3} \int q^2 dq d\Omega_q$$

and assuming $q = \frac{\omega}{c_s}$, we finally get

$$\beta_{ij} = \frac{m^* \Xi^2}{(2\pi)^5 \rho \hbar^6 c_s^3} \int_{E_j}^{\infty} d(\hbar\omega) (\hbar\omega)^3 \bar{n}(\hbar\omega) K(\hbar\omega) \int d\Omega_q \int d\Omega_K |M(K, j)|^2$$

which is the result quoted by Ascarelli and Rodriguez.

Turning to the matrix element $|M(K, j)|^2$, we attempted to evaluate it using plane waves for the continuum states. i.e.,

$$M(K, j) = \int e^{-i\vec{k}\cdot\vec{r}} e^{i\vec{q}\cdot\vec{r}} \psi_j(\vec{r}) d\vec{r}$$

This appears to appreciably underestimate the thermal ionization rate. Ascarelli and Rodriguez have given $|M(K, j)|^2$ in a closed form using Coulomb continuum functions. We have not checked their derivation, but merely state their result, and discuss the validity of their approximations. In the limit of $Q_j^2 \gg 1$, $q \gg K$, and $Ka^* \ll 1$,

($Q_j = jqa^*$, q and K are the phonon and electron wave vectors), Ascarelli and Rodriguez obtain the following results.

$$M(\vec{K}, j) = \frac{8^3 \pi^2}{j^3 q^8 a^{*6} K} \exp\left(-\frac{4}{jq^2 a^{*2}}\right) \quad (D.9)$$

We now consider their approximations to show their validity independent of temperature. From the conservation of energy contained in the delta function

$$\frac{\hbar^2 K^2}{2m^*} = \hbar\omega_j - E_j = \hbar c_s q - E_j$$

$$\frac{K^2}{q^2} = \frac{2m^* c_s}{\hbar} \frac{1}{q} - \frac{2m^*}{\hbar} E_j$$

The maximum value of k^2/q^2 is when $q = \frac{2E_j}{\hbar c_s}$ obtained from setting $\frac{d}{dq}\left(\frac{k^2}{q^2}\right) = 0$. This gives

$$\frac{K^2}{q^2} \leq \frac{1}{2} \frac{m^* c_s^2}{E_j}$$

so that

$$q^2 \geq \frac{1}{j^2} \left(\frac{2E_0}{m c_s^2}\right) K^2 \approx \left(\frac{700}{j^2}\right) K^2$$

therefore $q \gg K$ for $j \leq 5$ where E_0 , the ground state binding energy, is ≈ 10 meV and $m c_s^2 \approx 3 \times 10^{-2}$ meV. We also need the magni-

tude of $Q_j = jqa^*$. Now $\hbar\omega = E_j$ when $K = 0$, so that $\hbar\omega \geq E_j$ and

$$q \geq \frac{E_j}{\hbar c_s}$$

$$Q_j^2 = j^2 q^2 a^{*2} \geq \frac{E_0^2 a^{*2}}{j^2 \hbar^2 c_s^2} = \left(\frac{e^2}{2\hbar c_s}\right)^2 \frac{1}{j^2} \approx \frac{200}{j^2}$$

$Q_j^2 \gg 1$ is also valid for j up to 5. The last approximation they used in evaluating $|M(\vec{k}, j)|^2$ is that $ka^* \ll 1$. From the form of the integral for $M(\vec{k}, j)$, i.e., $[\exp i(\vec{q} - \vec{k})]$, $|\vec{q} - \vec{k}|$ will tend to be as small as is consistent with conservation of energy;

$$|\vec{q} - \vec{k}| = \frac{\hbar\omega}{\hbar c_s} - \left(\frac{2m^*}{\hbar^2}\right)^{\frac{1}{2}} [\hbar\omega - E_j]^{\frac{1}{2}}$$

This is a minimum for $\hbar\omega = E_j + \frac{1}{2} m^* c_s^2$, so that for $\frac{\hbar^2 k^2}{2m^*} \approx \frac{1}{2} m^* c_s^2$, $ka^* \approx \frac{m^* c_s a^*}{\hbar} \approx 0.05$. This approximation should be adequate.

Using their result (D.9) with

$$\frac{1}{j Q_j^2 a^{*2}} = j^3 \left(\frac{2k\hbar c_s}{e^2} \right)^2 \left(\frac{E_j}{\hbar\omega} \right)^2 \approx \frac{j^3}{200} \left(\frac{E_j}{\hbar\omega} \right)^2$$

in the integral for thermal emission rate, we get the following:

$$\beta_j = \frac{256 \hbar^2 c_s^3 m^* \Omega^2}{\pi \rho a^{*6} j^3} \int_{E_j}^{\infty} \frac{d(\hbar\omega)}{(\hbar\omega)^5} \frac{\exp\left[-\frac{j^3}{50} \left(\frac{E_j}{\hbar\omega}\right)^2\right]}{\left[\exp\left(\frac{\hbar\omega}{kT}\right) - 1\right]} \quad (D.10)$$

Since $|M(\vec{k}, j)|^2$ is spherically symmetric, the two angular integrations give $(4\pi)^2$. The lower limit of the integral arises from the requirement that the phonon must have at least as much energy as the binding energy.

We now want to expand the exponential in the denominator. For the temperature range 20°K to 100°K it will usually be adequate to approximate $[\exp\left(\frac{\hbar\omega}{kT}\right) - 1]$ by $\frac{\hbar\omega}{kT}$. This assumes that the maximum contribution to the integral comes near $\hbar\omega = E_j$. ($E_j < kT$ for $T > 30^\circ\text{K}$)

and $E_3 < kT$ for $T > 13^\circ\text{K}$.) We will not be able to calculate the ground state; its thermal emission rate, however, should be small.

We also have to approximate the exponential in the numerator. Since the lower limit of the integral is E_j , for $j = 2$ the exponential is essentially 1. For $j = 3, 4, 5$ we expand the exponential in a power series, and the integral eventually converges. For $j = 5$, satisfactory convergence required eight terms.

The results are

$$\beta_2 = \frac{256 \hbar^2 c_s^3 m^* \Xi^2 kT j^7}{5\pi a^{*6} E_0^5 \rho}$$

$$\beta_2 \approx 2.1 \times 10^8 \pi \text{ (sec}^{-1}\text{)} \quad (\text{D.11})$$

$$\beta_3 \approx 2.5 \times 10^9 \pi \text{ (sec}^{-1}\text{)} \quad (\text{D.12})$$

$$\beta_4 \approx 1.4 \times 10^{10} \pi \text{ (sec}^{-1}\text{)} \quad (\text{D.13})$$

$$\beta_5 \approx 2.5 \times 10^{10} \pi \text{ (sec}^{-1}\text{)} \quad (\text{D.14})$$

We have used the following values for the constants

$$\Xi = 20 \text{ ev}$$

$$E_0 = 9.6 \text{ mev}$$

$$m^* = 2 \times 10^{-28} \text{ gm}$$

$$c_s = 5 \times 10^5 \text{ cm/sec}$$

$$a^* = 4.5 \times 10^{-7} \text{ cm}$$

$$\rho = 5.4 \text{ gm/cm}^3$$

TRANSITIONS BETWEEN TWO BOUND STATES

We would like to briefly discuss the transition rate between two bound states j and j' . The derivation is similar to that of thermal ionization. If the electron is originally in state j , and j is greater (less) than j' , the transition occurs through phonon emission (absorption). The sum on the electron distribution $\sum_k \rightarrow 1$, and the Fermi distribution factor is omitted. This assumes that the electron is originally in state j , and we want to calculate the transition rate to a state j' which must be empty. We also assume that transitions with change of spin are less probable. Energy conservation is expressed by $\delta(E_j - E_{j'} \pm \hbar\omega)$.

The previous matrix element $M(\mathbf{K}, j)$ is replaced by $M(j, j')$ and only transitions between s states are considered.

For an s state with principal quantum number j , the wave function $F_{j0}(r)$ (i.e., the spherically symmetric envelope) can be written (see Landau and Lifschitz, p 124 ff and 496).

$$F_{j0}(r) = \frac{e^{-\frac{r}{a^*}}}{\sqrt{\pi} j^3 a^{*3}} \left[1 - \frac{(j-1)}{2} \frac{r}{a^*} + \frac{(1-j)(2-j)}{3 j^2} \left(\frac{r}{a^*}\right)^2 + \dots \right] \quad (\text{D.15})$$

and

$$M(j, j') = \frac{1}{\pi a^{*3} \sqrt{j^3 j'^3}} \int e^{\frac{-r}{a^*} \left[\frac{1}{j} + \frac{1}{j'} \right] \pm i \vec{q} \cdot \vec{r}} d\vec{r} \left[1 - \left\{ \frac{j-1}{j} + \frac{j'-1}{j'} \right\} \frac{r}{a^*} \right] \quad (\text{D.16})$$

The integration gives reciprocal powers of

$$\left[\frac{1}{a^{*2}} \left(\frac{1}{j} + \frac{1}{j'} \right)^2 + q^2 \right]$$

and for

$$q a^* \gg 1$$

we keep only the lowest order.

From the conservation of energy

$$q a^* = \frac{E_0 a^*}{\hbar c_s} \left(\frac{1}{j'^2} - \frac{1}{j^2} \right)$$

$$q a^* \approx 15 \left(\frac{1}{j'^2} - \frac{1}{j^2} \right)$$

For $q a^* \gg 1$, we can also neglect $(1/j + 1/j')^2$ with respect to $q a^*$.

Unfortunately, proceeding with the derivation we do not get the same result as Ascarelli and Rodriguez. We get a result which is higher than theirs. However, we are not actually calculating anything using these rates, but merely want to use them to illustrate

relative magnitudes. We, therefore, will use the results quoted in their paper (40).

For $j > j'$

$$W_{j \rightarrow j'} = \frac{(64 \pi^2 \hbar^4 C_s^3)}{(\pi \rho a^*{}^8 E_0^5)} \frac{(jj')^5}{(j-j')^5 (j+j')^3} \left[1 - e^{-\frac{\hbar \omega_{jj'}}{kT}} \right]^{-1} \quad (\text{D.17})$$

where

$$\hbar \omega_{jj'} = E_0 \left(\frac{1}{j'^2} - \frac{1}{j^2} \right) \quad (\text{D.18})$$

From detailed balance, we get

$$W_{j' \rightarrow j} = W_{j \rightarrow j'} \exp\left(-\frac{\hbar \omega_{jj'}}{kT}\right) \quad (\text{D.19})$$

We use the same values for the constants as in (D.11) to (D.14).

$$W_{j \rightarrow j'} \approx 4.0 \times 10^8 \frac{(jj')^5}{(j-j')^5 (j+j')^3} \left[1 - e^{-\frac{\hbar \omega_{jj'}}{kT}} \right]^{-1}$$

APPENDIX E

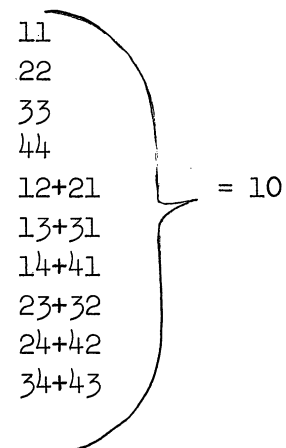
VALLEY STATISTICS

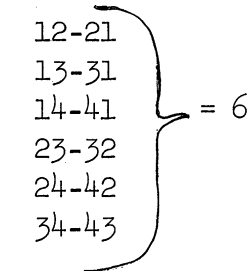
As was mentioned in Chap. V, Sec. E, the many-valley structure does not alter the exchange cross section. It is amusing, however, to consider how the many-valley structure affects the total cross section by virtue of altering the distinguishability of electrons. In a single-valley process, one requires that the product of spin function and space function be antisymmetric with respect to the interchange of the two electrons. In a many-valley process, the requirement is that the spin-valley function times the space function be antisymmetric.

For germanium, which has four valleys, there are ten symmetric valley functions and six antisymmetric valley functions.

Using the schematic notation that (12) means electron a in valley 1 and electron b in valley 2, and (21) means a in valley 2 and b in 1, we get the following valley functions:

<u>Symmetric</u>	<u>Antisymmetric</u>
11	12-21
22	13-31
33	14-41
44	23-32
12+21	24-42
13+31	34-43
14+41	
23+32	
24+42	
34+43	





For a two electron system, there are three symmetric spin functions ($\uparrow\uparrow, \downarrow\downarrow$, and $\uparrow\downarrow + \downarrow\uparrow$) and one antisymmetric spin function ($\uparrow\downarrow - \downarrow\uparrow$). There are therefore a total of 64 spin-valley functions of which 36 are symmetric and 28 are antisymmetric. (The 36 arises from ten symmetric valley functions times three symmetric spin functions plus six antisymmetric valley functions times one antisymmetric spin function.)

The total wave function must now be made antisymmetric in spin-valley times the orbital wave function. To conform to the hydrogen notation, we will call the total function the triplet if the orbital is antisymmetric, and the singlet if the orbital is symmetric. We have therefore 36 triplets and 28 singlets.

The total cross section is then written

$$\begin{aligned}\tilde{\sigma}_{total} &= \frac{28}{64} \tilde{\sigma}_S + \frac{36}{64} \tilde{\sigma}_T \\ &= \frac{7}{16} \tilde{\sigma}_S + \frac{9}{16} \tilde{\sigma}_T\end{aligned}\tag{E.1}$$

where the corresponding result for hydrogen is

$$\tilde{\sigma}_{total} = \frac{1}{4} \tilde{\sigma}_S + \frac{3}{4} \tilde{\sigma}_T\tag{E.2}$$

Using the previous hydrogen notation for the cross section in terms of the direct ($f(\theta)$) and exchange ($g(\theta)$) scattering ampli-

tudes (Eq. (5.29)).

$$\tilde{\sigma}_S = |f(\theta) + g(\theta)|^2 \quad (\text{E.3})$$

$$\tilde{\sigma}_T = |f(\theta) - g(\theta)|^2 \quad (\text{E.4})$$

and

$$\tilde{\sigma}_D = |f(\theta)|^2 \quad (\text{E.5})$$

$$\tilde{\sigma}_E = |g(\theta)|^2 \quad (\text{E.6})$$

so that

$$\begin{aligned} \tilde{\sigma}_{\text{total}} &= |f(\theta)|^2 + |g(\theta)|^2 - \frac{1}{4} |f(\theta)| |g(\theta)| \\ &= \tilde{\sigma}_E + \tilde{\sigma}_D - \frac{1}{4} |f(\theta)| |g(\theta)| \end{aligned} \quad (\text{E.7})$$

for donors in germanium, and

$$\begin{aligned} \tilde{\sigma}_{\text{total}} &= |f(\theta)|^2 + |g(\theta)|^2 - |f(\theta)| |g(\theta)| \\ &= \tilde{\sigma}_E + \tilde{\sigma}_D - |f(\theta)| |g(\theta)| \end{aligned} \quad (\text{E.8})$$

for hydrogen. The explanation for the above cross sections is as follows: When the particles are distinguishable (different valley or different spin), the total cross section is the sum of the direct and exchange cross sections, i.e., $|f(\theta)|^2 + |g(\theta)|^2$

In $3/4$ of the collisions, the electrons belong to different valleys, and in $1/2$ of the collisions they have opposite spins. Of the 64 spin-valley combinations, 48 are distinguishable as a result of valley, and half of the remaining 16 as a result of spin. For the remaining eight combinations, the antisymmetric space function must be used. This gives

$$\begin{aligned}
 \zeta_{\text{total}} &= \frac{56}{64} \left(|f(\theta)|^2 + |g(\theta)|^2 \right) + \frac{8}{64} |f(\theta) - g(\theta)|^2 \\
 &= |f(\theta)|^2 + |g(\theta)|^2 - \frac{1}{4} |f(\theta)| |g(\theta)| \\
 &= \zeta_D + \zeta_E - \frac{1}{4} |f(\theta)| |g(\theta)|
 \end{aligned} \tag{E.7}$$

The corresponding result for hydrogen is

$$\zeta_{\text{total}} = \frac{1}{2} \left(|f(\theta)|^2 + |g(\theta)|^2 \right) + \frac{1}{2} |f(\theta) - g(\theta)|^2$$

since in half of the collisions the electrons are distinguishable

so that

$$\zeta_{\text{total}} = \zeta_D + \zeta_E - |f(\theta)| |g(\theta)| \tag{E.8}$$

Since the cross term ($|f(\theta)| |g(\theta)|$) contribution would vanish in the limit of truly distinguishable particles, the many-valley model is seen to make electrons more distinguishable.

It is also seen that although the many-valley structure alters the total cross section by changing the contribution of the interference term, the individual direct and exchange or equivalently the "singlet" and "triplet" are not affected.

BIBLIOGRAPHY

1. G. Weinreich, T. M. Sanders, Jr., and H. G. White, *Phy. Rev.* 114, 33 (1959).
2. R. H. Parmenter, *Phy. Rev.* 89, 990 (1953) and *Phy. Rev.* 113, 102 (1959).
3. G. Weinreich, *Phy. Rev.* 104, 321 (1956).
4. T. Holstein, Westinghouse Research Memo 60-94698-3-M15 (1956). Unpublished.
5. E. I. Blount, *Phy. Rev.* 114, 418 (1959).
6. N. Mikoshiba, *J. Phy. Soc. Japan* 15, 1189 (1960).
7. Wen-Chung Wang, *Phy. Rev. Letters* 9, 443 (1962).
8. R. W. Keyes, *Phy. Rev.* 103, 1240 (1956).
9. F. J. Morin, T. H. Geballe and C. Herring, *Phy. Rev.* 105, 529 (1957).
10. W. Kohn, Solid State Physics, Vol. V (1957). (Academic Press, Inc., New York.)
11. P. J. Price, Private communication and unpublished work.
12. S. H. Koenig, International Conference on Semiconductors. Exeter, United Kingdom (1962) (to be published).
13. C. Herring, *Bell System Tech. J.* 34, 237 (1955).
14. R. W. Keyes, Solid State Physics Vol. XI (1960). (Academic Press Inc., New York.)
15. C. Kittel, Introduction to Solid State Physics, 2'nd Edition (1959). (Wiley and Sons Inc., New York.)
16. G. Weinreich, *Phy. Rev.* 107, 317 (1957).
17. B. D. Cullity, Elements of X-Ray Diffraction (1956). (Addison-Wesley Publishing Co., Reading, Mass.)

18. C. S. Fuller and J. D. Struthers, *Phy. Rev.* 87, 526 (1952).
19. Transistor Technology (1958). Edited by H. E. Bridges, J. H. Schaff, and J. N. Shive. (D. Van Nostrand Co., New York)
20. G. K. White, Experimental Techniques in Low Temperature Physics (1959). (Oxford University Press)
21. R. L. Powell and M. D. Bunch, Advances in Cryogenic Engineering, 6, 537 (1961). K. D. Timmerhaus-Editor. (Plenum Press Inc.)
22. Methods of Experimental Physics. Vol VI B, Solid State Physics. Edited by K. Lark-Horovitz and V. A. Johnson. (Academic Press Inc.)
23. P. P. Debye and E. M. Conwell, *Phy. Rev.* 93, 693 (1954).
24. Semiconductors. Edited by N. B. Hannay (1960). (Rheinhold Publishing Corporation, New York.)
25. H. Fritzsche, *Phy. Rev.* 115, 336 (1959).
26. C. Herring and E. Vogt, *Phy. Rev.* 101, 944 (1956).
27. P. J. Price, *Phy. Rev.* 104, 1223 (1956).
28. R. Truett and C. Elbaum, Handbuch Der Physik. Akustik II (1961). Vol. XI/2. Edited by S. Flügge (Springer-Verlag).
29. G. Weinreich and H. G. White, *Bull. of Amer. Phy. Soc.* 5, 60 (1960) and G. Weinreich, International Conference on Semiconductors. Prague, 1960 (Academic Press).
30. D. K. Wilson and G. Feher, *Bull. Amer. Phy. Soc.* 5, 60 (1960).
31. H. Fritzsche, *Phy. Rev.* 120, 1120 (1960).
32. R. E. Pontinen and T. M. Sanders, Jr., *Bull. Amer. Phy. Soc.* 6, 426 (1961).
33. G. Weinreich, *J. Phy. Chem. Solids*, 8, 216 (1959).
34. L. D. Landau and E. M. Lifshitz, Quantum Mechanics Non Relativistic Theory (1958). (Addison Wesley Co., Reading, Mass.)
35. E. M. Conwell and V. F. Weisskopf, *Phy. Rev.* 77, 388 (1950).

36. D. Bohm, Quantum Theory (1955). (Prentice-Hall Inc., New York)
37. M. Lax, Phy. Rev. 119, 1502 (1960).
38. M. Lax and J. J. Hopfield, Phy. Rev. 124, 115 (1961).
39. S. H. Koenig, R. D. Brown, and W. Schillinger, Phy. Rev. 128, 1668 (1962).
40. G. Ascarelli and S. Rodriguez, Phy. Rev. 124, 1321 (1961).
41. H. Y. Fan, Solid State Physics, Vol. I (1955). (Academic Press Inc., New York).
42. B. N. Brockhouse and P. K. Iyengar, Phy. Rev. 111, 747 (1958).
43. L. I. Schiff, Quantum Mechanics, 2'nd Edition (1955). (McGraw-Hill Co., New York).
44. P. G. Burke and K. Smith, Revs. Mod. Phys. 34, 458 (1962).
45. A. Temkin, Phy. Rev. 126, 130 (1962).
46. C. Schwartz, Phy. Rev. 124, 1468 (1961).
47. G. Ascarelli and S. C. Brown, Phy. Rev. 120, 615 (1960).
48. T. H. Geballe and G. W. Hull, Phy. Rev. 110, 773 (1958).
49. American Institute of Physics Handbook, (McGraw-Hill) (1957).
50. G. Feher, D. K. Wilson, and E. A. Gere, Phy. Rev. Letters 3, 25 (1959).
51. M. B. Prince, Phy. Rev. 92, 681 (1954).
52. N. Mikoshiba, J. Appl. Phys. 34, 510 (1963).
53. A. R. Hutson, Phy. Rev. Letters, 9, 296 (1962).
54. A. R. Hutson, J. H. McFee, and D. L. White, Phys. Rev. Letters, 7, 237 (1961)

UNIVERSITY OF MICHIGAN



3 9015 03526 8609